



Sudan University of Science and Technology
College of Graduate Studies



**Determination of Radiological Properties of 3D Dosimeters and
Human Tissues for Heavy Charged Particles Interaction
Using Srim program**

تحديد الخصائص الإشعاعية لمقاييس الجرعات ثلاثية الأبعاد والأنسجة البشرية
عند تفاعلها مع الجسيمات الثقيلة المشحونة
باستخدام برنامج سريم

**A thesis Submitted for Fulfillment of Requirements for
Degree of Doctor of Philosophy in Physics**

By

Maria Sid Ahmed Abdelrahim MohamedKheir

Supervisor

Prof. Khalid Mohammed Haroun

Co- Supervisor

Dr. Ahmed Elhassan Elfaki

August 2021



قَالُوا سُبْحَانَكَ لَا عِلْمَ لَنَا إِلَّا مَا عَلَّمْتَنَا

إِنَّكَ أَنْتَ الْعَلِيمُ الْحَكِيمُ ﴿٣٢﴾

صدق الله العظيم

(سورة البقرة الآية ٣٢)

ACKNOWLEDGMENT

In the name of Allah, The Most Gracious and Most Merciful, I am truly grateful to Allah, the most beneficent and the most merciful, for granting me health, patience, and strength throughout my research, without whom it would have been impossible to complete it successfully. I prayed for his kindness and forgiveness in our lives here and after. Firstly, I would like to thank my supervisor, Prof. Khalid Mohammed Haroun, for all his support and words of wisdom throughout my PhD research. His continual confidence in my ability as a scientist has pushed me to achieve my very best and I will be forever grateful for his guidance and encouragement over the past four years. Secondly, I would like to express my gratitude to my co-supervisor, Dr. Ahmed Elhassan Elfaki, for acting as my co-supervisor and for his support, and encouragement throughout this study. Finally, my most special thanks go to my family for their prayers, unconditional love, support, encouragement, and generosity and for fully supporting me and cheering for my success: my mother, brothers and sisters, especially Salwa, Zahia and Omiana.

ABSTRACT

This research discusses the relation between medium and incident heavy charged particles passing through it. The main objective of this research is investigation of the radiological properties of three dimensions (3D) dosimeters which include polymer gels, Fricke gel and PRESAGE gels dosimeters, and some human tissues, with respect to their mass stopping cross section, effective atomic number (Z_{eff}) and electron density (N_e) in the continuous energy range from 0.01-1000 MeV of ions. SRIM code was used to generate mass stopping power of elements. The effective atomic number (Z_{eff}) and electron density (N_e) were calculated for proton, ^4He , ^{11}B , ^{12}C and ^{16}O ion interactions using logarithmic interpolation method. Variations of effective atomic number (Z_{eff}) and electron density (N_e) with the kinetic energy of ions were observed over the whole energy range for all studied materials which is up to (24%,10%) for polymeric gels, (27%, 11%) for Fricke gel, and (17%, 8%) for PRESAGE gels for proton interaction. For ^4He ion, variations are up to (24%, 10%), (23%, 11%) and (18%, 9%) for polymeric gels, Fricke gel, and PRESAGE gels, respectively. For other ions, variation is up to (33%, 14%) for polymeric gels as well as Fricke gel, and (28%,13%) for PRESAGE gels. Maximum values of (Z_{eff}) have been observed in intermediate energies between 1-10 MeV for all dosimeters, except for PRESAGE gels where maximum values were observed in the low energy range 10 – 100 keV. For effective atomic number relative to water, polymeric gels and Fricke gel have shown excellent water equivalency with very small differences in (Z_{eff}) throughout the entire energy range for all incident ions studied, while PRESAGE dosimeters show good water equivalence properties only at high energies for all ions. For human tissues the highest variation in (Z_{eff}) for ion interaction is occur in bone, cortical (ICRU-103) for all ions. Skeletal Muscle (ICRP ICRU-201) and Striated Muscle (ICRP ICRU-202), have the best water equivalence in the entire energy range of proton, and Lung Tissue (ICRP), Striated Muscle (ICRP ICRU-202), have the best water equivalence in the entire energy range for other ions. MAGIC is an excellent tissue equivalent material for Lung Tissue (ICRP) and Skeletal Muscle (ICRP ICRU-201). Fricke and BANG-1 gel are an excellent tissue equivalent for Lung Tissue (ICRP), Skeletal Muscle (ICRP ICRU-201) and Striated Muscle, (ICRP ICRU-202), whereas PRESAGE could be considered as a good tissue equivalent to Lung Tissue (ICRP),

Skeletal Muscle (ICRP ICRU-201) and Striated Muscle (ICRP ICRU-202) at different ranges of proton energy. None of these dosimeters could simulate Adipose tissue (ICRP ICRU-103) for proton interaction above 1 MeV. For ^{12}C ion interaction, MAGIC, BANG-1 and Fricke gel have good tissue-equivalent properties throughout the entire energy range for Lung Tissue (ICRP), Skeletal Muscle (ICRP ICRU-201) and Striated Muscle, (ICRP ICRU-202). PRESAGE gel show low differences only for energies greater than 2 MeV. Generally, it is found that polymer and Fricke gels match human tissues more than water do. Data reported here give essential information about interaction of different types of charged particles with different materials and could be useful in the energy range specified.

المستخلص

هذا البحث يختص بمناقشة العلاقة بين الجسيمات المشحونة الثقيلة والوسط الذي تمر من خلاله. الهدف الرئيسي من هذا البحث هو التحقق من الخصائص الإشعاعية لمقاييس الجرعات ثلاثية الأبعاد والتي تشمل المقاييس البلومرية الهلامية السائلة بنوعها (ناقصة التأكسج والعادية)، ومقياس فريكي الهلامي والمقاييس البلومرية الهلامية الصلبة بالإضافة إلى بعض الأنسجة البشرية وذلك فيما يتعلق بالمقطع العرضي لقدرة الإيقاف، والعدد الذري الفعال (Z_{eff})، والكثافة الإلكترونية (N_e) في مدى الطاقة الممتد من 0.01 إلى 1000 ميغا إلكترون فولت من الأيونات. تم إستخلاص قدرة الإيقاف للعناصر المكونة لهذه المواد من برنامج سريم. ومن ثم تم حساب المقطع العرضي لقدرة الإيقاف والعدد الذري المؤثر (Z_{eff}) و الكثافة الإلكترونية (N_e) لهذه المواد عند تفاعلها مع الجسيمات الثقيلة المشحونة والتي تشمل البروتون و ^4He ، ^{11}B ، ^{12}C و ^{16}O بطريقة الإستيفاء اللوغاريتمي. تلاحظ وجود تباين في قيمة العدد الذري الفعال (Z_{eff}) والكثافة الإلكترونية (N_e) مع تغير الطاقة الحركية للأيونات الساقطة علي هذه المواد في كامل نطاق الطاقة لجميع المواد قيد البحث والذي يصل إلى (10%,24%). للمقاييس البلومرية السائلة و(11%, 27%) لهلام فريكي، و (8%, 17%) لهلاميات البوليمر الصلبة لتفاعلها مع البروتون. بالنسبة الي أيونات الهيلوم فانها تصل إلى (10%,24%)، (11%,23%)، (9%,18%) للمواد الهلامية البوليمرية، هلام فريكي، وهلاميات البوليمر الصلبة على التوالي. بالنسبة للأيونات الأخرى يصل التباين إلى (14%,33%) لكل من هلام البوليمر وهلام فريكي ويصل إلى (13%,28%) لهلاميات البوليمر الصلبة. لقد وجد أن القيم القصوى ل(Z_{eff}) قد لوحظت في الطاقات الوسيطة بين 1-10 ميغا إلكترون فولت لجميع مقاييس الجرعات الإشعاعية ثلاثية الأبعاد، باستثناء المواد الهلامية الصلبة حيث لوحظت القيم القصوى في نطاق الطاقة المنخفض نسبياً 10-100 كيلو فولت. أظهرت المقاييس الهلامية ومقياس فريكي خصائص مكافئة للماء بدرجة ممتازة في كامل نطاق الطاقة لكل انواع الأيونات بينما اظهرت المقاييس الهلامية الصلبة ذلك فقط في الطاقات العالية. أما بالنسبة للأنسجة البشرية فإن أعلى تباين في قيم (Z_{eff}) للتفاعل الأيوني لوحظ في مادة العظام المكتتزة (ICRU-119) بنسبة عالية لتفاعلها مع جميع الأيونات. أما فيما يتعلق بالخصائص المكافئة للماء للأنسجة البشرية، فقد لوحظ أن العضلات الهيكلية (ICRP ICRU-201) والعضلات المخططة (ICRP ICRU-202)، هما أفضل مكافئ للماء في كامل نطاق الطاقة

للبروتون، وأن أنسجة الرئة (ICRP)، والعضلات المخططة (ICRP ICRU-202) هما أفضل مكافئ للماء في كامل نطاق الطاقة لبقية الأيونات. وجد أن هلام البوليمر ماجيك هي مادة مكافئة بدرجة ممتازة لأنسجة الرئة (ICRP) والعضلات الهيكلية (ICRP ICRU-201)، أما هلام فريكي وهلام البوليمر بانغ-1 فهما نسيج مكافئ ممتاز لأنسجة الرئة (ICRP) والعضلات الهيكلية (ICRP ICRU-201) والعضلات المخططة (ICRP ICRU-202)، بينما يمكن اعتبار هلام البوليمر الصلب نسيجاً مكافئاً لها في نطاقات مختلفة من طاقة البروتون. لا يمكن لأي من مقاييس الجرعات المذكورة هذه محاكاة الأنسجة الدهنية (ICRP ICRU-103) في حالة تفاعل البروتون بطاقة أعلى من 1 ميغا إلكترون فولت. بالنسبة لتفاعل أيون ^{12}C ، يتمتع هلام ماجيك وهلام بانغ-1 وهلام فريكي بخصائص مكافئة للأنسجة ومتفاوتة في جميع أنحاء نطاق الطاقة الكامل لأنسجة الرئة (ICRP) والعضلات الهيكلية (ICRP ICRU-201) والعضلات المخططة (ICRP ICRU-202). يُظهر هلام البوليمر الصلب اختلافات منخفضة فقط للطاقات التي تزيد عن 2 ميغا إلكترون فولت. بشكل عام، وجد أن هلام البوليمر وهلام فريكي أكثر تطابقاً مع الأنسجة البشرية من الماء. المعلومات المقدمة هنا تمثل معلومات أساسية لتفاعل مختلف أنواع الجسيمات المشحونة مع مختلف المواد ويمكن الاستفادة منها في نطاق الطاقة المحدد.

TABLE OF CONTENTS

Subject	Page
Verse	I
Acknowledgment	II
Abstract	III
Abstract (Arabic)	V
Table of Contents	VII
List of Tables	XII
List of Figures	XII
List of Abbreviations	XIV
List of Appendices	XV
CHAPTER ONE	
INTRODUCTION	
1.1 Introduction	1
1.2 Problem Statement	6
1.3 Thesis Objectives	6
1.3.1 General Objectives	6
1.3.2 Specific Objectives	6
1.4 Methodology	7
1.5 Thesis Outline	7
CHAPTER TWO	
THEORETICAL BACKGROUND	
2.1 Introduction	9

Subject	Page
2.2 Interaction of charged particles with matter	9
2.2.1 Ionizing radiation	9
2.2.2 Mechanism of interaction	9
2.3 Interaction of heavy charged particles with matter	10
2.3.1 Electronic stopping power	11
2.3.2 Nuclear energy loss	13
2.3.3 Stopping of ions in compounds	15
2.3.3.1 Bragg's additivity rule	15
2.3.3.2 Core and bond (CAB) approach	16
2.3.4 Stopping cross-Section (σ)	17
2.4 The effective atomic number (Z_{eff})	18
2.4.1 Theoretical background	18
2.4.2 Methods of calculation of the effective atomic number	19
2.4.2.1 Atomic to electronic cross-section method	19
2.4.2.2 Logarithmic Interpolation method	20
2.5 The effective electron density, (N_e)	21
2.5.1 Electron density for elements	21
2.5.2 Electron density for chemical compounds	22
2.5.2.1 Average electron density $\langle N_e \rangle$	22
2.5.2.2 Effective electron density, N_e	22
2.6 Three Dimension (3D) Dosimeters	23

Subject	Page
2.6.1 Fricke Gel Dosimeters	24
2.6.2 Polymer gel dosimeters (PGD)	25
2.6.2.1 Hypoxic gel dosimeters	26
2.6.2.2 Normoxic gel dosimeters	26
2.6.3 PRESAGE™ Dosimeters	27
2.7 Water and Tissue Equivalence for Multi-element Materials	27
2.7.1 Tissue Equivalence for Multi-element Materials	27
2.7.2 Water Equivalence for Multi-element Materials	30
2.8 Literature Review	31
CHAPTER THREE	
MATERIALS AND METHODS	
3.1 Materials	36
3.1.1 Elemental Composition of The 3D Dosimeters	36
3.1.2 Elemental Composition of The Human Tissues and Substitutes	36
3.2 Computational Methods	37
3.2.1 Simulation Software	37
3.2.1.1 TRIM/SRIM Code	37
3.2.1.2 SRIM Applications	39
3.2.1.3 Accuracy of SRIM Stopping Calculations	40
3.2.2 Methods of Calculation of (Z_{eff})	41
3.2.2.1 Total Mass Stopping Power Calculation	41

Subject	Page
3.2.2.2 Stopping cross-section (σ_{comp}) of Compound	42
3.2.2.3 Effective Atomic Number (Z_{eff}) Calculation	42
3.2.2.4 Electron Density (N_e) Calculation	42
3.3 Water and Tissue Equivalency	43
CHAPTER FOUR	
RESULTS AND DISCUSSION	
4.1 Overview	44
4.2 Accuracy of Effective Atomic Number (Z_{eff}) Calculation	44
4.3 Effective Atomic Number (Z_{eff}) and Electron Density (N_e) for ions interaction	44
4.3.1 Z_{eff} and N_e of 3D Dosimeters	44
4.3.21 Z_{eff} and N_e of Human Tissues and Human Tissue Substitutes	48
4.4 Effective Atomic Number (Z_{eff}) and Electron Density (N_e) as Indicator for Radiological Water Equivalence of Substances	51
4.4.1 Water Equivalence of 3D Dosimeters	51
4.4.2 Water Equivalence of Human Tissues and Human Tissue Substitutes	54
4.5 Effective Atomic Number (Z_{eff}) and Electron Density (N_e) as Indicator for Tissue Equivalence of Substances	55
4.5.1 Tissue Equivalence of 3D Dosimeters	56
4.5.1.1 Tissue Equivalence for Proton Interaction	56
4.5.1.2 Tissue Equivalence for ^{12}C Ion Interaction	58
4.5.2 Tissue Equivalence of Human Tissue Substitutes	60

Subject	Page
4.6 Discussion	62
4.7 Comparison with Previous Studies	63
4.8 Conclusion	64
4.9 Recommendations	65
REFERENCES	66-75
Appendix A: Elemental composition for 3D dosimeters	76
Appendix B: Mass density (ρ) and relative atomic weight (A_r) of 3D dosimeters	78
Appendix C: Elemental composition for human tissues and substitutes	79
Appendix D: Mass density (ρ) and relative atomic weight (A_r) of human tissues and substitutes	80
Appendix E: Basic statistical information on the variation of (Z_{eff}) 3D dosimeters for ions interaction	81
Appendix F: Basic statistical information on variations of (N_e) of the 3D dosimeters for ions interaction	82
Appendix G: Basic statistical information on the variation of (Z_{eff}) of the 3D dosimeters for ions interaction	83
Appendix H: Basic statistical information on the variations of (N_e) of the 3D dosimeters for ions interaction	84
Appendix I: Published scientific paper 1	85
Appendix K: Published scientific paper 2	96

LIST OF TABLES

No.	CAPTION	Page
3.1	Accuracy of SRIM Stopping Power Calculations	41

LIST OF FIGURES

No.	CAPTION	Page
3.1	SRIM Title Page Window	38
3.2	SRIM Setup Window	39
4.1.a-e	Variation of effective atomic number (Z_{eff}) of 3D dosimeters with the kinetic energy of differently charged particles. (a) Proton, (b) ^4He , (c) ^{11}B , (d) ^{12}C and (e) ^{16}O ion	45
4.2.a-b	Variation of (a) effective atomic number Z_{eff} (b) electron density N_e of liquid water with the kinetic energy of differently charged particles	46
4.3.a-e	Variation of electron density N_e of 3D dosimeters with the kinetic energy of different charged particles. (a) Proton, (b) ^4He ion, (c) ^{11}B ion, (d) ^{12}C ion, (e) ^{16}O ion	48
4.4.a-e	Variation of effective atomic number (Z_{eff}) of human tissues and substitutes with the kinetic energy of differently charged particles. (a) Proton, (b) ^4He ion, (c) ^{11}B ion, (d) ^{12}C ion, and (e) ^{16}O ion	49
4.5.a-e	Variation of electron density (N_e) of human tissues and human tissue substitutes with the kinetic energy of differently charged particles. (a) Proton, (b) ^4He ion, (c) ^{11}B ion, (d) ^{12}C ion, and (e) ^{16}O ion	50
4.6.a-e	Percentage difference in (Z_{eff}) of 3D dosimeters relative to water For: (a) Proton (b) ^4He (c) ^{11}B (d) ^{12}C and (e) ^{16}O ions interaction	52
4.7.a-e	Percentage difference in (N_e) of 3D dosimeters relative to water for:	54

No.	CAPTION	Page
	(a)Proton, (b) ^4He ion, (c) ^{11}B ion (d) ^{12}C ion (e) ^{16}O ion interaction	
4.8.a-e	Percentage difference in (Z_{eff}) of human tissues and human tissue substitutes relative to water For: (a) Proton, (b) ^4He ion, (c) ^{11}B ion (d) ^{12}C ion (e) ^{16}O ion interaction	55
4.9.a-d	Z_{eff} : difference percent relative to tissues and muscles for (a) MAGIC gel (b) BANG-1 (c) PRESAGE [®] and (d) Fricke gel, for total proton interaction	57
4.10.a-d	Z_{eff} : difference percent relative to tissues and muscles for (a) MAGIC gel (b) BANG-1 (c) PRESAGE [®] and (d) Fricke gel, for total ^{12}C ion	58
4.11.a-f	Percentage difference in Z_{eff} of human tissue substitutes relative to human tissues for differently charged particles interaction	60
4.12.a-f	Percentage difference in electron density (N_e) of human tissue substitutes relative to human tissues for different charged particles interaction	62

LIST OF ABBREVIATIONS

Abbreviation	Material
SRIM	Stopping and Range of Ions in Matter
HEAG	Hydroxy-Ethyl-Acrylate Gel
MAGAS	Methacrylic Acid, Gelatine Gel with Ascorbic acid
MAGAT	Methacrylic Acid, Gelatine Gel and THPC
MAGIC	Methacrylic Acid, Ascorbic Acid In Gelatine Initiated By Copper
PAGAT	Polyacrylamide, Gelatin And Tetrakis Hydroxyl Methyl Phosphonium Chloride
ABAGIC	Ascorbic Acid, Bis-Acrylamide, In Gelatine Initiated By Copper)
BANG-1 & 2	Bis Acrylamide Nitrogen Gelatine
PABIG	Polyethylene Glycol DiacrylateBisGelatine
PAG	Polyacrylamide Gelatine
SRIM	Stopping Power And Range Of Ions In Matter
TRIM	Transport Of Ions In Matter
ICRP	International Commission on Radiological Protection
ICRU	International Commission on Radiation Units

LIST OF APPENDICES

No.	CAPTION	Page
A	Elemental composition for 3D dosimeters (weight fraction (%) denoted as w_i)	76
B	Mass density (ρ) and relative atomic weight (A_r) of the selected 3D dosimeters	77
C	Elemental composition for human tissues and substitutes (weight fraction (%) denoted as w_i)	78
D	Mass density (ρ) and relative atomic weight (A_r) of human tissues and human tissue substitutes	79
E	Basic statistical information on the variation of the (Z_{eff}) of the 3D dosimeters for Proton (^1H), ^4He , ^{11}B , ^{12}C and ^{16}O ions interaction	80
F	Basic statistical information on variations of electron density (N_e) of the 3D dosimeters for Proton (^1H), ^4He , ^6B , ^{12}C and ^{16}O ions interaction	81
G	Basic statistical information on the variation of the effective atomic number (Z_{eff}) of the different types of human tissues and human tissue substitutes, for Proton (^1H), ^4He , ^{11}B , ^{12}C and ^{16}O ions interaction.	82
H	Basic statistical information on electron density (N_e) of human tissues and human tissue substitutes variations for Proton (^1H), ^4He , ^6B , ^{12}C and ^{16}O ions interaction	83
I	Published scientific paper 1	84
K	Published scientific paper 2	95

CHAPTER ONE

Introduction

1.1 Introduction:

Heavy ion beams are of use in a wide range of industrial, medicine, agriculture and nuclear physics related applications such as ion implantation, radiation damage studies in reactor materials, material surface investigations, accelerator technology, and in radiotherapy. Micro- and ultra-filtration membranes can be produced by means of chemical etching of ion tracks in polymers and they have found several niches in the market since the seventies. With the help of ion track technology it is possible to produce low-cost templates for nanowires. Also, swift heavy ions can be used for electronic sputtering of metals and insulators, have studied changes in metal nanoparticle shape and size induced by swift heavy-ion irradiation.[1]

With this increasing use of charged particles in various fields, the study of their interaction with different composite materials has become an important issue for radiation physicists.

One of the most important applications of heavy charged particles is its applications in medicine, therapy and diagnosis. Interest in heavy charged particle beam therapy has gradually increased since Wilson (1946) [2] first proposed using particle beams in radiation therapy; he pointed out that the properties of specific ionization of heavy charged particles could be used for medical and biological applications [3]. Since then, heavy charged particle beams used in radiotherapy for the treatment of deep-seated and/or radio-resistant tumors, which are known to return poor prognosis in photon treatments, have included ^1H , ^4He , ^{12}C , and ^{16}O , which are considered the most relevant candidates for advancing particle therapy, and is presently available in the most advanced particle therapy clinical centers [4].

Particle therapy is a form of external beam radiotherapy using beams of energetic protons or positive ions for cancer treatment. The most common type of

particle therapy is proton therapy. Particle therapy is sometimes referred to, more correctly, as hadron therapy (that is, therapy with particles that are made of quarks). Charged Particle therapy (CPT) works by aiming energetic ionizing particles at the target tumor. These particles damage the DNA of tissue cells, ultimately causing their death. Because of their reduced ability to repair damaged DNA, cancerous cells are particularly vulnerable to attack.

For protons and heavier ions, the dose increases while the particle penetrates the tissue and loses energy continuously. Hence the dose increases with increasing depth up to the Bragg peak that occurs near the end of the particle's range. Beyond the Bragg peak, the dose drops to zero (for protons) or almost zero (for heavier ions). The advantage of this energy deposition profile is that the penetration depths of those ions can be projected to have a maximum absorption at the tumor position so that less energy is deposited into the healthy tissue surrounding the target tissue. In addition, the energies of heavy charged particle beams can be adjusted using modulating materials to treat any part of tumors within a patient. Beyond this peak, the dose deposition decreases very gradually in an exponential manner. This means that the irradiation of healthy tissue around the target tumor is significantly less during Proton and ions therapy in comparison to radiotherapy with photons where maximum dose deposition at high photon energies and therefore immediately after penetrating the body [3].

While tumor therapy with protons is well-established treatment modality with more than 60 000 patients treated worldwide, the application of heavy ions is so far restricted to a few facilities only.

It is concluded that a careful analysis of stopping power data for different tissues is necessary for radiation therapy applications, radiology, dosimetry, nuclear medicine and radiation protection as well as nuclear physics. The precision of a Monte Carlo technique for computation of ion trajectories in matter depends mainly on the precision of the calculation of the stopping power properties of the matter. A direct calculation of proton and heavy ions stopping powers in tissue is practically possible by using the SRIM computer program. Although not the only available program for the calculation of stopping powers, the SRIM code has become the de-facto standard for stopping power calculations [5]

Advances in radiotherapy in recent years have also challenged detector technology. Dosimetry studies, when the radiation is utilized to treat cancer in order to deliver a sufficient dose to target tissues without delivering excessive amount of dose that might affect the other healthy tissues is very important. In radiotherapy, dose measurement is of major significance, especially in medical practice. The accurate measurement of the dose imparted to target cells is fundamental in studies of clinical radiotherapy practice, as well as in biological effects of irradiation. Radiation dosimetry deals with methods of quantitatively determining the energy deposited in a given medium by direct or indirect ionizing radiation (IR)[6].

Dosimetry is a key component of radiotherapy that entails the measurement or calculation of a dose deposited in a given medium, in which dose is the differential energy imparted per unit mass. Dosimetry techniques are used to compare the planned (treatment planning system predicted) dose distribution to the measured dose distribution in a given volume. For a complex dose distribution, the measurement of the whole dose distribution would be preferential in evaluating whether the dose had been deposited accurately. A radiation dosimeter is a device, instrument, or system that measures or evaluates, either directly or indirectly, the quantity of exposure, absorbed dose or equivalent dose, their time derivatives (rates), or related quantities of IR [7]. To be effective, radiation dosimeters must display certain key features comprising sensitive response to dose, in which sensitivity is independent of dose rate and radiation energy, stability over time with high accuracy, and measurement precision. In other words, an ideal dosimeter offers the following main features: a distinctive accuracy and reproducible response that is independent of energy; capability of measuring the dose with a high spatial resolution; a linear response over a large dynamic range; non-disturbance of the dose to the medium; and the ability to measure the dose distribution in three dimensions. However, not all dosimeters can meet all of these requirements. Thus, the preference for a radiation dosimeter and its reader must be made systematically, with consideration of the measurement conditions the requirements [8].

According to IAEA recommendations, the dosimetry of proton beams can be performed with an ionization chamber dosimeter [9]. However, because of the steep dose gradients, dose measurements are difficult close to the Bragg peak. In addition, the ion chambers only provide point dose information and would require a large

number of them to provide two or three-dimensional dosimetric information. Therefore, 3D dosimetry techniques such as polymer gel dosimetry, has potential to be used as dosimeters for relative dose measurements to improve spatial resolution in CP Therapy, where the absorbed radiation dose distribution may be recorded in three dimensions based on the type of gel dosimeter utilized. They are manufactured from radiation sensitive chemicals that, upon irradiation with ionizing radiation, undergo a fundamental change in their physical and chemical properties as a function of the absorbed radiation dose [10]. These changes, including changes in color, transparency, and density, are measurable using different techniques [11]. Additionally, variations on the formulation of those types of dosimeters can be used to make it equivalent to soft tissue, as they are made up from elements with approximately the same density and atomic composition as tissue. As a result, the distribution of radiotherapy beams as they are scattered and attenuated or stopping by the 3D dosimeter will be the same compared to human tissue. This allows 3D dosimeters to act as a phantom for dose distribution measurements, and their physical properties (shape or form) can be changed to meet the needs for different specific purposes. To measure dose delivered in tissue, an ideal dosimeter should present tissue and/ or water-equivalent properties.

In application of 3D dosimetry, consideration of radiological properties of these materials for different types of radiation in different energy regions is a very important issue. This importance increases with the increasing use of heavy charged particles in medical applications, therapeutic and diagnostic.

There are various parameters used to characterize the materials in terms of radiation response such as mass stopping power and mass stopping cross section for electrons, protons and heavy ions, from which other parameters of dosimetric interest like effective atomic number and electron density could be derived, these help in the basic understanding of radiation interactions with multi-element materials. Effective atomic number of a multi-element material varies with respect to the atomic number of its constituent elements and the kinetic energy of the incident radiation [12], which result in different radiation interaction probabilities in different energy ranges, hence it could not be expressed with one single number as in the case of elements as pointed out by Hine [13], meaning that, at a given energy, a multi-element material

would interact with radiation in the similar way as a single element of atomic number equivalent to (Z_{eff}) of that multi-element material.

Since it is an energy dependant parameter, it could be used to evaluate radiological properties of compounds, mixtures and composites. Therefore, it is a crucial parameter giving information on how the radiation interacts with different types of materials in the entire energy region. However, the effective atomic number, (Z_{eff}), which represents a weighted average of the number of electrons per atom in a multi-element material, [14] could be used as an equivalence estimator and effective atomic number (Z_{eff}) of each material under investigation could be compared with calculated values of respective human tissues or any materials.

Early calculations of (Z_{eff}) were based on parameterization of the photon interaction cross section by fitting data over limited ranges of energy and atomic number. Today, accurate databases and interpolation programs, have made it possible to calculate (Z_{eff}) with much improved accuracy and information content over wide ranges of energy, for all types of materials [15]. Electron density (N_e) is closely related to the effective atomic number and represents the probability of finding an electron at a particular point in space. Both, effective atomic number and electron density have physical meanings and have been widely used in radiation dosimetry, radiation therapy, medical diagnosis and many technical and medical fields. For example, deviations of the physical parameters such as effective atomic number by 15–20% from their normal values can be used to estimate early detection of tumors, atherosclerosis and osteoporosis [16].

Today, it becomes a common practice to study the radiological properties of materials such as dosimeters, human tissues and phantom material, with respect to their effective atomic number and electron density, and use them as a tool for evaluation of radiation equivalence of two materials. That is water equivalence and tissue equivalence of dosimeters, human organs, human tissues and tissue substitute, and too many other substances. In the present study, we will define water equivalence and tissue equivalence of different types of 3D dosimeters and some human tissue substitutes in terms of the effective atomic number (Z_{eff}), which represents a weighted average of the number of electrons per atom in a multi-element material as mentioned before.

1.2 Problem Statement

Heavy ion therapy has the advantages of unique radiation dose profile which is very useful in medical applications, treatment and diagnosis. Many researches has been done for characterization of many materials used in these applications, such as biological materials, human tissues, and different types of dosimeters including the new type 3D dosimeters. In all these studies, experimental procedures have been followed which need advanced facilities to study these radiological properties. These facilities are not available in most research centers especially in developed countries. Instead, theoretical methods have been established to achieve this goal. This is the reasons to choice this topic of this research.

1.3 Thesis Objective

1.3.1 General Objective

The general objective of this research is investigation of the radiological properties of gel dosimeters, human tissues and tissue equivalent material with respect to their mass stopping cross section, effective atomic number and electron density in the continuous energy range from 0.01 -1000 MeV of heavy charged particle interaction of proton, Helium, Boron, Carbon and Oxygen ion, using SRIM data base.

1.3.2 Specific Objective

- To compute stopping cross-section of ions interaction with the materials under study and used it to drive effective atomic number (Z_{eff}) and electron density (N_e) of the materials.
- To Investigate effective atomic number (Z_{eff}) and electron density (N_e) variation induced by heavy charged particles passing through materials.
- To evaluate the water equivalence of 3D dosimeters in the wide energy range with respect to effective atomic number (Z_{eff}) and electron density (N_e).
- To evaluate the tissue equivalence of 3D dosimeters and tissue substitutes when interacting with the selected heavy charged particles in the wide energy range with respect to effective atomic number (Z_{eff}) and electron density (N_e).

- To provide the information for these quantities in order to achieve the best treatment and less harm to the patient.

1.4 Methodology

Monte Carlo code, SRIM- 2013 (Stopping Power and Ranges of Ions in Matter) software, is used to generate tables of the stopping power and range of Proton, ^4He , ^{11}B , ^{12}C and ^{16}O ion interactions with selected types of 3D dosimeters (Fricke gel, polymer gel and solid radiochromic polymers), human tissues, human tissue substitutes and water as a reference material, in the extended energy range from 0.01-1000 MeV. The data is used to compute stopping cross-sections of materials under study, which is used to compute the effective atomic number (Z_{eff}) using logarithmic interpolation method and the electron density (N_e) of the material is derived from effective atomic number values.

1.5 Thesis Outline

This research consist of five chapters, Chapter one is an introduction, provides a brief introduction to history and development of charged particle interactions with multi-element materials and usage in different branches of sciences specially in radiotherapy applications, for 3D gel dosimetry; followed by the problem statement, research significance and research objectives. Chapter Two presents theoretical background that covers a review of the mechanism of charged particle-matter interaction with consideration of heavy charged particle interactions, as well as theoretical background of (Z_{eff}) and (N_e) definition and their usage in radiological properties of multi-elements materials studies. Addressing water equivalence and tissue equivalence concept, and clarifying its importance in material characterization for dosimetric studies. Followed by the literature review which summarizes past and current research in the areas relevant to the thesis topic. Chapter three, is the materials and methods, include selected materials for this study, their physical properties and chemical elemental composition, Monte Carlo simulation and computational methods used to calculate mass stopping cross section, effective atomic number, electron density, and water and tissue equivalence. Part of the work presented in chapter four has been published in international journal and attached as Appendix I & K. Also this chapter entails the results and discussion of all the

computational work performed in this study. Finally, conclusion presents the major findings of this thesis, and suggested directions for future work arising from this study and concluding remarks.

CHAPTER TWO

Theoretical Background

2.1. Introduction:

This chapter summarizes and explains necessary physics on the quantities of interest for the conducted study. Section 2.2 explains interaction of charged particles with matter while section 2.3 contains four subsections. In the subsection 2.3.1, 2.3.2, 2.3.3, and 2.3.4 concentrate on heavy charged particle interactions with elements and compound include electronic, nuclear, cross section and stopping in compound. Sections 2.4 & 2.5 in which theory and computation related to the effective atomic number (Z_{eff}) and electron density (N_e) is briefly viewed. Section 2.6, viewed 3D dosimeters and in section 2.7, water and tissue equivalence are presented. Chapter is concluded with literature review, section 2.8.

2.2 Interaction of Charged Particles with Matter

2.2.1. Ionizing Radiation

Radiation is defined as the transport of energy by electromagnetic waves or atomic particles. The International Commission on Radiation Units and Measurements (ICRU) defines ionization as the liberation of one or more electrons in collision of particles with matter.[17] Radiation is classified into two main categories according to its ability to ionize matter, Direct ionizing radiations are charged particles (e.g. light electrons or heavy ions), which deposit energy in the medium through coulomb interactions with the orbital electrons of the atoms of the medium, while indirectly ionizing radiation (uncharged particles, e.g. photons, neutrons), create secondary charged particles which then deposit energy in the target medium[18].

2.2.2. Mechanism of Interaction

Charged particles passing through matter lose energy through several mechanisms when interacts with an atoms or nucleus of the material. These mechanisms depend meanly on both type and energy of the incoming particles:

Inelastic collisions with atomic nucleus: an interaction in which the incident particle is deflected by the nucleus, and a part of the particle energy goes into creating an emitted photon or into excitations of the nucleus. Elastic collisions with atomic nucleus: an interaction in which the incident particle is deflected and part of its kinetic energy is given up in imparting a kinetic energy to the targeted nucleus as required by conservation of momentum.

Elastic collisions with an atom: an interaction in which the incident particle is deflected elastically by the atom as a whole. In this interaction, energy transfer is less than the lowest energy required to remove any atomic electron from the atom.

Inelastic collisions with atomic electrons: in this interaction enough energy is transferred to one or more atomic electrons to experience a transition to higher energy state (excitation) or removed from the atom (ionization).

2.3 Interaction of Heavy Charged Particles with Matter

Charged particles may be classified as light or heavy, depending upon their masses. Electrons and positrons are called “light” particles because of their very tiny mass ($\sim 1/1840$ of mass of a proton). A charged particle is called “heavy” if its rest mass is large compared to the rest mass of an electron. Examples include protons, α -particles, and atomic nuclei (ions).

When an energetic heavy ion, passing through a medium, it immediately begins to transfer its energy to the medium system, through coulomb interactions with electrons and with atomic nuclei. The rate at which a charged particle loses energy as it passes through a material depends on the nature of both the target and the incident particles. This energy deposition is described by the ‘stopping power’ denoted $\left(-\frac{dE}{dx}\right)$. The stopping power of a material is defined as the average energy loss (dE) per unit path length (dx) which charged particle suffers when passing through a material. In practice, to stopping powers are tabulated in units of $(\text{MeV}/(\text{g}/\text{cm}^2))$. Thereby, the dependence of these quantities on the density of the medium is largely removed, with only a mild residual dependence found at high energies due to the density-effect correction. Stopping powers expressed in such

units are called mass stopping powers denoted by $-\left(\frac{1}{\rho}\right)\frac{dE}{dx}$ or $\left(\frac{1}{\rho}\right)S$, where ρ represents the density of the medium.

According to the dominant energy transfer mechanism, the stopping power can be classified into two scattering processes:

- Electronic stopping power, $S_{ele} = \left(-\frac{dE}{dx}\right)_{ele}$ arises from excitation and ionization of the target electrons, can be defined as the energy lost by the ion to the electronic system of the target atoms. Electronic stopping is the dominant process at high energies ($>1\text{MeV/nucleon}$), and
- Nuclear stopping power $S_{nucl} = \left(-\frac{dE}{dx}\right)_{nucl}$ arises from atomic collision with the target atoms

Then total stopping power $S_{tot} = \left(-\frac{dE}{dx}\right)_{tot}$ is the sum of the two components

$$S_{tot} = S_{ele} + S_{nucl} = \left(-\frac{dE}{dx}\right)_{elec} + \left(-\frac{dE}{dx}\right)_{nucl} \quad (2.1)$$

The electronic stopping force is the dominant term over a wide energy range. Nuclear stopping contributes less than 0.5 % to the total stopping force at projectile energies with corresponding particle speeds above the speed of orbital electrons in the target. However, for heavy projectiles, nuclear stopping becomes dominant for projectile speeds around and below the Bohr velocity v_0 , which corresponds to a particle energy of 25 keV/u. Radiative energy loss can be neglected for ions at energies available at medical accelerators. However, at energies above 106 MeV/u pair creation and Bremsstrahlung dominate the energy loss in heavy materials.

2.3.1. Electronic Stopping Power

The first successful attempt to derive a relation for the energy loss experienced by an ion moving in the electromagnetic field of an electron was made by Neil Bohr in 1915 [19] based on calculation of the momentum impulses of stationary, unbound electron and the impact parameter. This consideration led him to the following relation

$$\left[-\frac{dE}{dx}\right]_{Bohr} = \frac{4\pi q^2 e^4 N_e}{m_e v^2} \ln \left[\frac{\gamma^2 m_e v^3 f(Z)}{q e^2} \right] \quad (2.2)$$

Here e is the unit electron charge,

m_e is the mass of electron,

N_e is the electron number density,

Q is the charge of the ion,

v is the velocity of the ion,

$f(Z)$ is a function of the atomic number Z of the material, and

γ is the relativistic factor given by $(1 - v^2/c^2)^{-1/2}$.

This work was extended to the relativistic ions by Beth (1930) and Bloch (1933) and they solved the energy loss problem quantum mechanically in the first born approximation and derive another expression for the mass stopping power, known as Bethe-Bloch formula

$$\frac{S}{\rho} = \left[-\frac{dE}{\rho dx} \right]_{\text{Bethe-Bloch}} = 4\pi N_A r_e^2 m_e c^2 \frac{Z z^2}{A \beta^2} \left[\ln \left(\frac{2m_e c^2 \gamma^2 \beta^2}{I} \right) - \beta^2 - \frac{\delta}{2} - \frac{C}{Z} \right] \quad (2.3)$$

Where

$N_A = 6.022 \times 10^{23} \text{ mole}^{-1}$ is the Avogadro's number;

$r_e = 2.818 \times 10^{-15} \text{ m}$ is the classical electron radius;

$m_e = 9.109 \times 10^{-31} \text{ kg}$ is the rest mass of an electron;

z is the electrical charge of the ion in units of electrical charge;

ρ is the density of the medium;

A and Z is the mass number and atomic number of the medium;

I is the mean excitation potential of the medium;

$\beta = v/c$, and $\gamma = (1 - \beta^2)^{-1/2}$

This equation has been corrected for two factors that become significant at very high and moderately low energies. One is the shielding of distant electrons because of the polarization of electrons by the electric field of the moving ion. This effect depends

of the electron density (N_e) and becomes more and more important as the energy of incident particle increases. The second correction term applies at lower energies and depends on the orbital velocities of the electrons. Both of these correction terms are subtractive and represented by the symbols δ (density correction) and C (shell correction) respectively. [20]

2.3.2. Nuclear Energy Loss

As the energetic ion comes to rest in the target, it makes sufficient number of collisions with the lattice atoms. The elastic collision between the projectile ion and individual target atom is known as nuclear energy loss (S_{nuc}). The nuclear energy loss results in the creation of primary knock-on atoms (PKA). When the energy of the incident ion is sufficient to displace the lattice atom, then the displaced lattice atom is called PKA. The PKAs can in turn displace other atoms creating secondary knock-on atoms, tertiary knock-on atoms, etc thus creating a cascade of atomic collisions. The formation of PKAs leads to the distribution of vacancies, interstitial atoms and other types of lattice defects. The solution to nuclear energy loss is arrived by considering two assumptions, screened coulomb potential and impulsive approximation. The interaction potential $V(r)$ between two atoms Z_1 and Z_2 could be written in the form of a screened potential using χ as the screening function:

$$V(r) = \frac{z_1 z_2 E^2}{r^2} \chi\left(\frac{r}{A}\right) \quad (2.4)$$

If the screening potential is

$$\chi = \frac{a}{2R} \quad (2.5)$$

Where 'a' is Thomas-Fermi screening radius for collision,

$$a = \frac{0.885 a_0}{(z_1^{1/2} + z_2^{1/2})^{2/3}} \quad (2.6)$$

Where ' a_0 ' is the Bohr radius. The values of 'a' lay between 0.1 and 0.2 Å for most the interactions. In addition to Thomas-Fermi potential, the other potentials used to calculate S_{nuc} are Lenz-Jensen, Moliere and Bohr potentials. The expression of S_n is given as follows:

$$S_{\text{nucl}} = -\left(\frac{dE}{dx}\right)_n = \int_0^{\infty} T d\sigma = \int_0^{\infty} T(E, p) 2\pi p dp = 2\pi\gamma E \int_0^{p_{\text{max}}} \sin^2 \frac{\theta}{2} p dp \quad (2.7)$$

Where T is the energy transferred from an incident ion of energy E to an atom of the target material. p_{max} is the sum of the two atomic radii beyond which the interatomic potential and T, is zero. Lindhard et al. have discussed the calculation of nuclear stopping using Thomas-Fermi atoms and suggested a reduced energy coordinate system for nuclear stopping, then using Lindhard formulation to convert nuclear stopping from physical to LLS reduced units as follows:

$$S_n(\varepsilon) = \frac{\varepsilon}{\pi a_u \gamma E_0} S_n(E) \quad (2.8)$$

the reduced energy $\varepsilon = a_u M_2 E_0 / Z_1 Z_2 E^2 (M_1 + M_2)$

where a_u is the universal screening length. Then the universal nuclear stopping is calculated in reduced unit using reduced impact parameters:

$$S_n(\varepsilon) = \varepsilon \int_0^{\infty} \sin^2 \frac{\theta}{2} d(b^2) \quad (2.9)$$

For practical calculations, the universal nuclear stopping is

$$S_n(E_0) = \frac{8.462 \times 10^{-15} Z_1 Z_2 M_1 S_n(\varepsilon)}{(M_1 + M_2)(Z_1^{.23} + Z_2^{.23})} \frac{eV}{\left(\frac{\text{atom}}{\text{cm}^2}\right)} \quad (2.10)$$

With the reduced energy, ε , being calculated as:

$$\varepsilon = \frac{32,53 M_2 \varepsilon_0}{Z_1 Z_2 (M_1 + M_2) (Z_1^{.23} + Z_2^{.23})} \quad (2.11)$$

$$\text{for } \varepsilon \leq 30; \quad S_n(\varepsilon) = \frac{\ln(1+1.1383\varepsilon)}{2[\varepsilon+.0132\varepsilon^{.21226}+.19593\varepsilon^{-5}]} \quad (2.12)$$

$$\text{for } \varepsilon > 30; \quad S_n(\varepsilon) = \frac{\ln(\varepsilon)}{2\varepsilon} \quad (2.13)$$

[21].

2.3.3 Stopping of Ions in Compounds

The stopping power formula as introduced in Equation 2.3 yields values for elemental targets only. When mono-energetic ions penetrate a compound or mixture target, either Bragg's additivity rule or Core and bond (CAB) approach can be used to compute their stopping power with corrections due to chemical bonds.

2.3.3.1 Bragg's Additivity Rule

Bragg and Kleeman, in 1903, conducted stopping experiments to evaluate the dependence of alpha stopping on the atomic weight of the target, they also calculated the stopping contribution of hydrogen and carbon atoms in hydrocarbon target gases by assuming a linear addition based on the chemical composition of H and C atoms in the targets. This concept has come to be known as Bragg's Rule. [22]

Bragg's additivity rule states that the stopping of a compound may be estimated by the linear combination of the stopping powers of individual elements weighed by their weight fraction.[20]It is a simple alternative where experimental data are often lacking from which stopping powers for compounds could be extracted. According to this rule, the mass stopping power for a compound can be approximated by a linear combination of the stopping powers for the atomic constituents as follows:

$$\left(\frac{dE}{\rho dx}\right)_{\text{comp.}} = (S/\rho)_{\text{comp}} = \sum_{i=1}^n w_i (S/\rho)_i \quad (2.14)$$

$$w_i = \frac{N_i A_i}{\sum_i N_i A_i} \quad (2.15)$$

Where, $\left(\frac{dE}{\rho dx}\right)_{\text{comp.}}$ is the mass stopping power of the compound, $(S/\rho)_i$ is the mass collision stopping power of the i^{th} constituent element and w_i and N_i is the fraction by weight and number of atoms of the i^{th} constituent element respectively. [23]

For Bragg's rule accuracy, this rule is reasonably accurate, and the measurement of the stopping power of ions in compound deviates by less than 20% from those predicted by the Bragg's rule. Bragg rule is limited because the loss of energy of the electrons in any material depends on the detailed orbital structure and

excitation of the matter. Differences between the bonding in the base elemental material and the atoms in the compound can alter the transient ion charge and thus change the strength of its interaction with the target, which is assumed as drawback of this rule.[24]

2.3.3.2 Core and Bond (CAB) Approach:

Peter Sigmund [25] has developed a method to account for detailed internal motion within a medium that allows for arbitrary electron configuration in the target, and based on this work, Sabin and collaborators introduce the Core and Bond (CAB) approach for calculating stopping in compound.

CAB approach suggests that reducing each target atom to two parts: the core electrons which are unaffected by bonding and their stopping powers calculated using Bragg rule (as explained in 2.2.1), and the bonding electrons which would be evaluated depending on the chemical nature of the compound to made necessary stopping correction. The Core and Bond values may be determined by analyzing the stopping of ions over a great number of targets, and solving for the contribution from the Cores and the Bonds.

For practical use, chemical structure and phase of the compound should be known for the bond correction to be evaluated, without it, bond correction could not be carried out.

The corresponding relation for the mean excitation energy is: [26]

$$\ln I = \left[\sum_i w_i (Z_i/A_i) \ln I_i \right] / \langle Z/A \rangle \quad (2.16)$$

Where:

$$\langle Z/A \rangle = \sum_i w_i (Z_i/A_i) \quad (2.17)$$

Another expression for Bragg's additivity rule, which can be written in the form below, used by Sigmund [23]

$$-\frac{dE}{dx} = \sum_i n_i S_i \quad (2.18)$$

Where n_i and S_i are the number of atoms per volume and the stopping cross section, of the i^{th} constituent of target atoms respectively. This assumes that the stopping cross section of each species is unaffected by the state of aggregation. Hence the rule, when valid, pertains to both chemical and phase effects.

2.3.4 Stopping Cross-Section

Cross section (σ) is a fundamental quantity in radiation physics, it is a measure of probability for a reaction between a projectile and target particle to occur. It depends on strength and type of interaction between the projectile and target, and has the dimension of area. The interaction probability for a particle passing perpendicular through mater is directly proportional to the cross section (σ). The conventional unit of cross section is barn (b) with $1 \text{ b} = 10^{-24} \text{ cm}^2$.

In the experimental literature, the energy loss of charged particles is often described in terms of the stopping cross section (in units of 10^{-15} eV cm^2). The stopping cross section is usually denoted by the symbol σ , and is related as follows to the mass collision stopping power (in $\text{MeV cm}^2/\text{g}$):

$$\sigma(E) = 10^{21} (M_A/N_A) \frac{1}{\rho} S_{\text{col}}(E) \quad (2.19)$$

The mass stopping power is proportional to the total molecular interaction cross section of compound material through the relation:

$$\sigma_{\text{total}} = \frac{M}{N_A} \left(\frac{S}{\rho} \right)_{\text{comp}} \quad (2.20)$$

Where $M = \sum_i n_i A_i$, is the molecular weight of the compound, N_A is the Avogadro's number, n_i is the total number of atoms of the constituent element, and A_i is its atomic weight.

For any compound, a quantity called the effective atomic cross section σ_a , is defined from above equation. The total atomic cross section can be obtained by dividing the mass stopping power S/ρ (cm^2/g) of the compound by the total number of atoms present in one gram of that compound as follows,

$$\sigma_a = \frac{(S/\rho)_{\text{comp}}}{N_A \sum_i w_i/A_i} \left(\frac{\text{barn}}{\text{atom}} \right) \quad (2.21)$$

Where N_A is the Avogadro's number, w_i and A_i are the fraction by weight and the atomic weight of the constituent element i . Here $N_A \sum_i w_i/A_i$ is the total number of atoms of all types present in the compound as per its chemical formula.[27]

2.4 The Effective Atomic Number (Z_{eff})

2.4.1 Theoretical Background

The atomic number Z is a very important parameter in radiation physics and in nuclear and atomic physics, which occur in almost any formula. Hine (1952) [13] first appoints out that for a multi-elements medium, composed of several elements, such as biological materials, plastics, alloys, etc., a single number similar to that of atomic number of elements, cannot represent the effective atomic number of a multi-element material due to the different partial interaction processes at different energy regions and the various atomic numbers present in the compound have to be weighted differently. The effective atomic number (Z_{eff}) is a convenient parameter for representing characteristics of multi- element materials with respect to their radiation interaction depending mainly on atomic number of its constituent elements [12] which result in different radiation interaction probabilities in different energy ranges - and the energy of incident radiation, hence it could not be expressed with one single number. The idea of this coefficient is to assume that, a compound or mixture can be considered as a single element characterized by atomic number equals to effective atomic number (Z_{eff}) which is not constant, it varies with incident radiation or particle energy, so (Z_{eff}) could be used as a parameter for characterizing response of materials to ionizing radiation, especially in dosimetry, biology, medicine, radiation shielding, etc. In fact, the value of this parameter can provide an initial estimation of the chemical composition of the material. It is very useful in choosing a substitute composite material in place of an element or a material at a given energy depending on the requirements [28]. In addition, the energy absorption in the given medium can be calculated by means of well-established formulae if certain constants such as (Z_{eff}) and (N_e) of medium are known. For many applications, for example in radioisotope monitoring, cross-section studies of absorption, scattering and attenuation of electromagnetic radiation, testing of multi-component, heterogeneous and composite materials etc., this parameter is of principal significance. The effective atomic number also finds its utilization in the

computation of some other useful parameters, namely the effective dose and buildup factor [29]. The effective atomic number (Z_{eff}) is closely related to another important quantity, the electron density which will be discussed in the next section (2.4). The (Z_{eff}) and (N_e) represent the effective number of electrons per atom and per unit mass of the material respectively.

2.4.2 Methods of Calculation of the Effective Atomic Number

The effective atomic number (Z_{eff}) is calculated using atomic number of the constituent elements, weighed according to different interactions process of ionizing radiation. Commonly this method is based on determination of total mass stopping power cross-section for charged particle interaction. Early calculations of (Z_{eff}) were based on parameterization of the photon interaction cross section by fitting data over limited ranges of energy and atomic number. Today, accurate databases and interpolation programs, have made it possible to calculate (Z_{eff}) with much improved accuracy and information content over wide ranges of radiation energy, and for all types of materials. [29]

Different theoretical methods have been used to calculate effective atomic number for the selected composite materials, which have been discussed as follows:

2.4.2.1 Atomic to Electronic Cross-Section Method

The effective atomic number (Z_{eff}) of the selected composite materials is given by the ratio of atomic cross-section (σ_a) to the electronic cross-section (σ_e). Hence, it has been computed using following expression:

$$Z_{\text{eff}} = \frac{\sigma_a}{\sigma_e} \text{ (Dimensionless quantity)} \quad (2.22)$$

Where, (σ_a) is the atomic cross section and (σ_e) is the electronic cross section.

The (S/ρ) computed in the previous chapter for different types of materials, were further used to compute molecular cross-section given by:

$$\sigma_m = \frac{\left(\frac{S}{\rho}\right)_{\text{compositematerialial}}}{N} \sum_i n_i A_i \quad (\text{barnn/molecule}) \quad (2.23)$$

Where, n_i is the total number of atoms in the molecule, A_i is the atomic weight of the i^{th} element in the molecule and N is Avogadro's number. Then the atomic cross section (σ_a) can be computed using the following relation:

$$\sigma_a = \frac{\sigma_m}{\sum_i n_i} \quad (\text{barn/atom}) \quad (2.24)$$

Further, the electronic cross section (σ_e) can be given as:

$$\sigma_e = \left(\frac{1}{N}\right) (\sum f_i A_i) \left(\frac{S}{\rho}\right)_i \quad (\text{barn/electron}) \quad (2.25)$$

Where, f_i is the fractional abundance of atoms of i^{th} element present in the molecule of the selected composite materials. It can be defined as the ratio of number of atoms of i^{th} type to the total number of atoms present in the molecule and $(S/\rho)_i$ is the mass stopping power of the i^{th} element present in the molecule of the selected composite materials.[30]

2.4.2.2 Logarithmic Interpolation Method

As the materials are composed of various elements it is assumed that the contribution of each element of the compound to total mass stopping power interaction is additive, yielding the well-known mixture rule that represents the total mass stopping power of any compound as the sum of the appropriately weighed proportions of the individual atoms (see section of this chapter). The mass stopping power is proportional to the total molecular interaction cross-section through the relation

$$\sigma_m = \left(\frac{M}{N_A}\right) \left(\frac{S}{\rho}\right)_{\text{material}} \quad (2.26)$$

Where $\left(\frac{S}{\rho}\right)_{\text{material}}$ is the mass stopping power of the material, $M = \sum_i n_i A_i$ is the molecular weight of the material, $N_A = 6.022 \times 10^{23}$ is the Avogadro's number in atoms.gram⁻¹, n_i is the total number of atoms of the constituent element, and A_i is its atomic weight. For practical consideration, the total atomic cross section could be calculated from [31]

$$\sigma_a = \frac{1}{N_A} \frac{(S/\rho)_{\text{material}}}{\sum_i w_i/A_i} \quad (2.27)$$

Where w_i is the weight fraction of the constituent element i , and $\sum_i w_i/A_i$ is the total number of atoms present in the molecule. For calculating the cross section of the material from this equation, it is clear that an averaging is carried out over atoms of all elements in compound. The mass stopping cross section values of the selected composite materials so obtained were then interpolated in the mass stopping cross section values of elements in the energy range specified to compute the effective atomic number (dimensionless quantity) using the following logarithmic interpolation formula:

$$Z_{\text{eff}} = \frac{Z_1(\log\sigma_2 - \log\sigma) + Z_2(\log\sigma - \log\sigma_1)}{(\log\sigma_2 - \log\sigma_1)} \quad (2.28)$$

where σ_1 and σ_2 are the elemental cross-section (barn/atom) in between which the atomic cross-section σ_a of the multi element material lies, and Z_1 and Z_2 are the atomic numbers of the elements corresponding to the cross sections σ_1 and σ_2 , respectively. [32]

2.5 Effective Electron Density (N_e)

The number of electrons per unit mass is an important quantity that enters into many calculations in radiation, nuclear and atomic physics. It is the basic quantity required to determine the penetration of ionizing radiation in matter. This quantity known as electron density, abbreviated as (N_e). According to the quantum mechanics the position of an electron can be explained only statistically, so this quantity tell us the relative probability of finding an electron at a particular point in space. Electron density has units of (electrons/g), and related to another important quantity, effective atomic number, both play essential role in characterizing multi-element materials (compounds, composites and mixtures) and their interaction with ionizing radiation.

2.5.1. Electron Density for Elements

The number of atoms or electrons per unit mass of element can be obtained from the Avogadro constant, N_A , which has the value, $N_A=6.022 \times 10^{23} \text{ mol}^{-1}$. From definition of the Avogadro constant, one has

$$\text{Number of atoms per unit mass} = N_A/A \quad (2.29)$$

$$\text{Number of electrons per unit mass} = N_A Z/A = N_e \quad (2.30)$$

Where A is the atomic weight, Z is the atomic number and N_e is the electron density.

Low and medium Z elements have about the same number of protons and neutrons, so N_e is about one-half the Avogadro's number. So all elements have the same electron density of about 3×10^{23} electrons/gram, with the exception of Hydrogen.

2.5.2. Electron Density for Chemical Compounds

The molecular mass, M of the compound is given by

$$M = \sum n_i A_i \quad (2.31)$$

Where A_i and n_i are the atomic mass and the number of atoms of the i^{th} constituent element in the compound respectively. Replacing atom mass of element with the molecular mass of the compound in equation (2.2)

$$\text{No. of molecules per unit mass} = N_A/M = N_A/\sum n_i A_i \quad (2.32)$$

When dealing with electron density one can calculate the average electron density $\langle N_e \rangle$ which is single valued parameter or an effective electron density (N_e) which depends on the energy of incident radiation energy.

2.5.2.1. Average Electron Density $\langle N_e \rangle$

Generalizing equation 2.2 for chemical compound, using Z and A of the compound, we have the following formula for the average electron density:

$$\langle N_e \rangle = N_A \frac{\sum_i n_i Z_i}{\sum_i n_i A_i} = N_A \frac{\langle Z \rangle}{\langle A \rangle} = \frac{N_A}{M} \sum_i n_i Z_i \quad (2.33)$$

Where $\langle Z \rangle$ is the mean atomic number, and $\langle A \rangle$ is the mean atomic weight of compound. Since the ratio $\langle Z \rangle/\langle A \rangle$ is about 1/2 which means that $\langle N_e \rangle$ has a single value which is approximately equal to 3×10^{23} electrons/g for any material [29].

2.5.2.2. Effective Electron Density (N_e)

The effective electron density N_e is the quantity that tell us the relative probability of finding an electron at particular point in space, and could be defined in

terms of the effective atomic number, Z_{eff} where it is assumed that the actual atoms of a given molecule can be replaced by an equal number of identical atoms, each of which having Z_{eff} electrons. Substituting for Z and A for a compound in equation (2.5.2) we have:

$$N_e = N_A \frac{nZ_{\text{eff}}}{\sum_i n_i A_i} = N_A \frac{Z_{\text{eff}}}{\langle A \rangle} \quad (2.34)$$

Where $n = \sum_i n_i$ is the total number of atoms in the molecule. This equation show that N_e is directly proportional to Z_{eff} which means that N_e varies with incident charged particle energy in the same way as that of Z_{eff} . Note that $\langle A \rangle$ can be calculated in term of weight fractions (w_i) of constituent elements of the compound

$$\langle A \rangle = \sum_i w_i A_i \quad (2.35)$$

with condition $\sum_i w_i = 1$

High values of N_e mean more number of electrons per unit mass of the compound which leads to greater probability of interaction with ionizing radiation.

More general relations can be obtained in term of the atomic percent (molar fraction) of each element instead of n_i which have an integer value.

For a chemical compound the molar fraction, f_i of i^{th} element is defined as: $f_i = n_i/n$, where $\sum_i f_i = 1$

$$\langle N_e \rangle = N_A \frac{\sum_i f_i Z_i}{\sum_i f_i A_i} = N_A \frac{\langle Z \rangle}{\langle A \rangle} \quad (2.36)$$

$$N_e = N_A \frac{Z_{\text{eff}}}{\sum_i f_i A_i} = N_A \frac{Z_{\text{eff}}}{\langle A \rangle} \quad (2.37)$$

Which are valid for all types of materials, mixtures as well as compounds [29].

2. 6 Three Dimension (3D) Dosimeters

Polymer gel Fricke gel and solid radiochromic polymer dosimeters are technique being developed to meet challenges in measuring the radiation dose

distributions in three-dimensional space. The accurate quantification of radiation dose absorbed by the medium is the fundamental requirement in radiation physics generally and particularly, when the radiation is used for medical purpose. 3D dosimeters hold great promise for the future of radio therapy treatment planning and dosimetry. 3D dosimeter could be defined as a dose measurement device, which can record the 3D dose distribution in a continuous medium. The 3D radiation dosimeters are derived from radiation-sensitive materials that undergo transformations in their physical and chemical properties upon irradiation, as a basis for absorbed radiation dose. These transformations, including changes in color, transparency, and density, are measurable.[33] The response of a model 3D dosimeter is supposed to be firm, explicit, measurable, and reproducible. The following 3D dosimeters are currently available commercially or in research laboratories: The Fricke gel dosimeter (FGD), the polymer gel dosimeters (PGD) and the solid radio chromic polymer dosimeters often called (SPD).[34].

2.6.1 Fricke Gel Dosimeters

The Ferrous Sulphate dosimeters have been proposed by Fricke and Hart in 1966. The initial formulation was not a gel, but a solution consists of 1mmol/L ferrous sulphate (Fe SO_4), 1 mmol/L NaCl and 0.4 mmol/L sulfuric acid. Fe^{2+} ions of the Fricke solution are oxidized to Fe^{3+} ions when irradiated with ionized radiation, was capable of recording the dose in a 3D space [35].

In 1984, Gore J. C. et al demonstrated that changes of irradiated Fricke dosimetry solutions when Fe^{2+} ions converted to Fe^{3+} ions could be measured using nuclear magnetic resonance which then leads to that, by fixing the ferrous ions in a gel matrix (Gelatine, agarose, sephadex and polyvinyl alcohol (PVA), three dimensional (3D) spatial dose could be obtained using Magnetic Resonance Imaging (MRI). Fricke gels have been applied to study many dosimetric situations in the clinic including 3D conformal treatment planning, radiosurgery, brachytherapy and proton therapy. Fricke gels are currently available that measure doses of between 25 Gy and 30 Gy.

2.6.2 Polymer Gel Dosimeters (PGD)

Most of the polymer gel dosimeters are fabricated by radiosensitive monomers in gelatin matrix under normal atmospheric conditions. Upon irradiation, free radicals are generated in the gel medium making the monomers active. Activated monomers form the polymer network. The polymerization of the monomers causes a change in the molecular structure and the mass density which leads to an alteration of the mechanical, optical, and magnetic properties. Absorbed dose of the radiation is correlated with the amount of polymerization which can be evaluated or 'read-out' in many ways, including using magnetic resonance imaging (MRI), optical computer tomography (OCT), UV-visible spectrophotometer, ultrasound computed tomography (UCT) and Raman spectroscopy. [37]

Gel dosimeters have several useful advantages that make them highly desirable in radiotherapy dosimetry:

- Gels are tissue equivalent, they are composed of elements with the same density and atomic composition as tissue, and the distribution of energy deposited in gel is highly similar to human tissue, allowing use as both a dosimeter and phantom at the same time.
- Gels permit the formation of a three-dimensional image of the incident dose distribution. The degree of polymerization is dependent on the amount of incident radiation. By comparison, other techniques such as ionization chambers and radiochromic films are only capable of dose measurements at points or 2D planes.
- Variations on the formulation of the gel can be made to be suitable for any specific applications.
- Gels can be shaped to model various parts of a patient's anatomy.
- Gels are relatively energy independent.

Polymer gels do have several limitations. Firstly, they are sensitive to oxygen, which inhibits polymerization and thus reduces the sensitivity of the gel to radiation-induced polymerization. Secondly, polymer gels are not user-friendly as other dosimetry techniques, particularly as some of the chemicals they are composed of are hazardous to humans unless special precautions are taken. Polymer Gel

Dosimeters can be categorized into two main types, hypoxic and normoxic gel dosimeters.

2.6.2.1 Hypoxic Gel Dosimeters

Acrylamide-based polymer gel with N,N-methylene-bis-acrylamide (bis) monomers infused in aqueous agarose matrix. This type of PGD is known as PAG, have relatively stable post irradiation dose distribution, do not have diffusion limitations of Fricke gels. Many formulation of PAG (polyacrylamide gelatine) dosimeters where studied such as: BANG (bis-acrylamide nitrogen gelatine) with multiple formulations such as BANG-1, which made with powdered acrylamide and BANG-2 that made by using acrylic acid as monomer, PABIG (polyethylene glycol diacrylate bis gelatin) with reduced toxicity, and VIAR (N-vinyl pyrrolidone argon gel) [36]. Main disadvantage of this type, its high sensitivity to the oxygen contamination, which necessitate a hypoxic environment for the manufacturing.

A solution to this problem was the introduction of polymer gels with much-reduced sensitivity to oxygen known as Normoxic gel dosimeter.

2.6.2.2 Normoxic Gel Dosimeters

Normoxic PGD is composed of five chemical components: water, gelatin, monomer, catalyzer, and oxygen scavenger. [37] Oxygen scavenger is added to make PGD more resistant to oxygen contamination. Usually, we can group this type into two groups. Those with methacrylic as a monomer are called MAGAT/nMAG and those with acrylamide are called PAGAT/nPAG. There are many variations of those depending on the chemical agents. The first of these was called MAGIC (methacrylic acid, ascorbic acid in gelatin initiated by copper), which do not need an oxygen free environment to be prepared. HEAG (hydroxy-ethyl-acrylate gel), MAGAS (methacrylic acid, gelatin gel with ascorbic acid, MAGAT (methacrylic acid, gelatin gel and tetrakis hydroxyl methyl phosphonium chloride, PAGAT (polyacrylamide, gelatin and tetrakis hydroxyl methyl phosphonium chloride), and ABAGIC (ascorbic acid, bis-acrylamide, in gelatin initiated by copper) are different formulations of this type which will be studied in this thesis. [37]

2.6.3 PRESAGE™ Dosimeters

PRESAGE is a new type of 3D dosimeters often known as solid radiochromic gel dosimeter (SPD). Some plastic material such as polydiacetylene polymerizes when it interacts with radiation, the radiation causes copolymerization of the monomers and the change of color at the same time. The first 3D radiochromic dosimeter based on polyurethane with leuco-dye leucomalachite green (LMG), an alkyl diisocyanate prepolymer and a hydroxyl reactive polyol. The radiation sensitivity was enhanced by adding chemical catalyzer such as chloroform. [37] This dosimeter is available commercially, has a good temporal stability, linear dose response and is machinable to a variety of shapes. Commercial product which was developed by many companies made the production of SPD is directly obtained. Previous investigations show that PRESAGE has promising potential for particle dosimetry. Similar to 3D polymer gel dosimeters, PRESAGE can show saturation at the Bragg peak of high LET radiation such as protons. Basic studies on a new formulation of PRESAGE[®], developed for proton dosimetry, show promising results with respect to the saturation characteristics of high LET radiation for beam energies of 79 MeV and 153.2 MeV. [39] PRESAGE is not suitable for MRI evaluation but it contains leuco dyes which have a maximum absorbance at a wave length of 633 nm therefore it is suitable for evaluation with a He-Ne laser optical scanning system[35].

2.7 Water and Tissue Equivalence for Multi-element Materials

2.7.1 Tissue Equivalence for Multi-element Materials

Simulation of radiation dose distribution in human organs and tissues is done by tissue-equivalent materials. The tissue equivalent materials are used as tissue substitutes for various organs of the human body, having similar properties with respect to ionizing radiation interactions. Tissue substitutes are made of low-atomic-number materials (H, C, N, O, F, Cl, etc.).

The dosimetric and tissue equivalent properties of materials make them very useful in clinical applications such as radiological examinations and treatment planning. Since high doses, are sometimes used in radiation therapy, experiments are

done with water and tissue equivalents in order to get prior estimation about how radiation interacts with the real target [40]. The fundamental advantage of tissue equivalent materials is that they allow the absorbed dose to be determined when information on the energy and nature of the charged particles at the point of interest is incomplete. Since tissue equivalence describes the property of the material to respond to radiation in the same way as human tissue, phantoms made with tissue substitutes are widely used in medicine, radiation therapy, diagnostic radiology, radiation protection, and radiobiology to calibrate radiation detector systems and for depth-dose estimates. [41]

ICRU report 44 describes various types of tissue substitutes for human organs and tissues for diagnostic and therapeutic radiology, research, nuclear engineering, nuclear physics, health physics, radiation physics, medical physics, radiation dosimetry and radiation protection. This report states "Tissue substitutes are often mixtures formulated so that their radiation interaction properties rather than their atomic composition, match those of the body tissue to the degree necessary for the specific application". [42] Similarly, radiation detectors due to operational and construction requirements (such as electrical conductivity, stability, mechanical strength, and shape construction) are rarely made of components with identical composition to tissue. The IR interaction parameters like interaction cross section (σ), effective atomic number (Z_{eff}), and electron density (N_e) give the information about the elemental constituents and their proportion in the material. Hence, these parameters are very useful in choosing a substitute composite material in place of a tissue for a given energy depending on the requirement [41].

In the present study, we will define tissue equivalence in terms of the effective atomic number, (Z_{eff}), which represents a weighted average of the number of electrons per atom in a multi-element material. Early calculations of (Z_{eff}) were based on parameterization of the photon interaction cross section by fitting data over limited ranges of energy and atomic number. Today, accurate databases and interpolation programs have made it possible to calculate Z_{eff} with much improved accuracy and information content over wide ranges of IR energy, and for all types of materials [43].

The subject of tissue references is comprehensively discussed in ICRU report #44 and a report by the ICRP [180]. These reports identified the most important tissues needing simulation as muscle, adipose tissue and the skeleton. Together these make up over 70% of the body mass. Lung tissue is also important due to its large density difference. Muscle includes the connective tissue, blood vessels, blood, lymph, etc., generally associated with skeletal (striated) muscle [42]. ICRU report 44 identifies a composition called muscle (skeletal, ICRU, 1989) as the recommended muscle composition.[44]

For a given tissue substitute the quality of the tissue substitute depends on the type and energy of the radiation under investigation, so, tissue equivalence requires that the mass collision stopping powers of charged particles in the counter and the interaction cross section of the counter materials are identical to tissue. This requirement is fulfilled by utilizing materials with elemental compositions approaching that of standard muscle tissue as specified by ICRU report 44[45].

To facilitate the formulation of tissue substitutes for a wide range of applications (e.g., dosimetric phantoms, radiographic test objects, dosimeter components, etc.), a procedure has been proposed for photon interactions. This procedure involves the calculation and comparison of (Z_{eff}) of the material (to be used as tissue substitute material) with the present human organ/tissues in the extended energy region 1 keV–100 GeV, as described by Manohara et al.[46] For photons, (Z_{eff}) of the material should match as closely as possible to that of the human organ/tissues to be irradiated.

To measure dose delivered in tissue, an ideal dosimeter should present tissue- or water-equivalent properties. For dosimetry of proton beams, it should have a similar electronic mass stopping power and secondary particle production to tissue or water. Different methods have been used to investigate tissue and water equivalency of different materials for proton therapy, such as: calculation of the number of protons and fluence correction factors, absorbed dose, CT Hounsfield numbers, flux and water-equivalent depth, dose delivered by secondary neutrons. [45]

The increasing need for dedicated 3D quality assurance tools in modern radiation therapy is the main motivation behind the development of accurate and user-friendly 3D dosimetry tools. This development consists of two major parts: the

development of optical CT readout systems which is expected to facilitate the usability of 3D dosimeters by radiotherapy centers and the development of accurate and reliable 3D dosimeters able to record the radiation dose distribution [47].

2.7.2 Water Equivalence for Multi-element Materials

Since, water equivalency property is a major concern in radiation dosimeter, it is necessary to evaluate water equivalency for any medium which has to be used as an alternative for water. A method is described which determines the radiological equivalence of different materials by comparing their macroscopic photon and charged particle interaction parameters over the energy range of interest. This method has been applied to materials used for radiation dosimetry.

Dose protocols for radiotherapy (eg. IAEA 1997) recommended calibrations be expressed in terms of dose to water. Therefore, it is desirable for the composition of a dosimeter to be similar to that of water, so that (i) correction factors are not necessary and (ii) the beam is not perturbed by the presence of the dosimeter. If two materials have similar attenuation and absorption coefficients for photon beams, and stopping powers and scattering powers for charged particle beams, over the energy range of interest, then the particle transport and hence dose deposition will be similar throughout the volume.[48]

Phantoms are constructed from materials having good tissue equivalence with respect to absorption of ionizing radiation. Water is the standard phantom material for dosimetry measurements of IR, dosimetric measurements are often carried out in more practical solid materials, such as polystyrene, Lucite, A-150 tissue equivalent plastic, Solid Water (WT1), Solid Water (RMI-457), Plastic Water or Virtual Water. For a phantom to be water equivalent for charged particle dosimetry, it must match the linear stopping power and the linear scattering power of water. This is approximately achieved if the phantom material mimics water in terms of three parameters: mass density, number of electrons per gram and effective atomic number that depends on the atomic composition of the mixture as well as on the type and quality of the radiation beam.[49]

2.8 Literature Review

Effective atomic number (Z_{eff}) has proved to be a convenient parameter for representing the attenuation and stopping of ionizing radiation by a complex medium and particularly for the calculation of the dose in radiotherapy since 1981 by Daphne F. Jackson and D. J. Hawkes [50]. In 1946, Spiers F.W. et al [51], has extended the concept of effective atomic number and discussed energy absorption in biological tissues. Hine (1952) [13] suggests that, Z_{eff} varies with energy of incident radiation and could not be represented by single number in the extended energy range.

D.R. White (1978) [52] has study tissue substitute in experimental Physics and introduce the concept that (Z_{eff}) is to describe the properties of the composite materials in term of an equivalent element, since that time too many studies on (Z_{eff}) have been undertaken.

Now a days Literature is rich in studies dealing with calculation of effective atomic number (Z_{eff}) and electron density (N_e) for photons and electrons in biological materials and other compounds. Manjunatha guru and Umesh 2006 [53] have calculated effective atomic number (Z_{eff}) and electron density of some biologically important compounds containing H, C, N and O in the energy range 145–1330 keV, in semiconductors (Cevik et al. 2008) [54], in solutions (Kurudirek 2011) [55], in tissues from human organs (Manjunatha and Rudraswamy 2013) [56], in alloys (Han et al. 2012) [57], in dosimetric materials (Un 2013) [58] and in some polymers (Kucuk et al. 2013) [59]. White 1971 [60] have calculated the effective atomic number (Z_{eff}) of fat, muscle and bone for photons and with a restriction to the Z exponents and their variation with energy.

For gel dosimeters, Taylor M. L. et al. have calculated (Z_{eff}) for electron interaction in the energy range from 10 KeV to 100 MeV [61], and for photon interaction in the energy region of 10KeV to 10MeV. Studying the variation of (Z_{eff}), which is equivalent to taking into account the variation of mass attenuation coefficients with photon energy, it is found that gels typically match water better than water matches human tissues. As such, the differences in effective atomic number between water and gels are small and may be considered negligible.

Consideration of the mean disparity over a large energy range shows, broadly, BANG-1 to be the most water equivalent gel [38]. Also, (Z_{eff}) of a large number of biological and dosimetric materials for total electron interaction has been investigated in the wide energy region 10 keV–1 GeV by Kurudirek M. [62]. However studies on (Z_{eff}) and (N_e) for different types of radiations are rarely available.

Early trials to calculate (Z_{eff}) and electron density (N_e) for ion interaction was done by B. V. Thirumala Rao et al. (1985) [63], he reported a method for derivation of (Z_{eff}) from the cross section data of the constituent elements, where (Z_{eff}) can be read directly from a plot of stopping power expressed per atom Vs. elemental atomic number. Later, Parthasaradhi K.[64] used this method reported by B. V. Thirumala Rao to study (Z_{eff}) of biological materials include bones, muscles, spleen, liver and water, in the energy region 1-50MeV for photons, electrons and ^4He ions interaction. He found that (Z_{eff}) for photons and electrons increases as energy increases while it remain the same for ^4He ion.

Prasad et al.[65] have calculated effective atomic numbers for interaction of photons (1-50MeV), electrons (1-50MeV) and protons (1-200MeV) in multi-element materials such as bone cortical, muscle striated, water, polystyrene, Perspex and Nylon-6. He found that effective atomic number (Z_{eff}) for partial interaction of photons and electrons, remain the same, whereas the number for the total interactions increases as energy increase. For total proton interaction the number remains more or less the same. The (Z_{eff}) of biological materials have been studied in the energy region 1–50 MeV for photons, electrons and ^4He ions and it has been found that, in agree with later study, the (Z_{eff}) for photons and electrons increases with energy, and remains, about the same for ^4He ions [66]. However, those studies have been done for a limited number of materials and within a limited energy ranges. A study has been performed by Taylor , M. L.[67] based on (Z_{eff})s for electron interactions with TLD-100 and TLD-100H thermo luminescent dosimeters and investigated the influence of dopant concentrations and impurities on (Z_{eff}).

Now a days there is a renewed interest in studying of effective atomic number (Z_{eff}) and electron density (N_e) for charged particles interaction, and using them as a tool to investigate the radiological properties of compounds such as water and tissue

equivalence of different types of materials. Effective atomic number (Z_{eff}) of a large number of biological and dosimetric materials for total proton interaction has been investigated in the wide energy region 10 keV–1 GeV by Kurudirek M. [68].

Study for shielding materials was done by Kurudirek M.[69]. Murat Kurudirek (2016) [70] has perform a comparison of some biological materials with respect to the water and tissue equivalence properties for photon, electron, proton and alpha particle interactions as means of the effective atomic number (Z_{eff}) and electron density (N_e), using a Z-wise interpolation procedure that has been adopted for calculation of (Z_{eff}) using the mass attenuation coefficients for photons and the mass stopping powers for charged particles. In his study a comparison of (Z_{eff}) and (N_e) for different types of radiation such as photons, electrons, protons and alpha particles (heavy ions) in the energy region 10 keV–1 GeV has been performed.

Some gel dosimeters, water, human tissues and water phantoms were investigated with respect to their radiological properties in the energy region 10keV–10MeV. The effective atomic numbers (Z_{eff}) and electron densities (N_e) for some heavy charged particles interaction such as protons, ^4He ions, ^{11}B ions and ^{12}C ions have been calculated for the first time for Fricke, MAGIC, MAGAT, PAGAT, PRESAGE, water, adipose tissue, muscle skeletal (ICRP), muscle striated (ICRU), plastic water, WT1 and RW3 using mass stopping powers from SRIM Monte Carlo software. Two different set of mass stopping powers were used to calculate Z_{eff} for comparison. The water equivalence of the given materials was also determined based on the results obtained. Two different approaches namely CAB and Bragg's additivity rule were used to calculate mass stopping powers. Then, two different set of mass stopping powers were used to calculate (Z_{eff}) for comparison. This study has been done by Kurudirek M. (2015). [71].

Commonly used nuclear physics materials such as water, concrete, Pb-glass, paraffin, Freon and P 10 gases, some alloys such as brass, bronze, stainless-steel and some scintillators such as anthracene, stilbene and toluene have been investigated with respect to the heavy charged particle interaction as means of projected range and effective atomic number (Z_{eff}) in the energy region 10 keV-10 MeV. Calculations were performed for heavy ions such as H, C, Mg, Fe, Te, Pb and U, and (Z_{eff}) is calculated using logarithmic interpolation method.[1]

The effective atomic numbers (Z_{eff}) of different types of materials such as tissues, tissue equivalents, organic compounds, glasses and dosimetric materials have been calculated for total proton interactions in the energy region 1 keV–10 GeV. Also, effective atomic numbers relative to water ($Z_{\text{eff RW}}$) have been presented in the entire energy region for the materials that show better water equivalent properties. Some human tissues such as adipose tissue, bone compact, muscle skeletal and muscle striated have been investigated in terms of tissue equivalency by comparing (Z_{eff}) values and the better tissue equivalents have been determined for these tissues [62].

For the first time, effective atomic numbers (Z_{eff}) and electron densities (N_e) of some essential biomolecules such as fatty acids, amino acids, carbohydrates and nucleotide bases of DNA and RNA have been calculated for almost all types of ionizing radiation using the logarithmic interpolation method in the energy region 10keV-1 GeV. Variation of (Z_{eff}) and (N_e) with kinetic energy of charged particles and effective photon energy have been studied for total electron interaction, total proton interaction, total alpha particle interaction and multi-energetic photons Also, variation of (Z_{eff}) with weight fractions of H and O elements has been studied [72].

In 2015, Kurudirek M. et al. [73] has investigated (Z_{eff}) of some dosimetric materials just like water, CaF, air, Adipose tissue, bone compact, plastic scintillator and too many others in the energy range of 10 KeV-1GeV of electrons, protons and Alpha particles using direct method and compare his results to those obtained using logarithmic interpolation method, he found that (Z_{eff}) values using both methods generally agreed well with each other in the high energy region above 10 MeV for proton and Alpha particles.

For the first time, a study of effective atomic numbers and electron densities of some vitamins for electron, proton, ^4He and ^{12}C ion interactions in the energy range from 10KeV to 1GeV, have been done by Buyukyildiz M.[74] using logarithmic interpolation method. Significant variations of (Z_{eff}) have been observed for all types of interaction throughout the entire range of energy.

No studies have been performed for most of heavy charged particles such as ^4He , ^{12}C and ^{16}O ions, for biological and dosimetric materials in a wide range of energy, most calculations are conducted in small range of energy and have done for a

limited number of substances, which motivate conducting studies for charged particles as general.

CHAPTER THREE

Materials and Methods

3.1 Materials

3.1.1 Elemental Composition of the 3D Dosimeters

The chemical composition for selected gel dosimeters studied include different 3D dosimeter formulations including six normoxic gel formulations (HEAG, MAGAS, MAGAT, MAGIC, PAGAT, ABAGIC), and four hypoxic polymeric gels (BANG-1, BANG-2, PABIG, and PAG), BRESAGE, PREAGE® (for proton), Fricke gel dosimeters, and water. The data for normoxic, hypoxic polymeric gels and Fricke gel has been taken from the literature, [77]. Also, data for PRESAGE and PREAGE® are taken from references [78] and [79] respectively. The elemental compositions (weight fraction (%) of elemental components) of the selected 3D dosimeter are given in appendix A.

Also mass density (ρ) and relative atomic weight ($\langle A \rangle$) of the selected 3D dosimeters have been calculated using equation (2.34) and shown in appendix B.

3.1.2 Elemental Composition of the Human Tissues and Substitutes

The chemical composition of human tissues is of great importance in the study of micro-distributions in the treatment of human radiation. The chemical composition of human tissues is usually given in terms of biological molecules (eg, protein, fat, vitamins, etc.), and they are not readily adaptable to dosimetry calculations. In the usual energies of machine therapy, the effects of molecular association are negligible, and one can represent human tissue through its atomic structures (% by weight of elements. [80] Each tissue consists of basic elements are H, C, O, N, and some other elements such as P, S, Cl, K, etc. Therefore, the knowledge of the ratios of these elements is important to calculate the mass stopping power for heavy ion in the tissues as well as the density of the tissue. The elemental composition (weight fraction of tissue components), of the selected human tissues (Adipose Tissue (ICRP ICRU-103), Muscle, Skeletal (ICRP ICRU-201), Muscle, Striated (ICRP ICRU-202), Bone, Compact (ICRU-119), Bone, Cortical (ICRP-099),

MS₂₀ Tissue Substitute (ICRU-200), Muscle Equivalent Liquid with Sucrose (ICRU - 203), Muscle Equivalent Liquid Without Sucrose (ICRU - 204), B-100, Bone-Equivalent Plastic (ICRU-111)] and Water, was obtained from compound dictionary available within SRIM program, [81] Lung Tissue, ICRP[82] and LN10-75 LUNG was obtained from [83]. The elemental composition of these substances is given in Appendix C. Selected human tissue cover all density range, Low density (Lung and lung substitute), medium (Tissue, Muscles and substitutes) and high density (Bone compact cortical and substitute). Also, mass density (ρ) and relative atomic weight ($\langle A \rangle$) of the selected human tissues and human tissue substitutes have been calculated using equation (2.34) and shown in appendix D.

3.2 Computational Methods

3.2.1 Simulation Software

Monte Carlo (MC) is a well-established statistical technique for obtaining numerical solutions to physical or mathematical problems when physical measurements are either difficult or impossible. In charged particle transport, MC uses random numbers with probability distributions to estimate the energy, position, direction and path-length of individual particles, as well as the type of physical interactions that particles experience when passing a medium.

There are many number of computer simulation codes that study interactions of moving particles through a solid, among which the TRIM/SRIM code is widely used in the field due to its convenient graphical user interface and extensive database of electronic and nuclear stopping powers [84].

3.2.1.1 TRIM/SRIM Code

TRIM/SRIM [85] is a software package concerning the stopping and range of ions, from $Z=1-92$ in the energy range (10eV – 2GeV/amu), into matter using quantum mechanical treatment of ion-atom collisions. SRIM is developed by Ziegler and Biersack at 1985. Major upgrades are made about every six years since that time. SRIM is acronym of “Stopping power and Range of Ions in Matter”, and TRIM is the “Transport of Ions in Matter”. Monte Carlo (MC) simulation method known as

binary collision approximation (BCA) code is the fundamental basis for the SRIM simulations with statistical algorithms for calculation to be very efficient [86].

The binary collision approximation is the oldest computer simulation approach for calculating the passage of ions in solids. In this approach, the passage of an ion is calculated as a sequence of independent binary collisions by solving the classical scattering integral for purely repulsive interatomic potentials. It uses random algorithms to select the impact parameter of the next colliding atom and its type [87]. The target in SRIM simulations is treated as the collection of atoms of a gas, liquid, or solid having atomic number up to $Z = 92$. The code will accept targets made of compound materials with up to eight layers each of different materials. It calculates both 3D distribution of the ion and all kinetic processes associated with the ion's energy loss. Figure 3.1 and 3.2 below, show SRIM/TRIM title page and SRIM setup window.



Figure 3.1 SRIM title page window

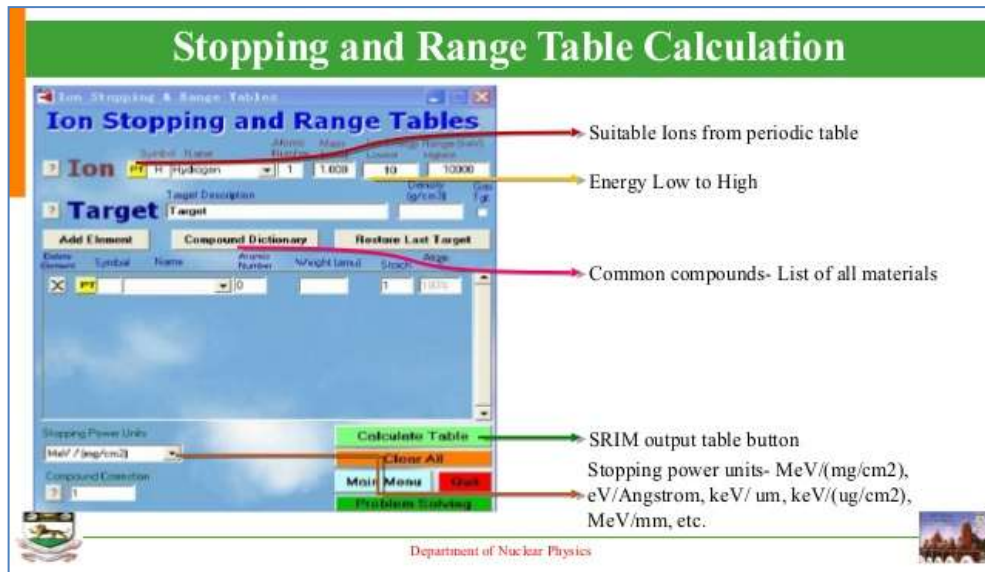


Figure 3.2 SRIM setup window

SRIM includes quick calculations that produce tables of electronic and nuclear stopping powers, range and straggling distributions for any ion at any energy (in the range 10 eV–2 GeV) and in any elemental or multi-elemental target [88].

3.2.1.2 SRIM Applications

Typical SRIM applications include:

1. Ion stopping and range in targets where calculation of most aspects of the loss of energy from the ions in the material. From SRIM simulations, tables of stopping powers, ranges and straggling distributions of any ion at any energy in any elemental or multi-elemental target can be quickly generated.
2. Ion implantation: Ion packages are used for the purpose of modifying samples by injecting atoms to change the chemical and electronic properties of the target. The ion beam causes the displacement of the atom and thus damage to the solid targets.
3. Sputtering: Is knock out target atoms, by ion beam.
4. Ion transmission: Ion beams can be followed through mixed gas/solid target layers, as occur in ionization chambers or in energy degrader blocks used to reduce ion beam energies.

5. Ion beam therapy: Ion beam can also be studied with the aid of SRIM simulations to be used for medical purposes [89].

Major improvements have been made: (1) About 2800 new experimental stopping powers were added to the database, increasing it to over 28,000 stopping values. (2) Improved corrections were made for the stopping of ions in compounds. (3) New heavy ion stopping calculations have led to significant improvements on SRIM stopping accuracy. (4) A self-contained SRIM module has been included to allow SRIM stopping and range values to be controlled and read by other software applications. (5) Individual interatomic potentials have been included for all ion/atom collisions, and these potentials are now included in the SRIM package [90].

3.2.1.3 Accuracy of SRIM Stopping Calculations

Shown in Table 3.1 below, are the statistical improvements in SRIM's stopping power accuracy when compared to experimental data and also compared to SRIM-1998. The right two columns show the percentage of data points within 5% and within 10% of the SRIM calculation. The experimental stopping powers for heavy ions contain far more scatter than for light ions, hence there are larger errors for heavy ions, Be–U. The SRIM-2013 have undergone several updates that ensures that the stopping power and range values are accurate and with less error [87].

The most successful approach to heavy ion stopping powers has been that of Brandt and Kitagawa. This approach is the most widely used method of calculating general heavy-ion stopping cross-sections. A significant systematic error in the Brandt-Kitagawa approach for heavy ions at the peak of the Bragg stopping curve is indicated. This is the velocity at which the ion approaches a fully stripped condition. James F. Ziegler et al. have reevaluated the Brandt-Kitagawa approach and introduce a new shielding functions inserted into the Brandt-Kitagawa theory. With these new shielding functions general heavy ion stopping powers can be calculated with an accuracy of better than 5%. [90] For calculation of the electronic stopping powers at energies above 1.0MeV the Bethe formula is used with correction terms, the uncertainties are stated to be about 2% for elements. [88].

Stopping power can now be calculated with an average accuracy of better than 10% for low energy heavy ion and to better than 2% for high velocity light ions [91].

Table 3.1 Accuracy of SRIM Stopping Power Calculations

	Approx. Data Pts.	SRIM-1998	SRIM- 2010-2013
H ions	9000	4.5 %	3.9 %
He ions	6800	4.6 %	3.5 %
Li ions	1700	6.4 %	4.6 %
Be-U Ions	10600	8.1 %	5.6 %
Overall Accuracy	28,000	6.1 %	4.3 %

3.2.2 Methods of Calculation of (Z_{eff})

Effective atomic number (Z_{eff}) and electron density (N_e) have been calculated for energy range 10 keV – 1.00 GeV of Proton, ^4He , ^{11}B , ^{12}C and ^{16}O ion total interactions using the method adopted by Kurudirek [92– 95] for highly charged particle interaction. In this method, effective atomic number of multi-element material is determined via exploitation of the smooth correlation between atomic cross sections and atomic numbers of the constituent elements. The effective atomic number of the sample was simply taken to be that value of the atomic number of an element whose cross section (σ) matched with that of the sample in a given energy region. Clearly, this method requires a large pool of the elemental cross-section data over a wide range of energies. In section 2.3, the theoretical calculations of all parameters were described in Equations (2.14), (2.21), (2.28) and (2.33).

3.2.2.1. Total Mass Stopping Power Calculation

As a first step, total mass stopping power of constituent elements of the multi element materials in units of ($\text{MeV}/(\text{mg}/\text{cm}^2)$) were obtained using Monte Carlo code, SRIM- 2013 (Stopping Power and Ranges of Ions in Matter) for Proton, ^4He ,

^{11}B , ^{12}C and ^{16}O ion interactions, spanning the continuous energy range from 10 keV to 1.0 GeV. Mass stopping power is used instead of linear stopping power so as to factor out mass density differences with other materials.

The mass stopping power values for the selected materials were estimated using the mixture rule (Bragg's additive law), the elemental stopping of the constituent elements obtained above, and the weight fraction of the individual element in a molecule of gel using equation (2.14).

3.2.2.2. Stopping Cross-Sections (σ_{comp}) of Compound

The Stopping cross-section (σ) values of the composite material were obtained by dividing the mass stopping power of the gel by $(N_A \sum_i (w_i/A_i))$ which represent the total number of atoms present in one gram of the molecule, weight fraction and atomic weight of the individual element in a molecule of the tissue substitutes, using equation (2.21).

3.2.2.3 Effective Atomic Number (Z_{eff}) Calculation

The obtained elemental cross-sectional values are constructed with the cross-section matrix as a function of Z of constitute elements [96], and the effective atomic number (Z_{eff}) values of molecules were then calculated by the logarithmic interpolation of Z values between the adjacent elemental stopping cross-section data in (barn/atom) between which the stopping cross-section lies, and the corresponding atomic numbers, using equation (2.28).

3.2.2.4 Electron Density (N_e) Calculation

The electron density of the materials has been calculated using the relative atomic mass $\langle A \rangle$ of the material and the effective atomic numbers calculated above in equation (2.33).

The data which was generated from SRIM code is in .txt file format and collected on the EXCEL program were then be converted to Origin lab software, (OriginPro 2016) for more specific resolution and more display options. Statistical analysis of the variation of effective atomic number (Z_{eff}) and electron density (N_e)

values with ion energy undertaken using Microsoft excel spread sheet, where, mean values, standard deviation, maximum and minimum values were calculated.

3.3 Water and Tissue Equivalency

A convenient method for evaluating the radiological characteristic equivalence of two materials is to compare (Z_{eff}) and (N_e) in a continuous energy region. Therefore, (Z_{eff}) of the materials relative to water/tissue were also calculated to show the water/tissue equivalence of each substance. Relative difference percent (RD%) between dosimeters and tissues samples and water are calculated to investigate their water and tissue equivalence with respect to their effective atomic number (Z_{eff}) and electron density (N_e), where the relative percentage difference is defined as [97]

$$(\text{RD}\%) = \frac{Z_{\text{eff}}(\text{Material}) - Z_{\text{eff}}(\text{Water/tissue})}{Z_{\text{eff}}(\text{Material})} \times 100 \quad (3.1)$$

CHAPTER FOUR

Results and Discussion

4.1 Overview

In this chapter the effective atomic number (Z_{eff}) and electron density (N_e) of 3D dosimeters, human tissues and human tissue substitutes, have been reported for total interaction processes with Proton (^1H), ^4He , ^{11}B , ^{12}C and ^{16}O ion in the wide energy range from 10 KeV to 1.0 GeV. The obtained values of effective atomic number (Z_{eff}) and electron (N_e), for all substances under study for selected energy values for the different ions are presented graphically in Figures 4.1.a-e and 4.3.a-e for 3D dosimeters and Figures 4.4.a-e and 4.5.a-e for human tissues and human tissue substitutes. Basic statistical information of the effective atomic numbers (Z_{eff}) and electron (N_e) of 3D dosimeters for all ions under study are presented in appendix E and appendix F. Also basic statistical information of the effective atomic numbers (Z_{eff}) and electron (N_e) of human tissues and human tissue substitutes, for all ions interaction studied are presented in appendix G and appendix H.

4.2 Accuracy of Effective Atomic Number (Z_{eff}) Calculation

Since the effective atomic number (Z_{eff}) and electron density (N_e) values were derived from mass stopping power data, accuracy in the effective atomic number (Z_{eff}) values are due to the accuracy in stopping powers calculation using SRIM code, which is stated to be 3.9%, 3.5%, 4.6%, and 5.6% for H ion, He ion, Li ions, and (Be-U), respectively, with an overall accuracy of 4.3% [90].

4.3 Effective Atomic Number (Z_{eff}) and Electron Density (N_e) for ions Interaction

4.3.1 Z_{eff} and N_e of 3D Dosimeters

The result below shown in Figures (4.1.a-e) and (4.3.a-e) are display the energy dependence of effective atomic number (Z_{eff}) and electron density (N_e) of all

types of 3D dosimeters studied, for total ion interaction in the energy region between 0.01 MeV and 1.0 GeV of proton, ^4He , ^{11}B , ^{12}C and ^{16}O ion.

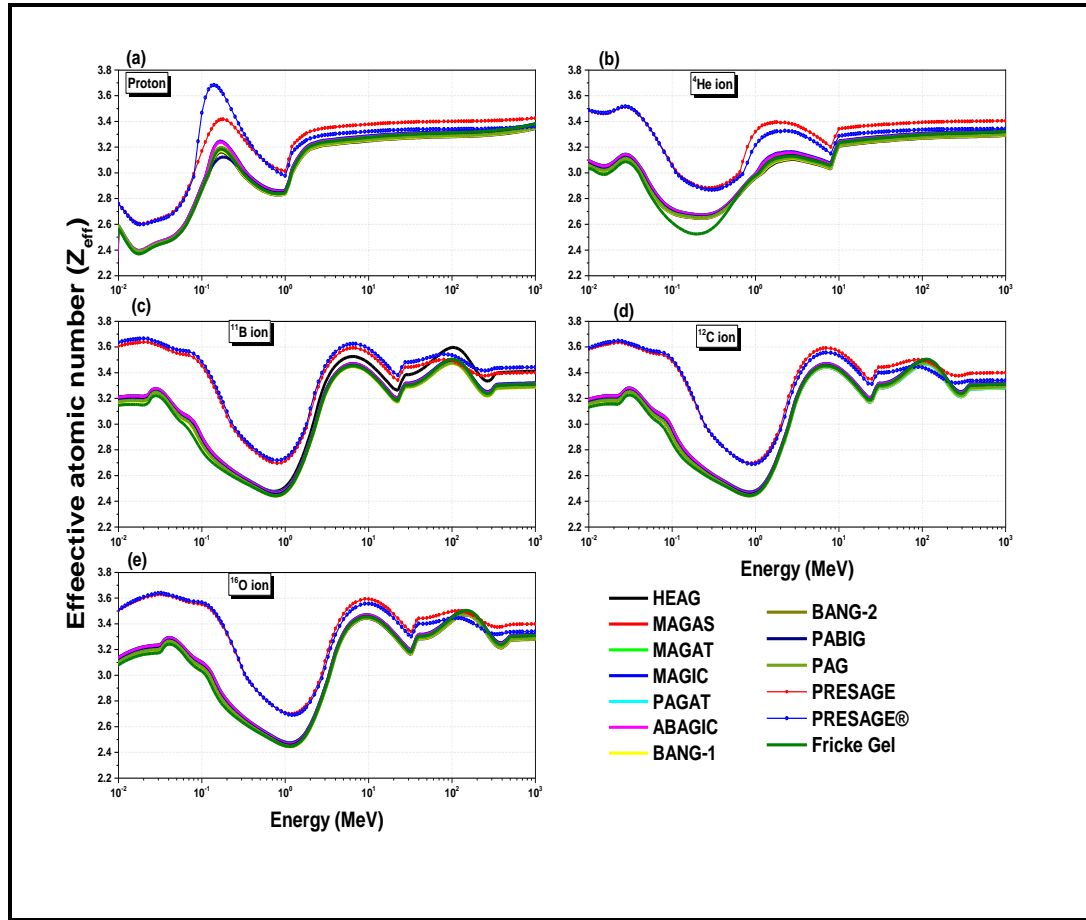


Figure 4.1.a-e Variation of effective atomic number (Z_{eff}) of 3D dosimeters with the kinetic energy of different charged particles. (a) Proton, (b) ^4He , (c) ^{11}B , (d) ^{12}C and (e) ^{16}O ion

According to Figure 4.1.a-e, it should be noted that variation of (Z_{eff}) with the energy varies depending on the type of radiation considered and the chemical composition of materials under test. There are different energy regions where (Z_{eff}) varies less for different types of radiation. This region boundary depends on incident ion specie (atomic number, Z). In general at low energies (< 100 KeV for proton), and at low energies ($< 0.25\text{MeV/nucleons}$) of ^4He , ^{11}B , ^{12}C and ^{16}O ion, the (Z_{eff}) seems to vary much more and the variation tends to be non-uniform for all types of radiation.

For different types of radiations, it has to be noted that the lowest values of (Z_{eff}) has been observed in the low energy region for protons while highest values is observed for other ions. At mid range of energy between (100 keV – 3.0 MeV),

(Z_{eff}) has the highest values at around 0.14 MeV for Proton interaction, and the lowest values are observed at mid range around energy of 0.2 MeV for ^4He , 0.7 MeV for ^{11}B , 0.8 MeV for ^{12}C , and 1.1 MeV for ^{16}O ion. At high-energy region, low variation of (Z_{eff}) values occurs around energy of 1 MeV, 10 MeV, 25 MeV, 30 MeV, and 35 MeV for proton, ^4He , ^{11}B , ^{12}C , and ^{16}O ion respectively, which tend to be more or less constant with energy increase. Meaning that effective atomic number (Z_{eff}) has less energy dependence at higher energies where its values reach a constant broad value for all heavy charged particles.

For each of the considered substances the lower and upper limit of their (Z_{eff}) is dictated by the range of atomic numbers of the constituent elements. Where the least value of (Z_{eff}) does not go below the least atomic number of the constituent element and the maximum value of (Z_{eff}) is also limited by the highest atomic number of the constituent elements.

Figure 4.2.a-b display variation of effective atomic number (Z_{eff}) and electron density (N_e) of liquid water for different types of ions. It is clear that the peaks of effective atomic number (Z_{eff}) are shifted toward higher energies with the increase of incident ion Z number. These peaks might be due to the fact that, (Z_{eff}) value derived

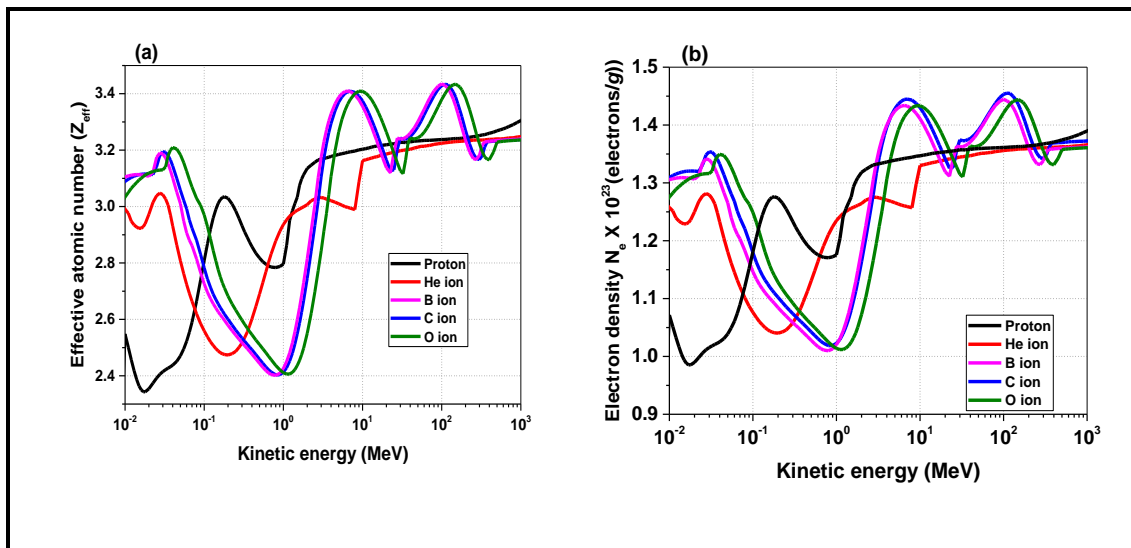


Figure 4.2.a-b Variation of (a) effective atomic number Z_{eff} (b) electron density N_e of liquid water with the kinetic energy of differently charged particles

mainly from the stopping power which exhibits a pronounced maximum at energy that depends on the ion species due to the interplay of decreasing effective charge, increasing scattering cross sections and decreasing maximum energy transfer.

Basic statistical information of the effective atomic number (Z_{eff}) of 3D dosimeters and its dependence on different chemical composition when interact with incident ion energy for all ions studied was been reported as appendix E .

The (Z_{eff}) variation for proton interaction is up to (23-24) % for polymeric (hypoxic and normoxic) gels, 27% Fricke gel, and (16-17)% for PRESAGE gels. For ^4He ion interaction, the (Z_{eff}) variation is up to (23-24) %, 23% and 18% for polymeric gels (hypoxic and normoxic), Fricke gel, and PRESAGE gels, respectively. For other ions, variation is up to (32-33) % for hypoxic and normoxic gels, 33% for Fricke gel, and 28% for PRESAGE gels. Comparing this variation of (Z_{eff}) here with results reported in paper (1) for energy range up to 100 MeV, we can conclude that variation in (Z_{eff}) value is decreases as energy of incident ion increases.

Figure 4.3.a-e below displays the variation of electron density (N_e) with ion energy for all dosimeters studied. It is clear that the variation of electron density (N_e) with the ion energy is closely related to that of effective atomic number (Z_{eff}) and has the same energy dependence as (Z_{eff}), this is expected due to that the two physical quantities are related through equation (2.36).

Appendix F displays statistical information on the variation of (N_e) with ion energy for different types of dosimeters studied. For proton interaction, variation of (N_e) is up to 10% for hypoxic and normoxic gels, 11% Fricke gel, and 8% for PRESAGE gels. For He ion interaction, the (N_e) variation is up to (10-11) %, 11% and 9% for polymeric gels (hypoxic and normoxic), Fricke gel, and PRESAGE gels, respectively. For other ions, variation of (N_e) is up to 14% for polymeric gels, 14% for Fricke gel, and 13% for PRESAGE gels. Generally, (N_e) variation for all ions interaction shows low values compared to that of (Z_{eff}). Highest values of (Z_{eff}) of (3.76, 3.51, 3.64, 3.63, 3.63) and (N_e) of (1.70, 1.59, 1.64, 1.64, 1.64) $\times 10^{23}$ electron/g, for proton, ^4He , ^{11}B , ^{12}C and ^{16}O , were observed for PRESAGE gel for all ion species studied. Also HEAG, BANG-1, PAG and Fricke gel show lowest values of Z_{eff} of (2.29, 2.65, 2.44, 2.44, and 2.45) for proton, ^4He , ^{11}B , ^{12}C and ^{16}O ion respectively. Lowest value of (N_e) of (0.96, 1.05, 1.02, 1.02 and 1.02) $\times 10^{23}$ electron/g, is observed for Fricke gel for proton, ^4He , ^{11}B , ^{12}C and ^{16}O ion interaction. Fricke gel is very close to water due to that both have close weight fractions of Oxygen and Hydrogen elements.

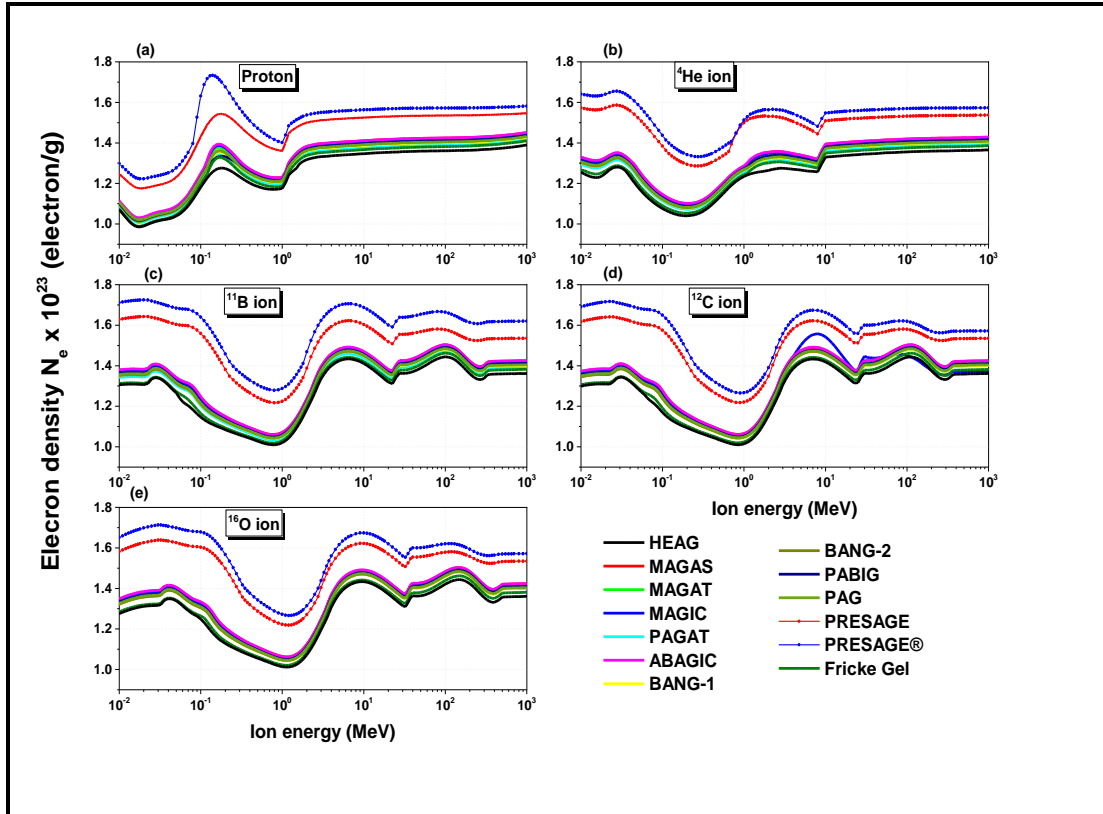


Figure 4.3.a-e Variation of electron density (N_e) of 3D dosimeters with the kinetic energy of different charged particles. (a) Proton, (b) ^4He , (c) ^{11}B , (d) ^{12}C (e) ^{16}O ion

The chemical composition (Z_{eff}) plays a significant part in the interaction of radiation with the selected materials. The values of (Z_{eff}) depend on the atomic number of the constituent elements of the interacting material. This can be described on the basis of weight fraction of different constituent elements. Higher is the weight fraction of higher atomic number element, higher will be its effective atomic number (Z_{eff}). As mentioned before PRESAGE dosimeter has the highest values of (Z_{eff}) and (N_e), this is due to the presence of Br ($Z=35$) maximum atomic number of constituent elements among the selected materials and high weight fraction of carbon element.

4.3.2 Z_{eff} and N_e of Human Tissues and Human Tissue Substitutes

The result below shown in Figure (4.4.a-e) displays the energy dependence of effective atomic number (Z_{eff}), electron density (N_e) shown in Figure (4.5.a-e) of all types of human tissues and human tissue substitutes studied, for total ion interaction

in the energy region between 0.01 MeV and 1.0 GeV of proton, ^4He , ^{11}B , ^{12}C and ^{16}O ion.

It is clear that, the general behavior of effective atomic number (Z_{eff}) for all materials, human tissues and human tissue substitutes and 3D dosimeter, is almost identical and have same trends, and variation of the effective atomic number (Z_{eff}) is observed throughout the whole energy range studied. As general, this variation is clearly confirming the comment by (Hine 1952) that, effective atomic number (Z_{eff}) of multi-element materials cannot be represented by single number throughout an extended energy range.

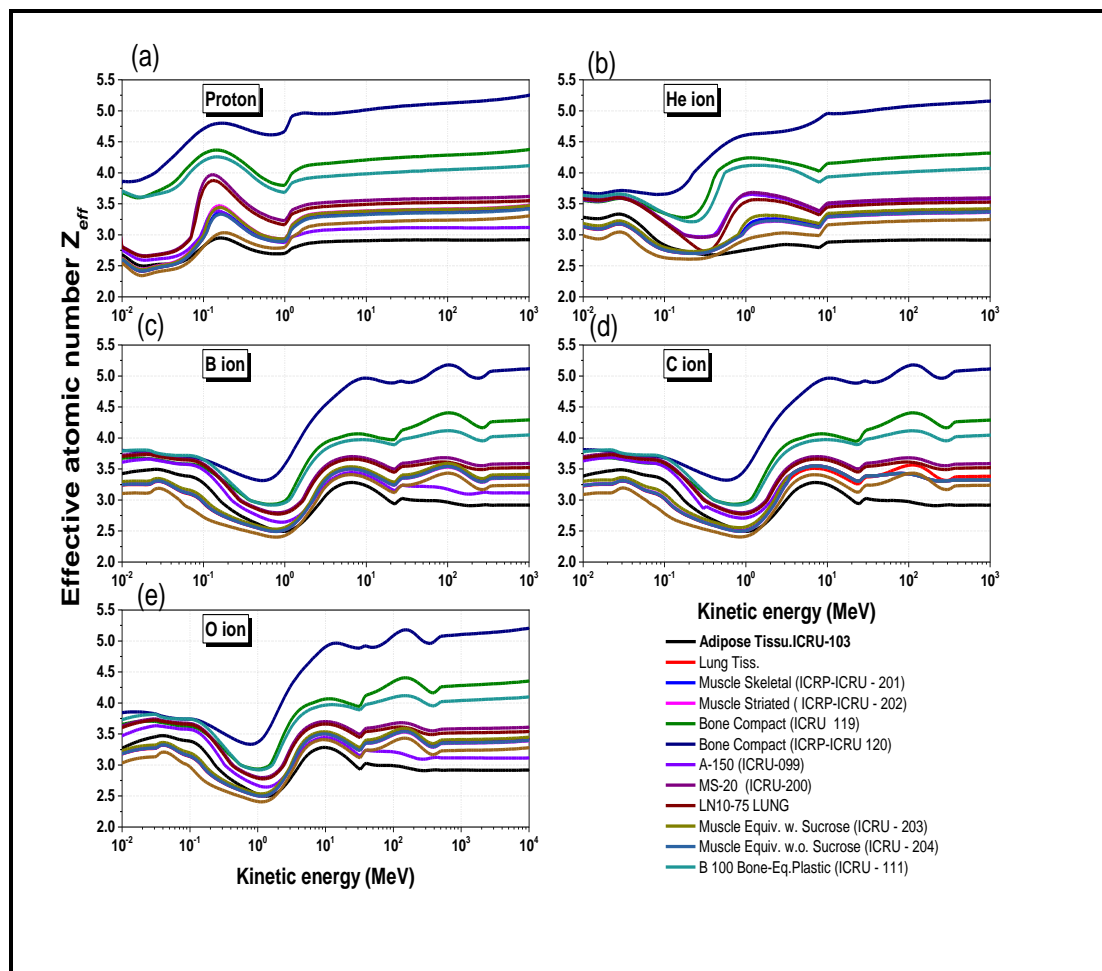


Figure 4.4.a-e Variation of effective atomic number (Z_{eff}) of human tissues and substitutes with the kinetic energy of differently charged particles. (a) Proton, (b) ^4He ion, (c) ^{11}B ion, (d) ^{12}C ion, and (e) ^{16}O ion

Highest values of (Z_{eff}) were observed for MS-20 (ICRU 200) and LN10/75 LUNG for all ions and observed for A-150 Tissue Equiv. Plastic (ICRU-099) for ^4He ion interaction only. Meanwhile lowest (Z_{eff}) values were observed for Adipose

Tissue (ICRP ICRU-103) and Muscle, Striated (ICRP ICRU-202) for all ions interaction, (except proton interaction for Striated (ICRP ICRU-202)).

Appendix G, shows basic statistical information on (Z_{eff}) for interaction of selected human tissues and human tissue substitutes with proton, ^4He , ^{11}B , ^{12}C , and ^{16}O ion. According to the type of incident ion, the highest variation in Z_{eff} for ion interaction is 35% (Tissue Substitute MS-20 ICRU-200), 23% (Lung ICRP, LN10-75 LUNG, Muscle Skeletal (ICRP ICRU-201), and Muscle Equiv. Liq. with Sucrose (ICRU - 203), 33% (Lung ICRP, Muscle Skeletal (ICRP ICRU-201), Muscle Equiv. Liq. with Sucrose (ICRU - 203)), 33% (Lung ICRP), and 33% (Lung ICRP and Skeletal (ICRP ICRU-201)) for Proton, ^4He , ^{11}B , ^{12}C and ^{16}O ion interaction, respectively. It is observed that (Z_{eff}) have less energy dependence at energies around and higher than 1.0 MeV, 10 MeV, 20 MeV, 30 MeV and 35 MeV for proton, ^4He , ^{11}B , ^{12}C and ^{16}O ion interaction, respectively.

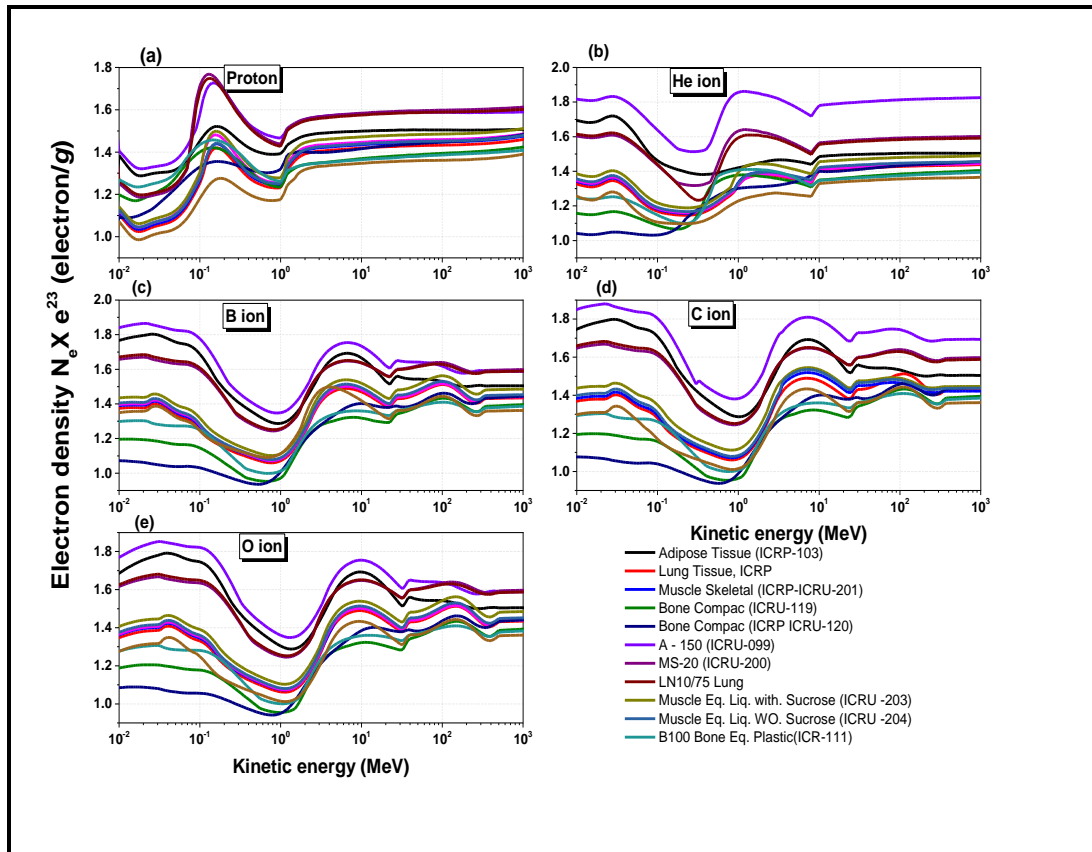


Figure 4.5.a-e Variation of electron density (N_e) of human tissues and human tissue substitutes with the kinetic energy of differently charged particles. (a) Proton, (b) ^4He ion, (c) ^{11}B ion, (d) ^{12}C ion, and (e) ^{16}O ion

The variation of effective electron density (N_e) with incident ion energy for the samples in this group, that displayed in Figure 4.5.a-e below, shows that the variation of the effective electron number (N_e), with the incident ion energy dependence, is similar to the variation of the effective atomic numbers (Z_{eff}), as mentioned before in case of 3D dosimeters.

Appendix H, displays basic statistical information of electron density (N_e) of biological samples interacting with different ions. Highest variation for electron density of 16% (Tissue Substitute MS-20 ICRU-200), 10% (Lung ICRP, LN10-75 LUNG, Muscle Skeletal (ICRP ICRU-201), A-150 Tissue Equiv. Plastic (ICRU-099), 15% A-150 Tissue Equiv. Plastic (ICRU-099) for proton, ^4He , ^{11}B ion interaction. Also variation between 13-14% (all tissues, muscles and substitutes) is observed for ^{12}C and ^{16}O ion interaction.

4.4 Effective Atomic Number and Electron Density as Indicator for Radiological Water Equivalence of Substances

Effective atomic number (Z_{eff}) and electron density (N_e) difference percentage (DR%) relative to water of the materials under study, were also calculated to evaluate degree of radiological water equivalence of the given substances for different ions interaction using equation (3.1).

4.4.1 Water Equivalence of 3D Dosimeters

Shown in Figure 4.6.a-e, below, the difference percentage (DR%) relative to water of polymeric (hypoxic and normoxic) gels, Fricke gel, PRESAGE and PRESAGE® for gels interaction with proton, ^4He , ^{11}B , ^{12}C and ^{16}O ion.

It can be seen that difference percent (DR%) in Z_{eff} relative to water for polymeric gels and Fricke gel, were <2.5% throughout the whole proton energy range. Highest difference percent of up (5-7) % occurs around proton energy of 0.15MeV, and constant difference of about 2.3% throughout energy range from 2.0 MeV to 1.0 GeV has been observed. This indicates good water equivalence properties in the entire energy region. Among this group, Fricke gel shows the best water equivalent properties. PRESAGE gels show high DR% relative to water up to 17% for PRESAGE® and 11.5% for PRESAGE dosimeter, within energy range from

0.01 MeV -1.0 MeV. PRESAGE dosimeters show good water equivalence properties at high energies >2.0 MeV with low variation of $\leq 5\%$ tends to decrease slightly as energy increase. For ^4He ion interaction, DR% relative to water for polymeric gels and Fricke gel is between (1.7–3.5%) for the whole energy range. Small peaks of $<5\%$ occurs at ^4He ion energy range between 0.01-10.0 MeV. PRESAGE® and PRESAGE show very high difference up to 17% in the range of energy between 0.01-1.0MeV, and up to 12% at range from 1.0-10MeV. PRESAGE® and PRESAGE show good water equivalence properties at high energies >10 MeV with low variation of $\leq 3.7\%$ and $\leq 5\%$ for PRESAGE® and PRESAGE dosimeter respectively, tends to decrease slightly as energy increase.

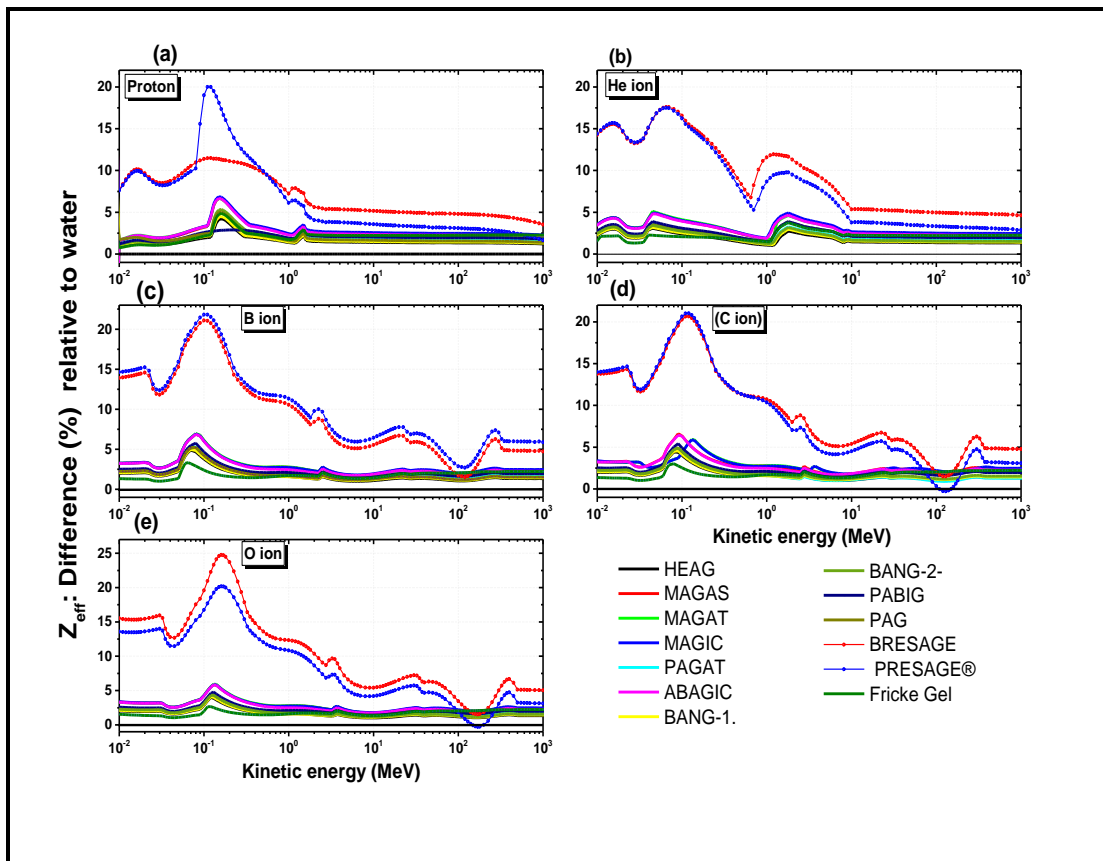


Figure 4.6.a-e Percentage difference in (Z_{eff}) of 3D dosimeters relative to water For: (a) Proton (b) ^4He (c) ^{11}B (d) ^{12}C and (e) ^{16}O ions interaction

In short, all polymeric gels and Fricke gel are good water equivalent materials throughout the whole energy range with percent difference DR% of $\leq 5\%$ relative to water. Note that, Hypoxic gels report less difference percent relative to water compared to normoxic polymer gels which may be due to the higher mass density of the normoxic polymer gel dosimeters and the higher concentration of water in the

hypoxic polymer gel. While PRESAGE® and PRESAGE dosimeters are considered as a good water equivalent material at high energy range (10MeV-1GeV) with difference percent relative to water of $\leq 5\%$ for PRESAGE $\leq 3\%$ for PRESAGE® for ^4He ion interaction.

For ^{11}B , ^{12}C and ^{16}O ion interaction, DR% for polymeric gels and Fricke gel has values between (1.1 – 2.5)%, (1.1 – 2.5)% and (1.0 – 2.7) % for ^{11}B , ^{12}C and ^{16}O ion interaction respectively, the whole energy range. Also, highest difference percent of 7% occurs at around 80KeV of ^{11}B ion, 6.4% occurs at ^{12}C ion energy of 90 KeV and 5.8 % occurs at ^{16}O ion energy of 130 KeV.

From above results, we conclude that (Z_{eff}) values of polymeric gels and Fricke gel and their behavior concerning ion energy are very close to those of water. They have shown excellent water equivalency, as differences in (Z_{eff}) between polymeric gels and Fricke gel and water were very small throughout the whole energy range from 0.01- 1000 MeV for all types of incident ion studied. The highest differences for all gels occur between 45 and 300 keV energies for all ions.

When it comes to PRESAGE and PRESAGE®, these gels show high differences of up to 12%, 17.5%, 22%, 21%, and 25% for proton, ^4He , ^{11}B , ^{12}C and ^{16}O ion respectively, at lower energy range. Also low variation in difference percentage (\sim constant) has been observed energy range (2.0 MeV, 10 MeV, 350 MeV, 375 MeV, and 500 MeV up to 1.0GeV) for proton, ^4He , ^{11}B , ^{12}C and ^{16}O ion respectively. Lowest point differences (almost zero) is observed at energies of 110MeV, 130MeV, and 170MeV, for ^{11}B , ^{12}C and ^{16}O ion. It is worth saying that PRESAGE® show great difference of 20% at 100kev of proton energy in comparison with PRESAGE which show differences of only 12% at same energy. These high values for PRESAGE gels are due to the presence of a high Z element (Br, Z= 35) with a relatively high weight fraction within its constituent elements and high weight fraction of carbon element.

Gels found to be most relative to water are Fricke, HEAG, and PAG gel for proton, BANG-1, HEAG, PAG and PAGAT for ^4He ion interaction, Fricke and HEAG for ^{11}B ion interaction, Fricke and HEAG for ^{12}C ion, and Fricke, HEAG, BANG-1 for ^{16}O ion interactions.

Data reported here gives essential information about the interaction of different types of charged particles with different materials and could be useful in the energy range specified. Lower differences observed for polymeric and Fricke gel dosimeters made it excellent water equivalent.

Differences percentage of electron density relative to water is calculated and displayed graphically in Figure 4.7.a-e below. It is observed that differences in (N_e) between gels are constant for all energies of ions.

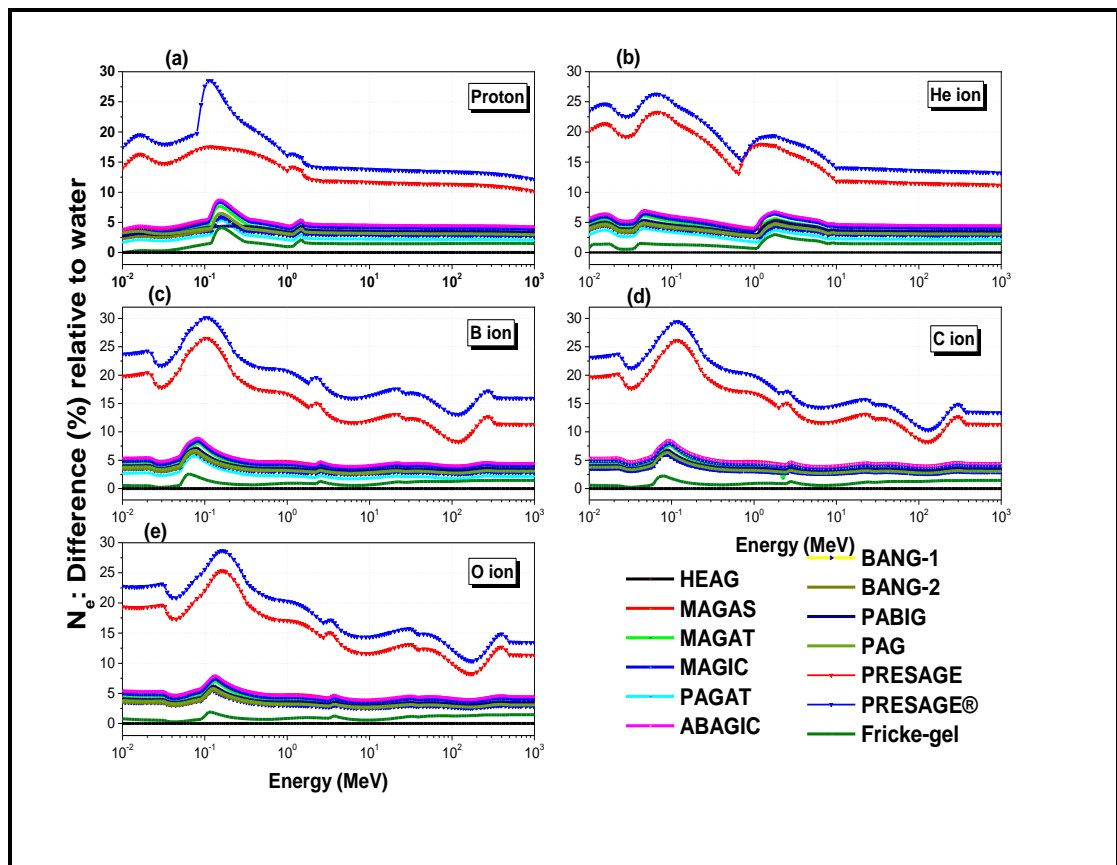


Figure 4.7.a-e Percentage difference in (N_e) of 3D dosimeters relative to water for: (a) Proton, (b) ^4He ion, (c) ^{11}B ion (d) ^{12}C ion (e) ^{16}O ion interaction

4.4.2 Water Equivalence of Human Tissues and Human Tissue Substitutes

The (Z_{eff}) difference percent relative to water (DR%) has been also calculated to evaluate degree of water equivalency of the given human tissues and human tissue substitutes for different ions interaction, and represented graphically in Figure 4.8.a-e. It has been observed that A-150 Tissue-Equivalent Plastic (ICRU-099), Muscle Equivalent Liquid Without Sucrose (ICRU-204), Skeletal (ICRP ICRU-201),

Muscle, Muscle Equivalent Liquid with Sucrose (ICRU-203) and Muscle, Striated (ICRP ICRU-202), have the best water equivalence in the entire energy range with relative difference of $\leq -3\%$, $\leq 4\%$, $\leq 5\%$, $\leq 5\%$, $\leq 6\%$ for proton. Also, Lung Tissue, ICRP, Muscle, Striated (ICRP ICRU-202), Muscle Equivalent Liquid with Sucrose (ICRU - 203), Muscle Equivalent Liquid without Sucrose (ICRU-204) show diff. of $\leq 5\%$ through entire energy range for ^{12}C , and ^{16}O ion.

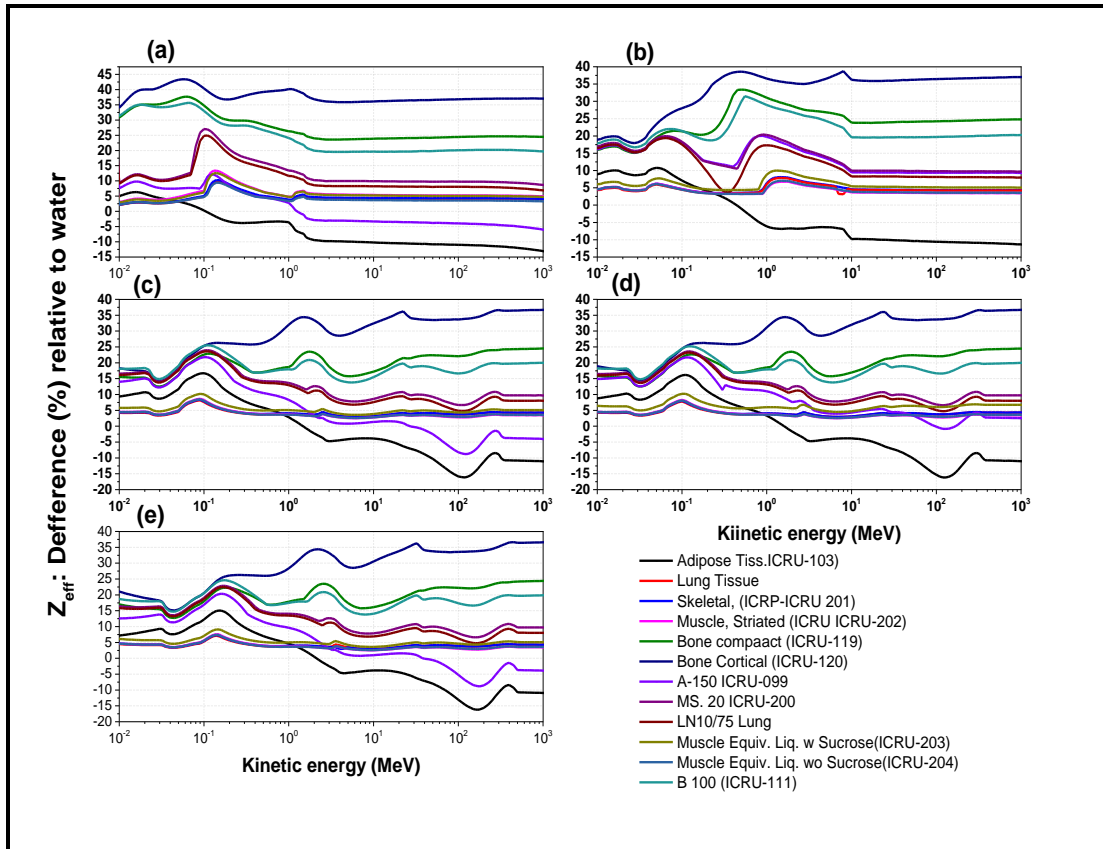


Figure 4.8.a-e Percentage difference in (Z_{eff}) of human tissues and human tissue substitutes relative to water For: (a) Proton, (b) ^4He ion, (c) ^{11}B ion (d) ^{12}C ion (e) ^{16}O ion interaction

4.5 Effective Atomic Number (Z_{eff}) and Electron Density (N_e) as Indicator for Tissue Equivalence of Substances

The (Z_{eff}) difference percent relative to tissue (DR %) has been calculated for some representative samples of 3D dosimeters relative to Adipose Tissue (ICRU-103), lung tissue ICRP, Muscle, Skeletal (ICRP ICRU-201) and Muscle, Striated (ICRP ICRU-202) for proton and ^{12}C ion interaction. In addition, difference percent of these tissues relative to corresponding equivalent substitutes has been calculated.

4.5.1 Tissue Equivalence of 3D Dosimeters

Four samples from 3D dosimeters studied have been chosen as representative to a group of 3D dosimeter: MAGIC, BANG-1, PRESAGE[®] and Fricke gel. Tissue and muscle equivalence of these dosimeters with respect to Adipose Tissue (ICRU-103), lung tissue ICRP, Muscle, Skeletal (ICRP ICRU-201) and Muscle, Striated (ICRP ICRU-202) is studied for proton and Carbon ion interaction with respect to its effective atomic number (Z_{eff}).

4.5.1.1 Tissue Equivalence for Proton Interaction

According to the variation of (Z_{eff}) of dosimeters with tissues and muscles, energy of proton could be divided into three main energy regions, low energy region from 0.01 – 0.1 MeV, mid energy region from 0.1 – 1.0 MeV and high energy region from 1.0 MeV to 1.0 GeV. Figure 4.9.a-d below show that MAGIC, Fricke and BANG-1 gel is a good tissue equivalent material throughout the whole range of proton energy. For lung tissue ICRP, and Muscle, Skeletal (ICRP ICRU-201) difference % is of $\leq -1.5\%$, $\leq -2.9\%$ and $\leq -3.7\%$ respectively, in the low and high energy regions, while difference % of up to -4.7% , -7.4% and -12% is observed in the mid energy region for MAGIC, Fricke and BANG-1 gel respectively. Also difference % of $\leq -3.5\%$, $\leq -4.4\%$ and $\leq -7.4\%$ is achieved for Muscle, Striated (ICRP ICRU-202) in the low and high energy range while high difference percent up to -9.4% , -12% and -12% is observed at mid range of energy for MAGIC, Fricke, and BANG-1 gel, respectively.

PRESAGE[®] could not be considered as tissue equivalent in case of lung tissue and skeletal muscle within the low and mid energy range of proton energy under study, where high difference % of up to 7.2% at low energy region decreasing to a difference % between 2.1% to 5% at mid range, then low difference % of 2.1% occur at high energy region for lung tissue ICRP, and Muscle, Skeletal (ICRP ICRU-201). For Muscle, Striated (ICRP ICRU-202), difference % of around 5%, between (-2% and 5%), and $\leq 0.8\%$ at low, mid and high energy respectively. Full matching of PRESAGE gel with Muscle, Striated (ICRP ICRU-202) is achieved in the high energy range from around 1.4MeV to 1.0 GeV. So for proton interaction, PRESAGE[®] is matching lung tissue ICRP, Muscle, Skeletal (ICRP ICRU-201) and

Muscle, Striated (ICRP ICRU-202) within high energy region with difference % of $\leq 2.1\%$.

For Adipose Tissue (ICRU-103), different behavior is observed. Increasing diff.% between (-5% to 3%), (-5% to 1.8%), (-5.6% to 1.9%) and (-2.8% - 11.1%) at low energy (0.1–1.4 MeV), for MAGIC, BANG-1, Fricke gel and PRESAGE[®]. between (3% -9%), (1.8% - 7.8%), (1,9% - 7.4%) and (11.1% - 14.2%) at mid range and 9.7%, 8,5%, 9,2% and 13.6% at 1.4MeV tends to increase slightly with energy increase for MAGIC, BANG-1, Fricke gel and PRESAGE[®], respectively. We can conclude that adipose tissue show the highest difference % for all dosimeters studied.

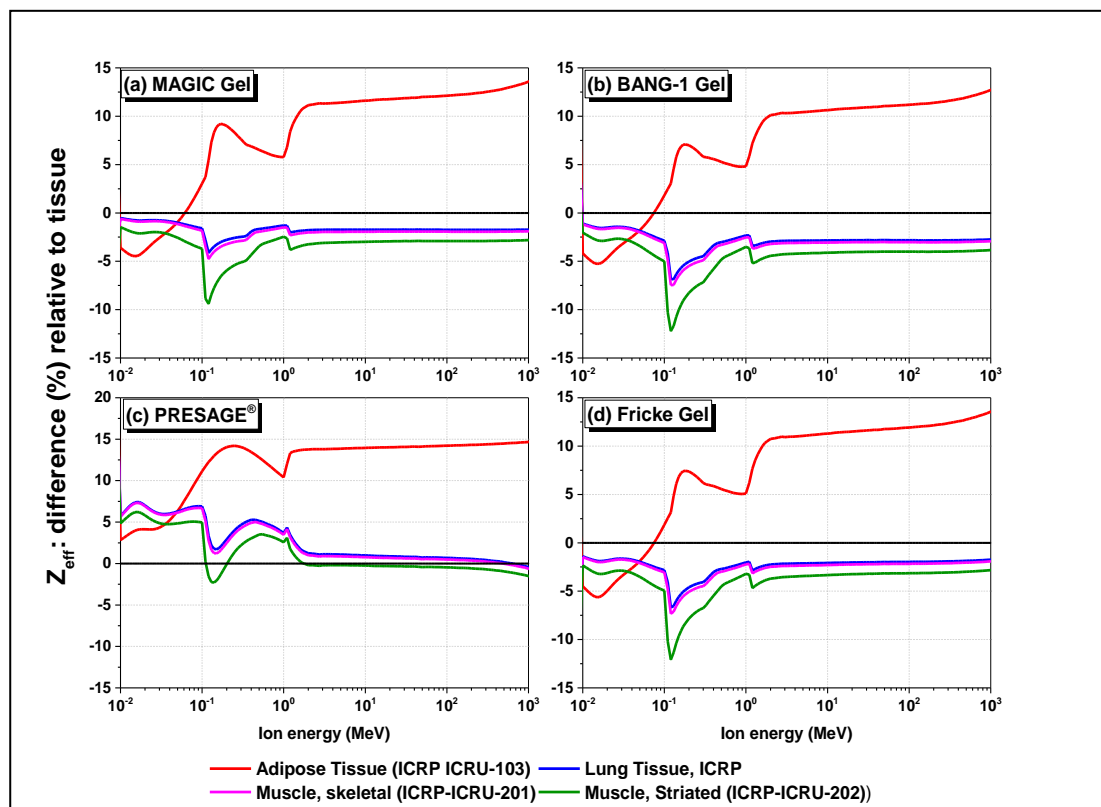


Figure 4.9.a-d Z_{eff} : difference percent relative to tissues and muscles for (a) MAGIC gel (b) BANG-1 (c) PRESAGE[®] and (d) Fricke gel, for total proton interaction

It can be seen that differences percent (DR%) in (Z_{eff}) of MAGIC gel relative to tissues for Lung and muscle skeletal, were $<1.5\%$ throughout the whole proton energy range, and difference percent of $\leq 9\%$ within energy region 0.1-1.0MeV. This indicates good water equivalence properties in the entire energy region.

4.5.1.2 Tissue Equivalence for ^{12}C Ion Interaction

According to the variation of (Z_{eff}) of dosimeters with tissues and muscles, energy range of carbon ion could be divided into three main energy regions, low energy region from 0.01– 3.0 MeV, mid energy region from 3.0 MeV to 400 MeV and high energy region from 0.4- 1.0 GeV.

Figure 4.10.a-d displays difference percent (diff.%) of the effective atomic number (Z_{eff}) between MAGIC, BANG-1, PRESAGE® and Fricke gel dosimeters versus Adipose Tissue (ICRU-103), lung tissue ICRP, Muscle, Skeletal (ICRP ICRU-201) and Muscle, Striated (ICRP ICRU-202) for ^{12}C ion interaction. It is shown in Figure 4.10.a that, MAGIC gel has shown low difference percent of $\leq -1.1\%$ for lung tissue ICRP throughout the low and mid range of energy, and low constant difference percent of -0.25% in the high range of energy. Also MAGIC gel show difference % of -1.1% in the low energies, diff.% between $(-3.0 \text{ to } 2.8)\%$ at mid energies and constant diff.% of -1.3% at high energies for Muscle, Skeletal (ICRP ICRU-201) and Muscle, Striated (ICRP ICRU-202). MAGIC shows very high difference with respect to Adipose tissue, where difference % between $(-12.5 \text{ to } 6.8)\%$, $(5.4 \text{ to } 15.6)\%$ and constant diff.% of $11/9\%$ at low, mid and high energies is observed.

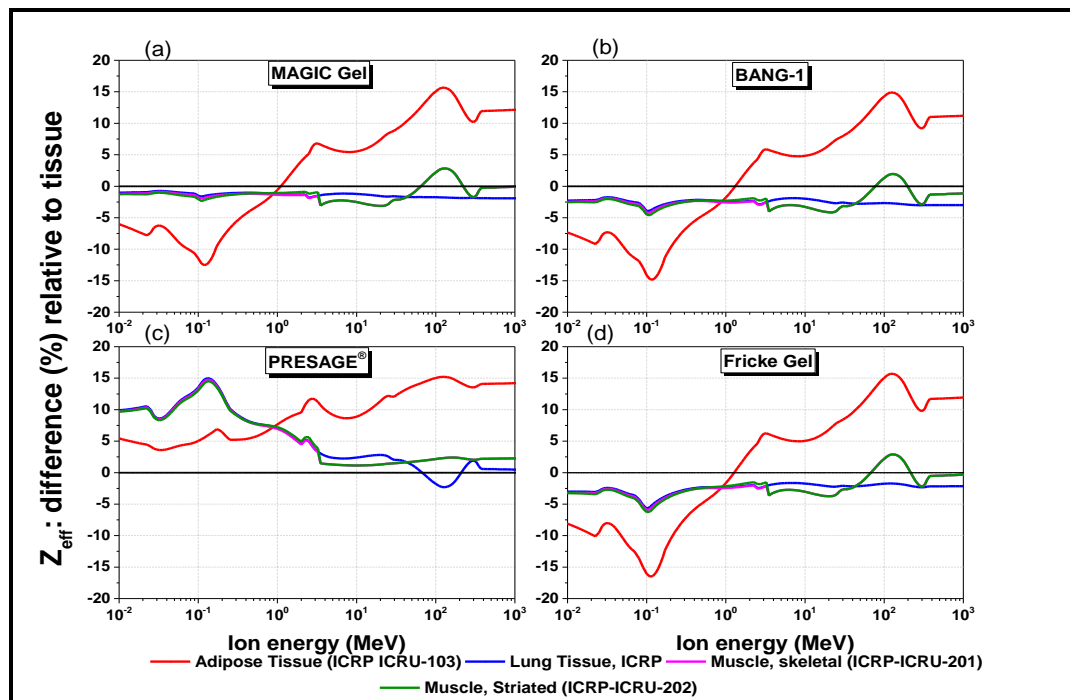


Figure 4.10.a-d Z_{eff} : difference percent relative to tissues and muscles for (a) MAGIC gel (b) BANG-1 (c) PRESAGE® and (d) Fricke gel, for total ^{12}C ion

From Figure 4.10.d, Fricke gel have shown difference percent of $\leq -3.4\%$ for Lung Tissue, ICRP, throughout the low and mid range of energy, and low constant difference percent of -2.1% in the high range of energy. Also Fricke gel gel show difference % of -3.2% in the low energies, diff.% between $(-3.6 \text{ to } 2.9)\%$ at mid energies and constant diff.% of -0.52% at high energies for Muscle, Skeletal (ICRP ICRU-201) and Muscle, Striated (ICRP ICRU-202). Fricke gel shows very high difference with respect to Adipose Tissue (ICRP ICRU-103), where difference % between $(-16.5 \text{ to } 6.2)\%$, $(5.0 \text{ to } 15.7)\%$ and constant diff.% of $11/7\%$ at low, mid and high energies is observed.

Figure 4.10.c, displays difference percent in (Z_{eff}) for PRESAGE[®] with respect to different types of tissues. High difference percent between $(4.9 \text{ to } 14.5)\%$ have been shown for Lung Tissue, ICRP, Muscle, Skeletal (ICRP ICRU-201) and Muscle, Striated (ICRP ICRU-202) within low range of energy. Difference % between $(2.4 \text{ to } 1.1)\%$ and $(-2.3 \text{ to } 2.8)\%$ at mid energies and 2.2% and 0.5% at high energies is observed for Lung Tissue, ICRP, Muscle, Skeletal (ICRP ICRU-201) and Muscle, Striated (ICRP ICRU-202) respectively. PRESAGE[®] shows difference % between $(3.6 \text{ to } 11.7)\%$, $(8.6 \text{ to } 15.2)\%$ and constant high diff.% of 14% at low, mid and high energies, with respect to Adipose Tissue (ICRP ICRU-103).

From the above discussion, we can conclude that MAGIC match well with low difference percent of $\leq -1.1\%$ for Lung Tissue, ICRP, $\leq -3\%$ for Muscle, Skeletal (ICRP ICRU-201) and Muscle, Striated (ICRP ICRU-202) throughout the whole range of ^{12}C ion energy. For BANG-1 gel, good tissue-equivalent properties with low difference % of $\leq -1.7\%$ and $\leq -4\%$ for Lung Tissue, ICRP, Muscle, Skeletal (ICRP ICRU-201) and Muscle, Striated (ICRP ICRU-202) throughout the whole energy range for ^{16}C ion interaction. Fricke gel has good tissue-equivalent properties with low difference % of $\leq -3.4\%$ for Lung Tissue, ICRP and $\leq -3.6\%$ Muscle, Skeletal (ICRP ICRU-201) and Muscle, Striated (ICRP ICRU-202) throughout the whole energy range for ^{16}C ion interaction. For PREAGE dosimeter, it shows good matching with low differences of $\leq 2.8\%$ that occurs at mid and high energies. All dosimeters show poor matching with Adipose Tissue (ICRP ICRU-103) for ^{16}C ion interaction.

4.5.2 Tissue Equivalence of Human Tissue Substitutes

The (Z_{eff}) difference percent relative to tissue (DR %) has been also calculated for some tissues of human organs relative to tissue substitutes and shown graphically in Figure 4.11.a-d below. It is found that A-150 Tissue Equiv. Plastic (ICRU-099), simulates Adipose through the entire energy range for all ions studied, with differences less than 6% while shows high differences (up to 15%), for proton

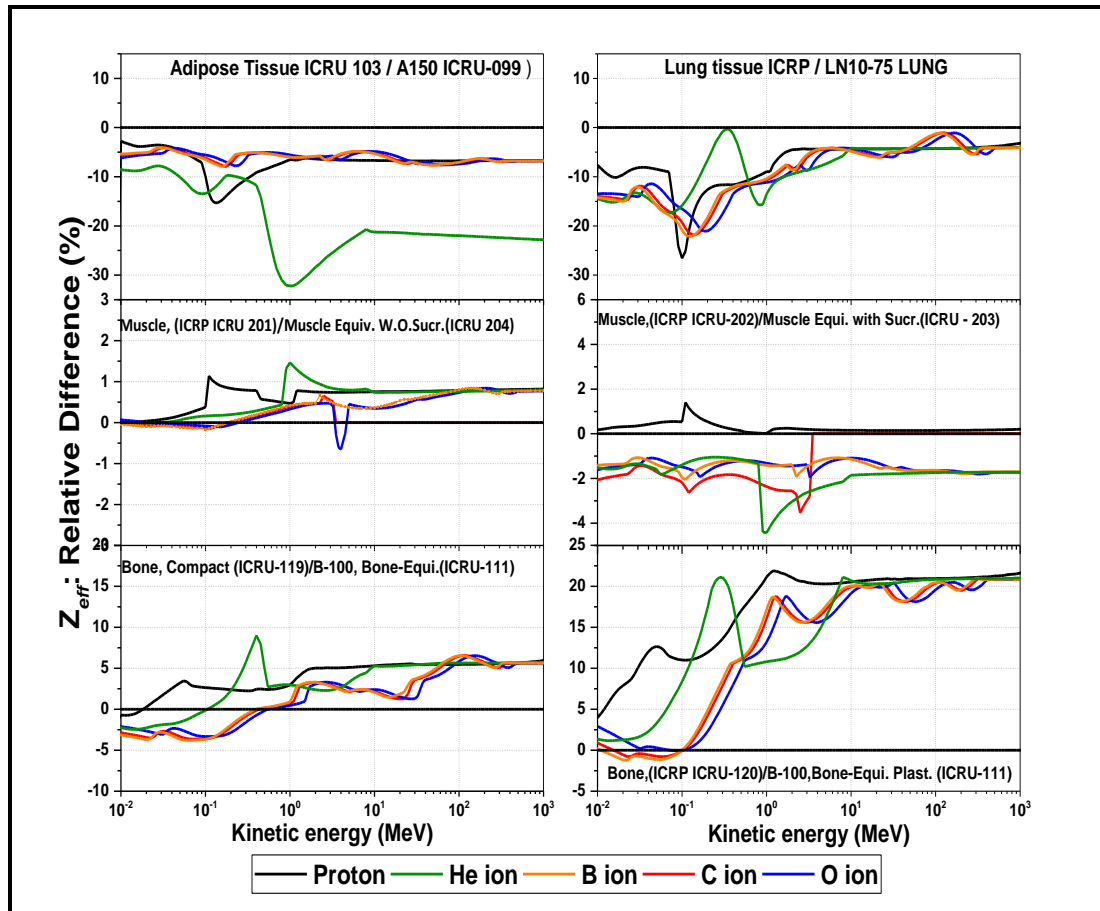


Figure 4.11.a-f Percentage difference in Z_{eff} of human tissue substitutes relative to human tissues for differently charged particles interaction

interaction in the energy range of (0.01-1.0 MeV) and differences up to about 30% for ^4He ion in the energy range of (0.04-1.0 GeV). Also, LN10/75Lung shows good tissue equivalence with Lung Tissue ICTP with differences less than 5% at energies of (1.5-1000MeV), (8-1000MeV) (3-1000MeV) (3-1000MeV), (4.5-1000MeV) for proton, ^4He , ^{11}B , ^{12}C and ^{16}O ion interaction, high difference up to (26% at 0.1 MeV), (17% at 0.07MeV and 0.8MeV), (22% at 0.14MeV), (22% at 0.14MeV) and (21% at 0.18MeV) is observed for proton, ^4He , ^{11}B , ^{12}C and ^{16}O ion respectively,

mean while full matching is observed around 0.035, 110, 170MeV for ^4He , ^{12}C and ^{16}O ion.

Muscle Equiv. Liq. without sucrose (ICRU - 204), matching well with muscle skeletal (ICRP ICRU-201) and Muscle Striated (ICRP ICRU-202) with relative differences of <1.0% for proton, <1.4 for the whole range of ^4He ion energy, < 0.6% for ^{11}B ion, <0.5% for ^{12}C ion, and < 0.6% for ^{16}O ion. With respect to Muscle Equiv. Liquid with Sucrose (ICRU-204), differences of 1.4% is observed at energy of 0.11MeV and difference is almost Zero for the rest of the energy regions for proton, and difference is <4% for the whole energy regions for other ions. B-100, Bone-Equivalent Plastic (ICRU-111) shows well matching with Bone Compact (ICRU-119), with low differences of < 3.3% in the first half of the energy range (up to 1.5 MeV) and constant difference of 5% in the rest of the range of proton interaction, also constant difference of 5% is achieved for ^4He ion interaction in the energy range of 10MeV up to end of range. For ^{11}B , ^{12}C and ^{16}O ion interaction, differences of $\leq -3.8\%$ up to 0.5MeV ion energy, $\leq 3.3\%$ between 1.0-100 MeV, and $\leq 6.5\%$ up end energy range. Full matching is achieved at energy of 0.5-1.0MeV. We can conclude that B-100, Bone Equiv. Plastic (ICRU-111) simulate Bone, Compact (ICRU-119) throughout the whole energy range with differences of $\leq 6.5\%$ for all ions studied. This substitute show high differences related to Bone, Cortical (ICRP ICRU-120), least and constant variation of 20% is observed for proton interaction in the energy region between 3.0 MeV to 1.0 GeV.

From Figure 4.12.a-f below, (Ne) difference percentage of different human tissues and tissue substitutes show same trends as for (Z_{eff}) with lower RD% values of 2% for Adipose Tissue ICRU 103 versus A150 ICRU-099, 7.5% for Lung tissue ICRP versus LN10-75 LUNG, 1.0 % for Muscle Skeletal (ICRP ICRU 201) versus Muscle Equiv. without Sucrose (ICRU 204), 2% for Muscle Striated (ICRP ICRU-202) versus Muscle Equiv. Liquid with Sucrose (ICRU-203), 4.6% for Bone, Compact (ICRU-119) versus B-100, Bone-Equiv. Plastic (ICRU-111), and 7.6% for Bone, (ICRP ICRU-120) versus B-100, Bone-Equiv. Plastic (ICRU-111). This is due to different values of relative atomic weights (A_r) of each material.

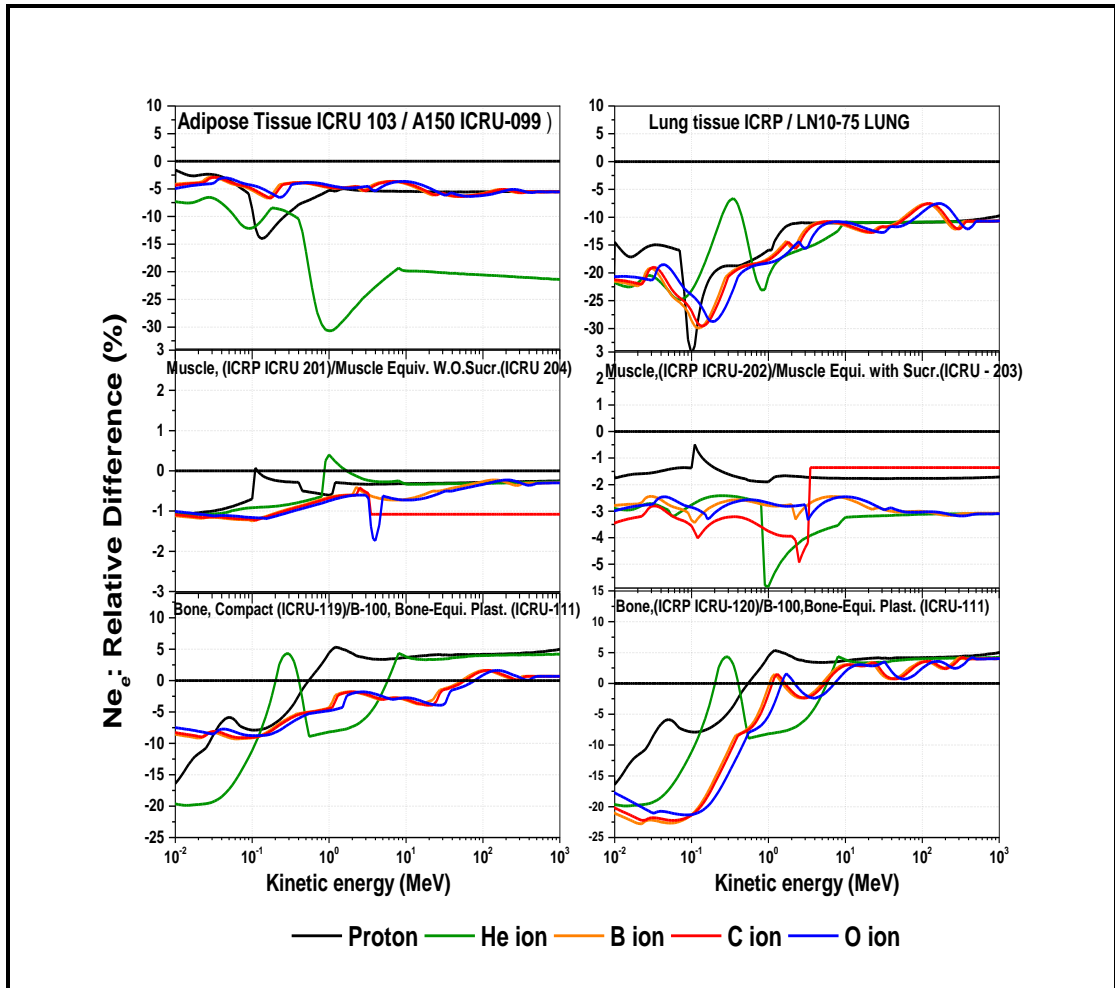


Figure 4.12.a-f Percentage difference in electron density (N_e) of human tissue substitutes relative to human tissues for different charged particles interaction

4.6 Discussion

In general, variation of effective atomic number (Z_{eff}) and electron density (N_e) was observed for all materials in the entire energy region under study. The significant variation of these curves over the keV-MeV energy range is confirming the comment by (Hine 1952) that, the effective atomic number Z_{eff} of multi-element material cannot be represented by a single number throughout an extended energy range of ionizing radiation. Beside, this variation show that the use of a single (Z_{eff}) value may be problematic if this energy dependence is not counted for. Effective atomic number (Z_{eff}) have less energy dependence at energies around and higher than 1.0 MeV, 10 MeV, 25 MeV, 30 MeV and 40 MeV for proton, ^4He , ^{11}B , ^{12}C and ^{16}O ion interaction, respectively. Beside that the peaks of effective atomic number (Z_{eff}) are shifted toward higher energies with the increase of incident ion Z number. These

peaks might be due to the fact that the stopping power exhibits a pronounced maximum at an energy that depends on the ion species due to the interplay of decreasing effective charge, increasing scattering cross sections and decreasing maximum energy transfer. For each of the considered substances in this study the lower and upper limit of their Z_{eff} is dictated by the range of atomic numbers of the constituent elements. Whereas the least value of Z_{eff} does not go below the least atomic number of the constituent element and the maximum value of Z_{eff} is also limited by the highest atomic number of the constituent element.

Considering the variation of (Z_{eff}), which is equivalent to taking into account the variation of mass stopping power with charged particles energy, it is found that gels (polymer and Fricke) typically match water in terms of (Z_{eff}) better than water matches tissue and the slight differences in effective atomic number between water and polymeric gels and Fricke gel may be considered negligible. The radiological properties of the hypoxic polymer gels typically match water better than normoxic polymer gels; this may be due to the higher mass density of the normoxic polymer gel dosimeters and the higher concentration of water in the hypoxic polymer gel formulation.

In spite of its lack of water equivalence at low and medium energies, the PRESAGE formulation dosimeter offers some advantages in terms of ease of use and its lack of water equivalence may be overcome with dosimetric correction factors. These results indicate that Fricke gel and the different polymer gel formulations is more radiological water equivalent than the PRESAGE formulation in the entire energy region, Although, the PRESAGE dosimeters show good water equivalence properties only in high energies above (2.0 MeV, 10 MeV, 350 MeV, 375 MeV, and 500 MeV for proton, ^4He , ^{11}B , ^{12}C and ^{16}O ion respectively).

4.7 Comparison with previous studies

Comparison with previous studies is undertaken with values of (Z_{eff}) of liquid water reported in different studies. This is because that water is a reference material in dosimetry.

Guru Prasad et al (1997),[65] have calculate the mean value of effective atomic number (Z_{eff}) for water and Nylon6 in the energy range from 1MeV to

100MeV of proton, they found a value of 3.3 for both water and nylon6. Murat kurdierk et al. (2015),[64] found that the mean value of (Z_{eff}) for water and nylon6 is also equals to 3.3 for proton interaction, which agreed with the interpolated values of (Z_{eff}) for water obtained in the present study that record a mean value of 3.3 in the energy region from 1keV to 200 MeV. Parthasaradhi, K. (1989) [66], has report a value of 3.2 versus 3.08 for present study, for ^4He ion interaction. Also kurudierk et al. [73] report a value of 3.13 and 3.06 of (Z_{eff}) of liquid water for total proton and ^4He ion interaction in the energy range of 0.01-1000MeV using direct method, while this study report a value of 2.99 and 3.0 for proton and ^4He ion interaction, these differences may be due to different methods of calculation or different database used. Another study by Kurudierk et al. (2015) [71] report values of 2.83 viz 2.83, 2.86 viz 2.84 and 2.88 viz 2.88 for proton, ^4He , ^{11}B and ^{12}C ion interaction respectively, in the energy range of 10KeV-10 MeV using SRIM database. We can conclude that the results of this study are in consistence with previous investigations. Small differences arise between values of effective atomic number due to different calculation methods or different sets of data of stopping power used.

4.6 Conclusion

In the present study, effective atomic numbers (Z_{eff}) different materials of dosimetric interest have been calculated for total proton, ^4He , ^{11}B , ^{12}C and ^{16}O ion interactions in the wide energy region 10keV– 1 GeV. The effective atomic number (Z_{eff}) and electron density N_e of the materials were calculated based on its mass stopping power and mass stopping cross section, which is generated from SRIM software. Radiological properties with respect to effective atomic number and electron density of all materials such as (Z_{eff}) difference percent relative (DR)% to water and tissues was calculated to evaluate their simulation accuracy of water and respective human tissue substitute. The effective atomic number (Z_{eff}) values of all materials were varying throughout the whole energy range of incident ions. Water match human tissue less than polymer and Fricke gels do, while Polymer gels and Fricke gels are matching water well, where as Fricke gel is more matching than polymer gels. Also, the PRESAGE dosimeters show good water equivalence properties only in high energies.

We conclude that MAGIC is an excellent tissue equivalent material for Lung Tissue, ICRP and Muscle, Skeletal (ICRP ICRU-201) throughout the whole range, Fricke and BANG-1 gel are an excellent tissue equivalent for Lung Tissue, ICRP, Muscle, Skeletal (ICRP ICRU-201) and, Striated (ICRP ICRU-202) throughout low and high energy for proton interaction. All three gels show high differences with adipose tissue at all energies. when it come to PRESAGE gel, it is observed that PRESAGE could be considered as a good tissue equivalent to Lung Tissue, ICRP, Muscle, Skeletal (ICRP ICRU-201) and, Striated (ICRP ICRU-202) throughout mid and high range of proton energy under study. Adipose tissue show the highest difference % for all dosimeters studied, none of dosimeters could simulate it above 1.0 MeV of proton energy.

4.7 Recommendations

- Determination of radiological properties for interaction of ion with different materials used in many applications could be done using effective atomic number (Z_{eff}) and electron density (N_e) as characterization tool
- Calculation of effective atomic number (Z_{eff}) and electron density (N_e) for heavy charged ion interaction using different computational methods such as direct method.
- Calculation of effective atomic number (Z_{eff}) and electron density (N_e) for light charged particles such electron mion interaction with materials.
- Calculation of stopping power using different databases just like NIST (National Institute of Standard and Technology) database [90].

REFERENCES

- [1] Kurudirek, M., 2016. Effective atomic number, energy loss and radiation damage studies in some materials commonly used in nuclear applications for heavy charged particles such as H, C, Mg, Fe, Te, Pb and U. *Radiation Physics and Chemistry*, 122, pp.15-23.
- [2] Wilson, R.R., 1946. Radiological use of fast protons. *Radiology*, 47(5), pp.487-491.
- [3] Zhang, R., Taddei, P.J., Fitzek, M.M. and Newhauser, W.D., 2010. Water equivalent thickness values of materials used in beams of protons, helium, carbon and iron ions, *Physics in Medicine & Biology*, 55(9), p.248.
- [4] Tommasino, F., Scifoni, E. and Durante, M., 2015. New ions for therapy *International Journal of Particle Therapy* 2 (3), 428–438. URL: [http://dx. doi. org/10.14338/IJPT-15-00027.1](http://dx.doi.org/10.14338/IJPT-15-00027.1).
- [5] Mayer, M., Eckstein, W., Langhuth, H., Schiettekatte, F. and Von Toussaint, U., 2011. Computer simulation of ion beam analysis: Possibilities and limitations. *Nuclear Instruments and Methods in Physics Research Section B: Beam Interactions with Materials and Atoms*, 269(24), pp.3006-3013.
- [6] Podgorsak, E.B., 2003. *Review of radiation oncology physics: a handbook for teachers and students*. Vienna, Austria: IAE Agency.
- [7] Attix, F.H., 2008. *Introduction to radiological physics and radiation dosimetry*. John Wiley & Sons.
- [8] Rosenberg, I., 2008. *Radiation oncology physics: a hand book for teachers and students*, *British journal of cancer*, 98 (5), pp. 1020- 1020.
- [9] Vatnitsky, S. and Andreo, P., 2002. *Codes of practice and protocols for the dosimetry in reference conditions of proton and ion beams*.
- [10] Baldock, C., 2017. *Review of gel dosimetry: a personal reflection*. In *Journal of Physics: Conference Series* (Vol. 777, No. 1, p. 012029). IOP Publishing.

- [11] Hurley, C., McLucas, C., Pedrazzini, G. and Baldock, C., 2006. High-resolution gel dosimetry of a HDR brachytherapy source using normoxic polymer gel dosimeters: preliminary study. *Nuclear Instruments and Methods in Physics Research Section A: Accelerators, Spectrometers, Detectors and Associated Equipment*, 565(2), pp.801-811.
- [12] Murty, R.C., 1965. Effective atomic numbers of heterogeneous materials. *Nature*, 207(4995), pp.398-399.
- [13] Hine, G.J., 1952. The effective atomic numbers of materials for various gamma ray processes. *Phys Rev*, 85, p.725.
- [14] Manohara, S.R., Hanagodimath, S.M., Thind, K.S. and Gerward, L., 2008. On the effective atomic number and electron density: a comprehensive set of formulas for all types of materials and energies above 1 keV. *Nuclear Instruments and Methods in Physics Research Section B: Beam Interactions with Materials and Atoms*, 266(18), pp.3906-3912.
- [15] Manohara, S.R., Hanagodimath, S.M. and Gerward, L., 2011. Energy absorption buildup factors of human organs and tissues at energies and penetration depths relevant for radiotherapy and diagnostics. *Journal of applied clinical medical physics*, 12(4), pp.296-312.
- [16] Grinyov, B., Ryzhikov, V., Lecoq, P., Naydenov, S., Opolonin, A., Lisetskaya, E., Galkin, S. and Shumeiko, N., 2007. Dual-energy radiography of bone tissues using ZnSe-based scintielectronic detectors. *Nuclear Instruments and Methods in Physics Research Section A: Accelerators, Spectrometers, Detectors and Associated Equipment*, 571(1-2), pp.399-403.
- [17] International Commission on Radiation Units and Measurements. 2011. Fundamental quantities and units for ionizing radiation (revised) – ICRU report no. 85. *Journal of the ICRU*, 11(1):pp.7–28
- [18] Khan, F. M., and Gibbons, J. P., 2014. Khan's the physics of radiation therapy. Lippincott Williams & Wilkins. (Fifth edition , page: 58 chapter 5-1)

- [19] Bohr, N., 1915. XLII. On the Quantum theory of radiation and the structure of the atom. The London, Edinburgh, and Dublin philosophical magazine and Journal of Science, 30(177), pp.394-415.
- [20] Ahmed, S. N., 2007. Physics and engineering of radiation detection. Academic Press. pp.110-113.
- [21] Ziegler J. F. Biersack J. P. and Ziegler M. D. 2015. SRIM – The Stopping and Range of Ions in Matter, pp.2.33-2.37.
- [22] Bragg, W. H. and Kleeman, R., 1905. On the Alpha Particles of Radium, and Their Loss of Range in Passing Through Various Atoms and Molecules. The London, Edinburgh, and Dublin Philosophical Magazine and Journal of Science, 10(57), pp.318–340.
- [23] Berger, M.J., Inokuti, M., Andersen, H.H., Bichsel, H., Powers, D., Seltzer, S.M., Thwaites, D. and Watt, D.E., 1993. Report 49. Journal of the International Commission on Radiation Units and Measurements, (2), pp. 15-17.
- [24] Ziegler J. F. Biersack J. P. and Ziegler M. D. 2015. SRIM – The Stopping and Range of Ions in Matter, p. 5-17.
- [25] Sigmund, P. 2004. Stopping of heavy ions: a theoretical approach (Vol. 204). Springer Science & Business Media.
- [26] Ziegler J. F. Biersack J. P. and Ziegler M. D. 2015. SRIM – The Stopping and Range of Ions in Matter. PP (2-34)- (2-36).
- [27] Singh, K., 2002. Effective atomic number studies in different body tissues and amino acids. Indian Journal of Pure & Applied Physics, Vol. 40, pp. 442-449.
- [28] White, D.R., 1978. Tissue substitutes in experimental radiation physics. Medical physics, 5(6), pp.467-479.
- [29] Manohara, S.R., Hanagodimath, S.M., Thind, K.S. and Gerward, L., 2008. On the effective atomic number and electron density: a comprehensive set of formulas for all types of materials and energies above 1 keV. Nuclear Instruments and Methods in Physics Research Section B: Beam Interactions with Materials and Atoms, 266(18), pp.3906-3912.

- [30] Singh, T., Kaur, P. and Singh, P.S., 2007. A study of photon interaction parameters in some commonly used solvents. *Journal of Radiological Protection*, 27(1), pp.79-85.
- [31] Prasad, S.G., Parthasaradhi, K. and Bloomer, W.D., 1998. Effective atomic numbers for photoabsorption in alloys in the energy region of absorption edges. *Radiation Physics and Chemistry*, 53(5), pp.449-453.
- [32] Akkurt, I., Mavi, B., Akkurt, A., Basyigit, C., Kilincarslan, S. and Yalim, H.A., 2005. Study on Z dependence of partial and total mass attenuation coefficients. *Journal of Quantitative Spectroscopy and Radiative Transfer*, 94(3-4), pp.379-385.
- [33] Hurley, C., Venning, A. and Baldock, C., 2005. A study of a normoxic gel dosimeter comprising methacrylic acid, gelatin and tetrakis (hydroxymethyl) phosphonium chloride (MAGAT). *Applied Radiation and Isotopes*, 63(4), pp.443-456.
- [34] De Deene, Y., 2004. Essential characteristics of polymer gel dosimeters. In *Journal of Physics: Conference Series* (Vol. 3, No. 1, p. 006). IOP Publishing.
- [35] Attix, A. F., 2004. *Introduction to Radiological Physics and Radiation Dosimetry*. Weinheim, Germany: Wiley-VCH Verlag GmbH & Co. KGaA,
- [36] Gore, j. C. and Kang, Y. S., 1984. Measurement of radiation dose distributions by nuclear magnetic resonance (NMR) imaging. *Physics in Medicine & Biology*, 29(10), p.1189.
- [37] Baldock, C., 2017. Review of gel dosimetry: a personal reflection. In *Journal of Physics: Conference Series* (Vol. 777, No. 1, p. 012029). IOP Publishing.
- [38] Taylor, M.L., Franich, R.D., Trapp, J.V. and Johnston, P.N., 2008. The effective atomic number of dosimetric gels. *Australasian Physics & Engineering Sciences in Medicine*, 31(2), pp.131-138.
- [39] Watanabe, Y., Warmington, L. and Gopishankar, N., 2017. Three-dimensional radiation dosimetry using polymer gel and solid radiochromic polymer: From basics to clinical applications. *World journal of radiology*, 9(3), pp.112-125.

- [40] Singh, V.P., Badiger, N.M. and Kucuk, N., 2014. Assessment of methods for estimation of effective atomic numbers of common human organ and tissue substitutes: waxes, plastics and polymers. *Radioprotection*, 49(2), pp.115-121.
- [41] Gorjiara, T., Kuncic, Z., Doran, S., Adamovics, J. and Baldock, C., 2012. Water and tissue equivalence of a new PRESAGE® formulation for 3D proton beam dosimetry: a Monte Carlo study. *Medical physics*, 39(11), pp.7071-7079.
- [42] Goldstone, K.E., 1990. Tissue Substitutes in Radiation Dosimetry and Measurement, in: ICRU Report 44, International Commission on Radiation Units and Measurements, USA (1989).
- [43] Manohara, S.R., Hanagodimath, S.M. and Gerward, L., 2009. The effective atomic numbers of some biomolecules calculated by two methods: a comparative study. *Medical physics*, 36(1), pp.137-141.
- [44] Peter D. Bradley, 2000. The Development of a Novel Silicon Microdosimeter for High LET Radiation Therapy. A thesis: (Doctoral dissertation), University of Wollongong, Department of Engineering Physics.
- [45] Constantinou, C. (1978). Tissue substitutes for particulate radiations and their use in radiation dosimetry and radiotherapy (Doctoral dissertation). link. <http://qmro.qmul.ac.uk/jspui/handle/123456789/1718>
- [46] Manohara, S.R., Hanagodimath, S.M. and Gerward, L., 2011. Energy absorption buildup factors of human organs and tissues at energies and penetration depths relevant for radiotherapy and diagnostics. *Journal of applied clinical medical physics*, 12(4), pp.296-312.
- [47] Vandecasteele, J., Ghysel, S., Baete, S.H. and De Deene, Y., 2011. Radio-physical properties of micelle leucodye 3D integrating gel dosimeters. *Physics in Medicine & Biology*, 56(3), pp.627-651.
- [48] Sathiyaraj, P. and Samuel, E.J.J., 2017. Energy Dependent Effective Atomic Number Calculation for Newly Developed 2-Acrylamido-2-methyl propane Sulfonic Acid Polymer Gel Dosimeter. *Asian Journal of Chemistry*, 29(6) pp.1225-1228.

- [49] Podgorsak, E.B. 2005. Radiation Oncology Physics: A Handbook for Teachers and Students, STI/PUB/1196, p. 310
- [50] Jackson, D.F. and Hawkes, D.J., 1981. X-ray attenuation coefficients of elements and mixtures. Physics Reports, 70(3), pp.169-233.
- [51] Spiers, F.W., 1946. Effective atomic number and energy absorption in tissues. The British journal of radiology, 19(218), pp.52-63.
- [52] White, D.R., 1978. Tissue substitutes in experimental radiation physics. Med. Phys. Radiation Research, 76:pp. 23-31.
- [53] Manjunathaguru, V. and Umesh, T.K., 2006. Effective atomic numbers and electron densities of some biologically important compounds containing H, C, N and O in the energy range 145–1330 keV. Journal of Physics B: Atomic, Molecular and Optical Physics, 39(18), pp.3969-3981.
- [54] Cevik, U.Ğ.U.R., Bacaksiz, E.M.İ.N., Damla, N. and Çelik, A.K.İ.N., 2008. Effective atomic numbers and electron densities for CdSe and CdTe semiconductors. Radiation measurements, 43(8), pp.1437-1442.
- [55] Kurudirek, M., 2011. Estimation of effective atomic numbers of some solutions for photon energy absorption in the energy region 0.2–1.5 MeV: an alternative method. Nuclear Instruments and Methods in Physics Research Section A: Accelerators, Spectrometers, Detectors and Associated Equipment, 659(1), pp.302-306.
- [56] Manjunatha H.C, Rudraswamy B., 2013. Study of effective atomic number and electron density for tissues from human organs in the energy range of 1 keV–100 GeV. Health Physics, 104(2),158–162.
- [57] Han, I., Aygun, M., Demir, L. and Sahin, Y., 2012. Determination of effective atomic numbers for 3d transition metal alloys with a new semi-empirical approach. Annals of Nuclear energy, 39(1), pp.56-61.
- [58] Un, A., 2013. Investigation of dopant effect on some TL dosimeters containing boron. Radiation Physics and Chemistry, 85, pp.23-35.

- [59] Kucuk, N., Cakir, M. and Isitman, N.A., 2013. Mass attenuation coefficients, effective atomic numbers and effective electron densities for some polymers. *Radiation protection dosimetry*, 153(1), pp.127-134.
- [60] White, D.R., 1977. An analysis of the Z-dependence of photon and electron interactions. *Physics in Medicine and Biology*, 22(2), pp.219-228.
- [61] Taylor, M.L., Franich, R.D., Trapp, J.V. and Johnston, P.N., 2009. Electron interaction with gel dosimeters: effective atomic numbers for collisional, radiative and total interaction processes. *Radiation research*, 171(1), pp.123-126.
- [62] Kurudirek, M., 2014. Effective atomic numbers of different types of materials for proton interaction in the energy region 1 keV–10 GeV. *Nuclear Instruments and Methods in Physics Research Section B: Beam Interactions with Materials and Atoms*, 336, pp.130-134.
- [63] Rao, B.T., Raju, M.L.N., Narasimham, K.L., Parthasaradhi, K. and Rao, B.M., 1985. Interaction of low- energy photons with biological materials and the effective atomic number. *Medical physics*, 12(6), pp.745-748.
- [64] Parthasaradhi, K., Rao, B.M. and Prasad, S.G., 1989. Effective atomic numbers of biological materials in the energy region 1 to 50 MeV for photons, electrons, and He ions. *Medical physics*, 16(4), pp.653-654.
- [65] Prasad, S.G., Parthasaradhi, K. and Bloomer, W.D., 1997. Effective atomic numbers of composite materials for total and partial interaction processes for photons, electrons, and protons. *Medical physics*, 24(6), pp.883-885.
- [66] Parthasaradhi, K., Rao, B.M. and Prasad, S.G., 1989. Effective atomic numbers of biological materials in the energy region 1 to 50 MeV for photons, electrons, and He ions. *Medical physics*, 16(4), pp.653-654.
- [67] Taylor, M.L., 2011. Robust determination of effective atomic numbers for electron interactions with TLD-100 and TLD-100H thermoluminescent dosimeters. *Nuclear Instruments and Methods in Physics Research Section B: Beam Interactions with Materials and Atoms*, 269(8), pp.770-773.

- [68] Kurudirek, M. 2014. Effective atomic number of different types of materials for proton interaction in the energy region 1KeV-10GeV. Nuclear instrumentation and methods B. 336, pp130-134.
- [69] Kurudirek, M., 2014. Radiation shielding and effective atomic number studies in different types of shielding concretes, lead base and non-lead base glass systems for total electron interaction: A comparative study. Nuclear Engineering and Design, 280, pp.440-448.
- [70] Kurudirek, M., 2016. Water and tissue equivalence properties of biological materials for photons, electrons, protons and alpha particles in the energy region 10 keV–1 GeV: a comparative study. International journal of radiation biology, 92(9), pp.508-520.
- [71] Kurudirek, M., 2015. Studies on heavy charged particle interaction, water equivalence and Monte Carlo simulation in some gel dosimeters, water, human tissues and water phantoms. Nuclear Instruments and Methods in Physics Research Section A: Accelerators, Spectrometers, Detectors and Associated Equipment, 795, pp.239-252.
- [72] Kurudirek, M. and Onaran, T., 2015. Calculation of effective atomic number and electron density of essential biomolecules for electron, proton, alpha particle and multi-energetic photon interactions. Radiation Physics and Chemistry, 112, pp.125-138.
- [73] Kurudirek, M., Aksakal, O. and Akkuş, T., 2015. Investigation of the effective atomic numbers of dosimetric materials for electrons, protons and alpha particles using a direct method in the energy region 10 keV–1 GeV: a comparative study. Radiation and environmental biophysics, 54(4), pp.481-492.
- [74] Büyükyıldız, M., 2017. A study of effective atomic numbers and electron densities of some vitamins for electron, H, He and C ion interactions. The European Physical Journal Plus, 132(9), pp.1-8.
- [75] Brown, S., Venning, A., De Deene, Y., Vial, P., Oliver, L., Adamovics, J. and Baldock, C., 2008. Radiological properties of the PRESAGE and PAGAT polymer dosimeters. Applied Radiation and Isotopes, 66(12), pp.1970-1974.

- [76] Gorjiara, T., Kuncic, Z., Doran, S., Adamovics, J. and Baldock, C., 2012. Water and tissue equivalence of a new PRESAGE® formulation for 3D proton beam dosimetry: a Monte Carlo study. *Medical physics*, 39(11), pp.7071-7079.
- [77] Young S. K. 1974. Human Tissues: Chemical Composition and Photon Dosimeter Data. *Radiation Research*, 57, pp. 38–45.
- [78] Ziegler, J. F., Ziegler, M. D. and Biersack, J. P., 2019. SRIM - The Stopping and Range of Ions in Matter, Version 2013.00, Available at: <http://www.srim.org>
- [79] White, D. R., Booz, J., Griffith, R.V., Spokas, J. J., Wilson, I. J. 1989. Report 44. *Journal of the International Commission on Radiation Units and Measurements*, 23(1).
- [80] Singh, K., 2002. Effective atomic number studies in different body tissues and amino acids. *Indian Journal of Pure & Applied Physics*, 40, pp.442-449.
- [81] Ziegler, J.F., Ziegler, M.D. and Biersack, J.P., 2010. SRIM–The stopping and range of ions in matter (2010). *Nuclear Instruments and Methods in Physics Research Section B: Beam Interactions with Materials and Atoms*, 268(11-12), pp.1818-1823.
- [82] Nordlund, K. and Djurabekova, F., 2014. Multiscale modelling of irradiation in nanostructures. *Journal of Computational Electronics*, 13(1), pp.122-141.
- [83] Ziegler, J.F., Ziegler, M.D. and Biersack, J.P., 2015. SRIM-The Stopping and Ranges of Ions in Matter, V15. p. 8-2.
- [84] Ziegler, J.E. and Sabin, J.A., 1995. Problems and corrections to heavy Ion Stopping Theory. IBM-Research, Yorktown, NY, U.S.A.
- [85] Ziegler, J.F., Ziegler, M.D. and Biersack, J.P., 2015. SRIM-The Stopping and Ranges of Ions in Matter, V15. Page 1-6.
- [86] Kurudirek, M., 2014. Effective atomic numbers, water and tissue equivalence properties of human tissues, tissue equivalents and dosimetric materials for total electron interaction in the energy region 10 keV–1 GeV. *Applied radiation and Isotopes*, 94, pp.1-7.

[87] Kurudirek, M., 2014. Effective atomic numbers and electron densities of some human tissues and dosimetric materials for mean energies of various radiation sources relevant to radiotherapy and medical applications. *Radiation Physics and Chemistry*, 102, pp.139-146.

[88] Taylor, M.L., Smith, R.L., Dossing, F. and Franich, R.D., 2012. Robust calculation of effective atomic numbers: The Auto- Zeff software. *Medical physics*, 39(4), pp.1769-1778.

[89] Kurudirek, M., 2016. Water and tissue equivalence properties of biological materials for photons, electrons, protons and alpha particles in the energy region 10 keV–1 GeV: a comparative study. *International journal of radiation biology*, 92(9), pp.508-520.

[90] Berger, M.J., Coursey, J.S., Zucker, M.A. and Chang, J., 2005. calculated using online database: ESTAR, PSTAR, and ASTAR: Computer Programs for Calculating Stopping-Power and Range Tables for Electrons, Protons, and Helium Ions (Version 1.2.3). [Physics nist. gov/StarS](http://physics.nist.gov/StarS), National Institute of Standards and Technology, Gaithersburg, MD.

Appendix A

Elemental composition for 3D dosimeters (weight fractions denoted as w_k)

S.N.	Material	w_H	w_C	w_N	w_O	w_{Na}	w_P	w_S	w_{Cl}	w_{Cu}	w_{Fe}	w_{Br}
1	HEAG	10.7641	5.7243	1.1452	82.0964	----	----	----	----	----	----	----
2	MAGAS	10.5087	9.3591	1.3799	78.7523	----	----	----	----	----	----	----
3	MAGAT	10.5220	9.5417	1.3660	77.6988	----	0.4064	----	0.4651	----	----	----
4	MAGIC	10.5473	9.2231	1.9316	78.8373	----	----	0.0003	----	0.0005	----	----
5	PAGAT	10.7257	6.2174	1.9688	80.2166	----	0.4064	----	0.4651	----	----	----
6	ABAGIC	10.5263	8.9630	3.1050	77.4054	----	----	0.0003	----	0.0005	----	----
7	BANG-1	10.7685	5.6936	2.0063	81.5316	----	----	----	----	----	----	----
8	BANG-2-	10.6369	5.6728	1.1452	81.7004	0.5748	----	----	----	----	----	----
9	PABIG	10.6454	6.8373	1.5649	80.9524	----	----	----	----	----	----	----
10	PAG	10.7367	6.2009	2.1804	80.8820	----	----	----	----	----	----	----
11	PRESAGE	08.9200	60.7400	04.4600	21.7200	----	----	----	3.3400	----	----	00.8400
12	PRESAGE®	09.0300	64.1000	04.9200	20.0000	----	----	5.63×10^{-3}	----	----	----	01.4000
13	Fricke Gel	10.7360	2.0000	0.6700	85.7360	0.0021	----	0.8500	0.0033	----	0.0026	----
14	Water	11.1900	----	----	88.8100	----	----	----	----	----	----	----

Appendix B

Mass density (ρ) and relative atomic weight (A_r) for 3D dosimeters:

No.	Material	Mass Density ρ (g cm ⁻³)	Relative atomic weight (A_r)
1	HEAG	0.920	14.091059001
2	MAGAS	1.000	14.022912267
3	MAGAT	1.127	14.165238265
4	MAGIC	1.040	14.098256074
5	PAGAT	1.040	14.255266906
6	ABAGIC	1.110	14.002073266
7	BANG-1	1.070	14.117667901
8	BANG-2	1.850	14.152381640
9	PABIG	1.850	14.099303754
10	PAG	1.450	14.098735843
11	PRESAGE	1.101	13.340313600
12	PRESAGE®	1.110	12.799478778
13	Fricke Gel	1.024	14.434803030
14	Water	1.000	14.321507100

Appendix C

Elemental composition for human tissues and human tissue substitutes (weight fractions denoted as w_k)

S.N.	Material	w_H	w_C	w_N	w_O	w_F	w_{Na}	w_{Mg}	w_P	w_S	w_{Cl}	w_K	w_{Ca}	w_{Fe}
1	Adipose Tissue (ICRP ICRU-103)	11.960	63.79	00.80	23.26	---	0.05	00.002	00.02	---	00.12	---	---	---
2	Lung Tissue, ICRP	10.128	10.231	02.865	75.707	Zn=.001	0.184	0.073	0.08	0.225	0.266	0.194	0.009	0.037
3	Muscle, Skeletal (ICRP ICRU-201)	10.10	10.83	2.78	75.78	---	0.08	0.02	0.18	0.24	---	---	---	---
4	Muscle, Striated (ICRP ICRU-202)	10.23	12.34	3.51	73.12	---	0.08	0.02	0.2	0.50	---	---	---	---
5	Bone, Compact (ICRU 119)	6.4	27.8	2.70	41.0	---	---	0.20	7.00	0.19	---	---	14.7	---
6	Bone, Cortical (ICRP ICRU-120)	4.72	14.43	4.20	44.61	---	---	0.22	10.50	0.32	---	---	21.00	---
7	A-150 Tissue-Equiv. Plastic (ICRU-099)	10.13	77.55	3.51	5.23	1.74	---	---	---	---	---	---	1.84	---
8	MS-20 Tissue Substitute (ICRU)	08.12	58.34	1.78	18.64	---	---	13.03	---	---	0.09	---	---	---
9	LN10/75 Lung	8.40	60.40	1.70	17.30	---	---	11.40	---	---	0.1	Si=0.7	---	---
10	Muscle Equiv. Liqu. with Sucrose (ICRU - 203)	09.82	15.62	03.55	71.01	---	---	---	---	---	---	---	---	---
11	Muscle Equiv. Liquid without Sucrose (ICRU - 204)	10.20	12.01	03.55	74.25	---	---	---	---	---	---	---	---	---
12	B-100 Bone-Equiv. Plastic (ICRU-111)	06.55	53.69	02.15	03.21	16.74	---	---	---	---	---	---	17.66	---

Appendix D

Mass density (ρ) and relative atomic weight (A_r) of human tissues and human tissue substitutes

No.	Material	Mass Density $\rho(\text{g cm}^{-3})$	Relative atomic weight (A_r)
1	Adipose Tissue (ICRP ICRU-103)	0.920	11.6765166
2	Lung Tissue, ICRP		14.196680552
3	Muscle, Skeletal (ICRP ICRU-201)	1.040	14.0720007
4	Muscle, Striated (ICRP ICRU-202)	1.040	14.0209213
5	Bone, Compact (ICRU 119)	1.850	18.510519
6	Bone, Cortical (ICRP ICRU-120)	1.850	21.3257112
7	A-150 Tissue-Equiv. Plastic (ICRU-099)	1.127	11.8130715
8	MS-20 Tissue Substitute (ICRU)	1.000	13.5194544
9	LN10-75 LUNG		13.348087
10	Muscle Equiv. Liquid with Sucrose (ICRU - 203)	1.110	13.8332422
11	Muscle Equiv. Liquid without Sucrose (ICRU - 204)	1.070	13.9218431
12	B-100 Bone-Equiv. Plastic (ICRU-111)	1.450	17.5594502

Appendix E

Basic statistical information on the variation of the effective atomic number (Z_{eff}) of 3D dosimeters, for Proton (^1H), ^4He , ^{11}B , ^{12}C and ^{16}O ions interaction. (1) HEAG (2) MAGAS (3) MAGAT (4) MAGIC (5) PAGAT (6) ABAGIC (7) BANG-1 (8) BANG-2 (9) PABIG (10) PAG (11) PRESAGE (12) PRESAGE[®] (13) Fricke Gel (14) Water.

S.N.	Proton				^4He ion				^{11}B ion				^{12}C ion				^{16}O ion			
	Mean	STD	Min	Max	Mean	STD	Min	Max	Mean	STD	Min	Max	Mean	STD	Min	Max	Mean	STD	Min	Max
1	3.10	0.24	2.29	3.35	3.13	0.23	2.65	3.42	3.08	0.32	2.44	3.47	3.09	0.32	2.44	3.47	3.09	0.32	2.45	3.47
2	3.14	0.23	2.39	3.38	3.17	0.23	2.67	3.45	3.12	0.32	2.47	3.50	3.12	0.32	2.47	3.50	3.12	0.32	2.47	3.50
3	3.14	0.23	2.40	3.38	3.17	0.23	2.67	3.45	3.12	0.32	2.47	3.50	3.12	0.32	2.47	3.50	3.12	0.32	2.48	3.50
4	3.14	0.23	2.39	3.38	3.17	0.23	2.67	3.46	3.12	0.32	2.47	3.51	3.12	0.33	2.47	3.65	3.12	0.32	2.47	3.50
5	3.11	0.23	2.35	3.36	3.14	0.23	2.66	3.44	3.09	0.32	2.45	3.48	3.09	0.32	2.44	3.47	3.10	0.32	2.45	3.48
6	3.13	0.24	1.91	3.37	3.16	0.23	2.67	3.45	3.12	0.32	2.46	3.50	3.12	0.32	2.47	3.50	3.12	0.32	2.47	3.50
7	3.10	0.23	2.33	3.35	3.13	0.23	2.65	3.43	3.09	0.32	2.44	3.47	3.09	0.32	2.44	3.47	3.09	0.32	2.44	3.47
8	3.12	0.24	2.34	3.37	3.15	0.24	2.66	3.45	3.10	0.33	2.45	3.49	3.10	0.32	2.45	3.49	3.10	0.32	2.46	3.49
9	3.11	0.23	2.34	3.35	3.15	0.23	2.66	3.44	3.10	0.32	2.45	3.49	3.10	0.32	2.46	3.49	3.10	0.32	2.46	3.49
10	3.10	0.23	2.34	3.35	3.14	0.23	2.65	3.43	3.09	0.32	2.44	3.48	3.09	0.32	2.45	3.48	3.09	0.32	2.45	3.47
11	3.36	0.17	2.76	3.76	3.30	0.18	2.88	3.51	3.34	0.28	2.70	3.64	3.34	0.28	2.70	3.63	3.34	0.28	2.70	3.63
12	3.31	0.16	2.75	3.68	3.26	0.18	2.87	3.52	3.37	0.29	2.72	3.67	3.32	0.28	2.69	3.65	3.32	0.28	2.69	3.64
13	3.27	0.27	2.30	3.51	3.07	0.23	2.65	3.32	3.09	0.33	2.44	3.51	3.09	0.33	2.44	3.51	3.09	0.33	2.45	3.51
14	2.99	0.31	2.34	3.30	3.00	0.22	2.61	3.25	3.03	0.33	2.40	3.44	3.04	0.32	2.40	3.43	3.04	0.32	2.41	3.43

Appendix F

Basic statistical information on variations of electron density (N_e) of the 3D dosimeters for Proton (^1H), ^4He , ^6B , ^{12}C and ^{16}O ions interaction, (1) HEAG (2) MAGAS (3) MAGAT (4) MAGIC (5) PAGAT (6) ABAGIC (7) BANG-1 (8) BANG-2 (9) PABIG (10) PAG (11) PRESAGE (12) PRESAGE[®] (13) Fricke Gel (14) Water.

N_e	Proton				^4He ion				^{11}B ion				^{12}C ion				^{16}O ion			
S.N.	Mean	STD	Min	Max	Mean	STD	Min	Max	Mean	STD	Min	Max	Mean	STD	Min	Max	Mean	STD	Min	Max
1	1.32	0.10	0.98	1.43	1.30	0.10	1.08	1.41	1.32	0.14	1.04	1.48	1.32	0.14	1.04	1.48	1.32	0.14	1.05	1.48
2	1.35	0.10	1.03	1.45	1.32	0.11	1.10	1.43	1.34	0.14	1.06	1.50	1.34	0.14	1.06	1.50	1.34	0.14	1.06	1.50
3	1.34	0.10	1.02	1.44	1.31	0.10	1.09	1.41	1.33	0.14	1.05	1.49	1.33	0.14	1.05	1.49	1.33	0.14	1.05	1.49
4	1.34	0.10	1.02	1.44	1.32	0.11	1.09	1.42	1.33	0.14	1.05	1.50	1.33	0.14	1.06	1.50	1.33	0.14	1.06	1.50
5	1.31	0.10	0.99	1.42	1.29	0.10	1.07	1.40	1.31	0.14	1.03	1.47	1.32	0.14	1.04	1.48	1.32	0.14	1.04	1.47
6	1.35	0.10	0.82	1.45	1.32	0.10	1.10	1.43	1.34	0.14	1.06	1.50	1.34	0.14	1.06	1.50	1.34	0.14	1.06	1.50
7	1.32	0.10	1.00	1.43	1.30	0.10	1.08	1.41	1.32	0.14	1.04	1.48	1.32	0.14	1.04	1.48	1.32	0.14	1.04	1.48
8	1.33	0.10	1.00	1.43	1.30	0.11	1.08	1.41	1.32	0.14	1.04	1.49	1.32	0.14	1.04	1.49	1.32	0.14	1.05	1.49
9	1.33	0.10	1.00	1.44	1.31	0.11	1.09	1.41	1.32	0.14	1.05	1.49	1.33	0.14	1.05	1.49	1.33	0.14	1.05	1.49
10	1.33	0.10	1.00	1.43	1.30	0.10	1.08	1.41	1.32	0.14	1.04	1.49	1.32	0.14	1.04	1.48	1.32	0.14	1.05	1.48
11	1.52	0.08	1.25	1.70	1.49	0.09	1.29	1.59	1.51	0.13	1.22	1.64	1.51	0.13	1.22	1.64	1.51	0.13	1.22	1.64
12	1.56	0.08	1.29	1.73	1.53	0.09	1.33	1.65	1.59	0.13	1.28	1.72	1.56	0.13	1.27	1.72	1.56	0.13	1.27	1.71
13	1.36	0.11	0.96	1.46	1.27	0.11	1.05	1.39	1.29	0.14	1.02	1.46	1.29	0.14	1.02	1.46	1.29	0.14	1.02	1.46
14	1.26	0.13	0.99	1.39	1.26	0.10	1.04	1.37	1.28	0.14	1.01	1.44	1.28	0.14	1.01	1.44	1.28	0.14	1.01	1.44

Appendix G

Basic Statistical information on the variation of the effective atomic number (Z_{eff}) of human tissues and human tissue substitutes for Proton (^1H), ^4He , ^{11}B , ^{12}C and ^{16}O ions interaction: (1) Adipose Tissue (ICRP ICRU-103), (2) Lung Tissue, ICRP (3) Muscle, Skeletal (ICRP ICRU-201) (4) Muscle, Striated (ICRP ICRU-202), (5) Bone, Compact (ICRU-119), (6) Bone, Cortical (ICRP ICRU-120) (7) A-150 Tissue Equiv. Plastic (ICRU-099), (8) MS_20 Tissue Substitute (ICRU-200), (9) LN10-75 LUNG, (10) Muscle Equiv. Liq. with Sucrose (ICRU - 203), (11) Muscle Equiv. Liq. without Sucrose (ICRU - 204), (12) B-100, Bone-Equivalent Plastic (ICRU-111).

S.N.	Proton				^4He				^{11}B ion				^{12}C ion				^{16}O ion			
	Z_{eff}	Mean	STDV	Min	Max	Mean	STDV	Min	Max	Mean	STDV	Min	Max	Mean	STDV	Min	Max	Mean	STDV	Min
1	2.82	0.14	2.50	2.95	2.91	0.18	2.68	3.34	3.03	0.28	2.49	3.50	3.03	0.28	2.50	3.49	3.04	0.28	2.50	3.47
2	3.13	0.33	2.41	3.44	3.15	0.23	2.70	3.39	3.16	0.33	2.50	3.57	3.17	0.33	2.50	3.57	3.17	0.33	2.50	3.57
3	3.14	0.33	2.42	3.45	3.16	0.23	2.70	3.39	3.17	0.33	2.50	3.57	3.16	0.32	2.50	3.55	3.17	0.33	2.51	3.57
4	3.18	0.34	2.45	3.48	3.1	0.22	2.70	3.36	3.15	0.32	2.50	3.53	3.16	0.32	2.50	3.55	3.16	0.32	2.50	3.53
5	4.13	0.23	3.60	4.38	3.97	0.36	3.28	4.32	3.79	0.45	2.93	4.41	3.79	0.44	2.93	4.41	3.78	0.43	2.94	4.41
6	4.81	0.39	3.86	5.25	4.52	0.57	3.65	5.15	4.33	0.68	3.31	5.18	4.32	0.67	3.32	5.18	4.31	0.66	3.33	5.18
7	3.02	0.20	2.59	3.39	3.46	0.19	2.97	3.65	3.21	0.29	2.64	3.66	3.32	0.28	2.71	3.69	3.22	0.29	2.64	3.64
8	3.42	0.35	2.66	3.97	3.48	0.21	2.96	3.69	3.47	0.29	2.79	3.75	3.48	0.29	2.79	3.75	3.48	0.29	2.80	3.74
9	3.36	0.33	2.65	3.88	3.40	0.23	2.73	3.60	3.44	0.29	2.77	3.73	3.44	0.29	2.77	3.73	3.44	0.29	2.78	3.73
10	3.18	0.34	2.44	3.47	3.20	0.23	2.73	3.42	3.20	0.33	2.53	3.59	3.19	0.30	2.55	3.55	3.20	0.32	2.53	3.59
11	3.12	0.32	2.42	3.42	3.14	0.22	2.70	3.37	3.16	0.32	2.49	3.54	3.16	0.32	2.49	3.55	3.16	0.32	2.50	3.54
12	3.96	0.17	3.61	4.26	3.83	0.28	3.21	4.12	3.73	0.36	2.92	4.12	3.72	0.36	2.92	4.12	3.72	0.36	2.92	4.12

Appendix H

Basic statistical information on variation of electron density (Ne) of human tissues and human tissue substitutes for Proton (^1H), ^4He , ^{11}B , ^{12}C and ^{16}O ions interaction, (1) Adipose Tissue (ICRP ICRU-103), (2) Lung Tissue, ICRP (3) Muscle, Skeletal (ICRP ICRU-201) (4) Muscle, Striated (ICRP ICRU-202), (5) Bone, Compact (ICRU-119), (6) Bone, Cortical (ICRP ICRU-120) (7) A-150 Tissue Equiv. Plastic (ICRU-099), (8) MS_20 Tissue Substitute (ICRU-200), (9) LN10-75 LUNG, (10) Muscle Equiv. Liq. with Sucrose (ICRU - 203), (11) Muscle Equiv. Liq. without Sucrose (ICRU - 204), (12) B-100, Bone-Equivalent Plastic (ICRU-111).

S.N.	Proton				^4He				^{11}B ion				^{12}C ion				^{16}O ion			
	Ne	Mean	STDV	Min	Max	Mean	STDV	Min	Max	Mean	STDV	Min	Max	Mean	STDV	Min	Max	Mean	STDV	Min
1	1.45	0.07	1.29	1.52	1.50	0.09	1.38	1.72	1.56	0.14	1.29	1.80	1.56	0.14	1.29	1.80	1.57	0.14	1.29	1.79
2	1.33	0.14	1.02	1.46	1.34	0.10	1.15	1.44	1.34	0.14	1.06	1.51	1.34	0.14	1.06	1.51	1.34	0.14	1.06	1.51
3	1.34	0.14	1.03	1.47	1.35	0.10	1.16	1.45	1.36	0.14	1.07	1.53	1.35	0.14	1.07	1.52	1.36	0.14	1.07	1.53
4	1.36	0.14	1.04	1.49	1.35	0.09	1.16	1.44	1.36	0.14	1.07	1.52	1.36	0.14	1.07	1.52	1.36	0.14	1.07	1.52
5	1.34	0.07	1.17	1.42	1.29	0.12	1.07	1.40	1.23	0.15	0.95	1.43	1.23	0.14	0.95	1.43	1.23	0.14	0.96	1.43
6	1.36	0.11	1.09	1.48	1.28	0.16	1.03	1.46	1.22	0.19	0.94	1.46	1.22	0.19	0.94	1.46	1.22	0.19	0.94	1.46
7	1.54	0.10	1.32	1.73	1.76	0.10	1.51	1.86	1.64	0.15	1.35	1.87	1.69	0.14	1.38	1.88	1.64	0.15	1.35	1.85
8	1.52	0.16	1.19	1.77	1.55	0.09	1.32	1.64	1.55	0.13	1.24	1.67	1.55	0.13	1.24	1.67	1.55	0.13	1.25	1.67
9	1.52	0.15	1.20	1.75	1.54	0.10	1.23	1.62	1.55	0.13	1.25	1.68	1.55	0.13	1.25	1.68	1.55	0.13	1.25	1.68
10	1.38	0.15	1.06	1.51	1.39	0.10	1.19	1.49	1.39	0.14	1.10	1.56	1.39	0.13	1.11	1.55	1.39	0.14	1.10	1.56
11	1.35	0.14	1.05	1.48	1.36	0.10	1.17	1.46	1.36	0.14	1.08	1.53	1.36	0.14	1.08	1.54	1.37	0.14	1.08	1.53
12	1.36	0.06	1.23	1.46	1.31	0.10	1.10	1.41	1.28	0.12	1.00	1.41	1.28	0.12	1.00	1.41	1.27	0.12	1.00	1.41

EFFECTIVE ATOMIC NUMBERS AND ELECTRON DENSITIES OF GEL DOSIMETERS FOR He, B, C, AND O HIGHLY CHARGED PARTICLES INTERACTION IN THE ENERGY RANGE 10 keV–100 MeV

M. S. ABDELRAHIM^a, KH. M. HAROUN^c, A. H. ALFAKI^a, H. S. BUSH^d,
O. ALDAGHRI^b, M. H. EISA^{a,b,*}

^aPhysics Department, College of Science, Sudan University of Science and Technology, Khartoum 11113, Sudan

^bDepartment of Physics, College of Sciences, Imam Mohammad Ibn Saud Islamic University (IMSIU), Riyadh 11623, Saudi Arabia

^cDepartment of Physics, College of Education, Alzaiem Alazhari University, Omdurman, Sudan

^dDepartment of Physics, faculty of Sciences, Islamic University of Madinah, P.O. POX 170, Madinah, Saudi Arabia

The radiological properties of different gel dosimeter formulations including six normoxic and four hypoxic polymeric gels, BRESAGE, PREAGE®, Fricke gel dosimeters, and water were investigated using SRIM code. The effective atomic number Z_{eff} and electron density (N_e) for heavily charged particle interaction were calculated and performed for Helium (He), Boron (B), Carbon (C), and Oxygen (O) ion interactions in the energy range from 10 keV to 100 MeV. Variations of effective atomic number (Z_{eff}) and electron density (N_e) with the kinetic energy of ions, (He, B, C, and O), were observed over the whole energy range for all studied materials. Variations of Z_{eff} for He ion are up to 21%, 25%, and 20% for hypoxic and normoxic gels, Fricke gel, and PRESAGE gels, respectively. For other ions, variation is up to 34% for hypoxic and normoxic gels as well as Fricke gel, and 32% for PRESAGE gels. It is found that the maximum values of Z_{eff} have been observed in intermediate energies between 1-10 MeV for all dosimeters, except for PRESAGE and PRESAGE®, where maximum values were observed in the relatively low energy range 10 – 100 keV. For effective atomic number relative to water, polymeric gels and Fricke gel showed better water equivalence with differences <7%, while PRESAGE and PRESAGE® showed high differences up to 17.5%, 22%, 21%, and 25% for He, B, C, and O ion, respectively. Gels found to be most relative to water are (Fricke, HEAG, and PAG), Fricke and HEAG), (Fricke and HEAG), and (Fricke, HEAG, and BANG-1) for He, B, C, and O ion interactions, respectively. Data reported here gives essential information about the interaction of different types of charged particles with different materials and could be useful in the energy range specified.

(Received October 28, 2020; Accepted January 13, 2021)

Keywords: Effective atomic number, Electron density, Highly charged ions, Gel dosimeters, SRIM code

1. Introduction

Effective atomic number Z_{eff} and electron density N_e of materials are of the most convenient parameters that represent characteristics of multi-element materials for radiation interaction depending mainly on the atomic number of its constituent elements [1], which result in different radiation interaction probabilities in different energy ranges and the energy of incident radiation; hence, it could not be expressed with one single number. Since it is energy dependant parameter, it could be used to evaluate the radiological properties of compounds, mixtures, and composites. Atomic numbers Z_{eff} and N_e are widely used in radiation dosimetry, radiation therapy, medical diagnosis, and in many technical and medical fields.

* Corresponding author: mheisas@hotmail.com

Polymeric gel dosimeters are fabricated from radiation-sensitive chemicals [2] which are polymerized as a function of radiation absorbed dose. It gains its importance from its ability to record radiation dose distribution in three dimensions compared to other types of dosimeters.

In the application of gel dosimetry, consideration of the radiological properties of these materials for different types of radiation in different energy regions is a very important issue. This importance increases with the increasing use of highly charged particles in medical applications, including both therapeutic and diagnostic. In literature, several studies of Z_{eff} in gel dosimeters are being carried out for photon [3] and electron interactions [4], but studies regarding highly charged particles are very few. Recently, a method adopted by Kurudirek [5–8] for calculation of effective atomic number for highly charged particle interaction has been used to investigate Z_{eff} for different materials, such as human tissues, dosimetric materials [9,10], vitamins, and biomolecules [5–6], [11,12].

No study is carried out regarding Z_{eff} and N_e of gel dosimeters for charged particle interaction except work done by Kurudirek [9] for a limited number of gels within limited energy range, thus this is the promotion behind this work.

The present study deals with calculations of the effective atomic number Z_{eff} and electron density N_e of gel dosimeters developed for 3D optical dosimetry, which includes Fricke gel, four hypoxic and six normoxic polymeric gel dosimeter formulations, PRESAGE gel, and PRESAGE®. The calculation is performed in the energy range 10 keV – 100 MeV for He, B, C, and O ion total interactions.

2. Materials and methods

The elemental composition of gel dosimeters studied is available for polymeric gels and Fricke gel in [3], PRESAGE gel [13], and PRESAGE® [14]. Their effective atomic number and electron density have been calculated for energy range 10 keV – 100 MeV, using the method adopted by Kurudirek [5–8] for highly charged particle interaction.

2.1. Stopping powers calculation

Mass stopping powers of constituent elements of the gel molecule were obtained using the Stopping and Range of Ions in Matter (SRIM) code [15-17], spanning the range from 10 keV to 100 MeV. The mass stopping power values for the selected gels were estimated using the mixture rule (Bragg's additive law) [18] and the elemental stopping of the constituent elements obtained above are as follows:

$$(S/\rho)_{gel} = \sum_{i=1}^n w_i (S/\rho)_i \quad (1)$$

where $(S/\rho)_i$ is the mass stopping of i^{th} element in the molecule of gel, n is the number of constituent elements and w_i is the weight fraction of the i^{th} element in a molecule of gel so that

$$\sum_{i=1}^n w_i = 1 \quad (2)$$

2.2. Stopping cross-sections (σ_{gel})

Stopping cross-sections were obtained by dividing the mass stopping power of the gel by the total number of atoms present in one gram of the gel:

$$\sigma_{gel} = \frac{(S/\rho)_{gel}}{N_A \sum_i (w_i/A_i)} (\text{barn/atom}) \quad (3)$$

where $N_A (= 6.022 \times 10^{23})$ is Avogadro's number in atom g^{-1} , w_i is the weight fraction of the i^{th} element in a molecule of gel, and A_i is the atomic weight of i^{th} element in the molecule.

2.3. Z_{eff} calculation

The Z_{eff} values were calculated by the logarithmic interpolation of Z values between the adjacent stopping cross-section data as follows:

$$Z_{eff} = \frac{Z_1(\log \sigma_2 - \log \sigma) + Z_2(\log \sigma - \log \sigma_1)}{\log \sigma_2 - \log \sigma_1} \quad (4)$$

where (σ) is the cross-section of the material, σ_1 and σ_2 are the elemental cross-sections between which the stopping cross-section of the material lies, and Z_1 and Z_2 are the atomic numbers of the elements corresponding to σ_1 and σ_2 , respectively.

2.4. Electron density N_e

The electron density of the gels has been calculated using the following formula:

$$N_e = Z_{eff} N_A / \langle A \rangle \text{ (electrons/g)} \quad (5)$$

where N_A is the Avogadro's number and $\langle A \rangle$ is the relative atomic mass of the gel.

3. Results and discussion

Since Z_{eff} and N_e values were derived from mass stopping power data, accuracy in Z_{eff} values are due to the accuracy in stopping powers calculation using SRIM code, which is stated to be 3.9%, 3.5%, 4.6%, and 5.6% for H ion, He ion, Li ions, and (Be-U), respectively, with an overall accuracy of 4.3% [15]. The obtained values of Z_{eff} and N_e for selected energy values for the different ions are presented in Fig.1 to Fig.8. Table1 shows basic statistical information of the effective atomic numbers for all ions studied. Figure 1 below shows that variation in Z_{eff} and N_e values have been observed through the entire energy range (10 keV–100 MeV) for all types of charged particles studied.

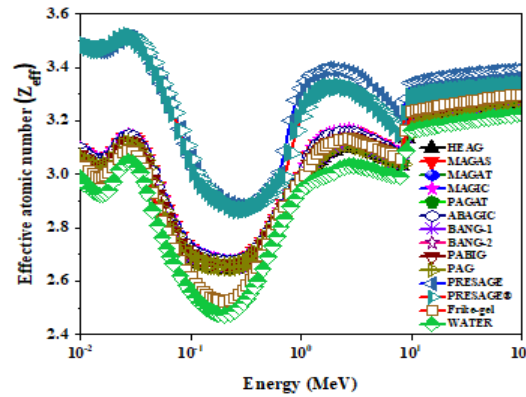


Fig. 1. Variation of effective atomic number Z_{eff} of dosimetric gels with the kinetic energy of He ion.

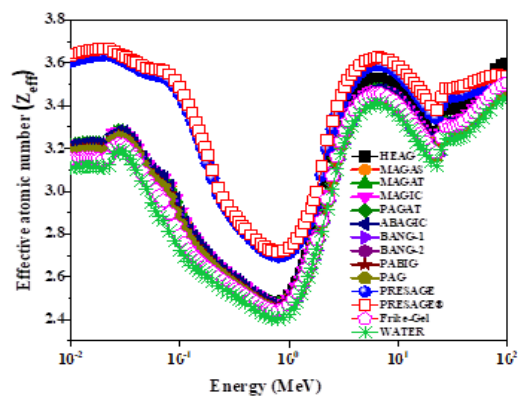


Fig. 2. Variation of effective atomic number Z_{eff} of dosimetric gels with the kinetic energy of B ion.

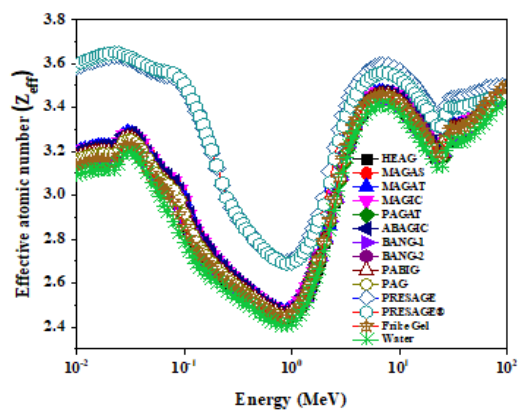


Fig. 3. Variation of effective atomic number Z_{eff} of dosimetric gels with the kinetic energy of C ion.

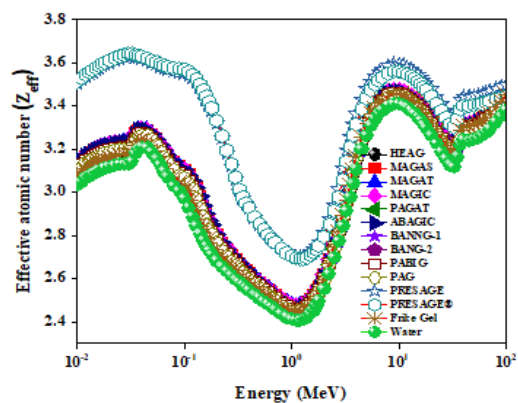


Fig. 4. Variation of effective atomic number Z_{eff} of dosimetric gels with the kinetic energy of O ion.

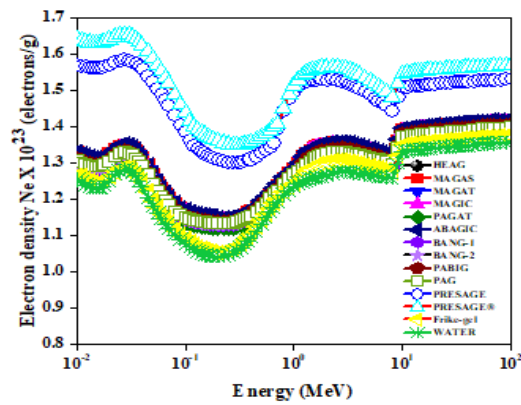


Fig. 5. Variation of electron density N_e of dosimetric gels, with the kinetic energy of He ion.

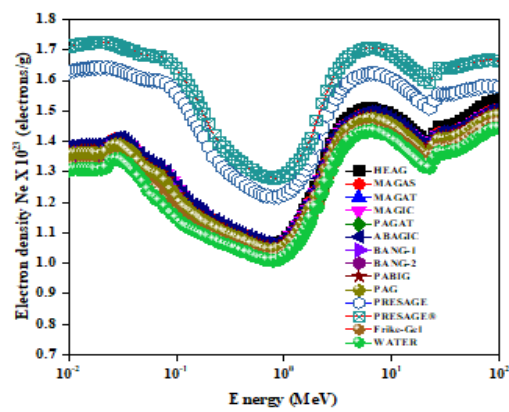


Fig. 6. Variation of electron density N_e of dosimetric gels, with the kinetic energy of B ion.

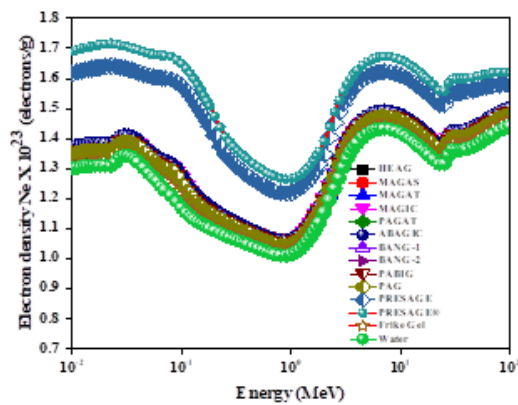


Fig. 7. Variation of electron density N_e of dosimetric gels, with the kinetic energy of C ion.

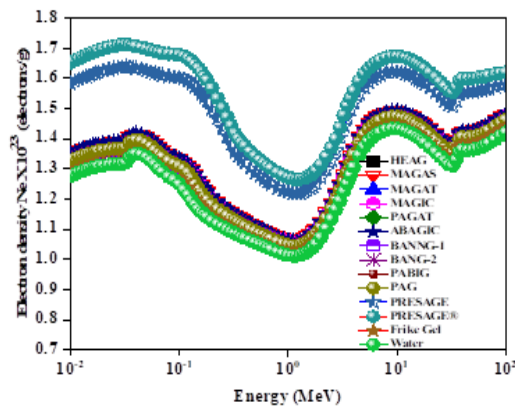


Fig. 8. Variation of electron density N_e of dosimetric gels, with the kinetic energy of O ion.

Table 1. Statistical information on Z_{eff} of the Gel dosimeters for He, B, C, and O ions. (1) HEAG (2) MAGAS (3) MAGAT (4) MAGIC (5) PAGAT (6) ABAGIC (7) BANG-1 (8) BANG-2 (9) PABIG (10) PAG (11) PRESAGE (12) PRESAGE® (13) Fricke Gel (14) Water.

S. N	He ion				B ion				C ion				O ion			
	Mean	STD	Min	Max	Mean	STD	Min	Max	Mean	STD	Min	Max	Mean	STD	Min	Max
1	3.00	0.21	2.65	3.27	3.03	0.34	2.44	3.47	3.03	0.33	2.44	3.47	3.03	0.32	2.45	3.44
2	3.04	0.21	2.67	3.30	3.06	0.34	2.47	3.50	3.06	0.33	2.47	3.50	3.06	0.32	2.47	3.47
3	3.04	0.21	2.67	3.30	3.06	0.33	2.47	3.50	3.06	0.33	2.47	3.49	3.06	0.32	2.48	3.47
4	3.04	0.21	2.67	3.31	3.07	0.34	2.47	3.51	3.07	0.33	2.47	3.50	3.06	0.32	2.47	3.47
5	3.01	0.21	2.66	3.28	3.04	0.34	2.45	3.48	3.03	0.33	2.44	3.46	3.03	0.32	2.45	3.45
6	3.04	0.21	2.67	3.30	3.06	0.34	2.46	3.50	3.06	0.33	2.47	3.49	3.06	0.32	2.47	3.47
7	3.00	0.21	2.65	3.27	3.03	0.34	2.44	3.47	3.03	0.33	2.44	3.47	3.03	0.32	2.44	3.45
8	3.02	0.21	2.66	3.29	3.04	0.34	2.45	3.49	3.04	0.34	2.45	3.49	3.04	0.33	2.46	3.46
9	3.02	0.21	2.66	3.29	3.05	0.34	2.45	3.49	3.05	0.33	2.46	3.49	3.04	0.32	2.46	3.46
10	3.01	0.21	2.65	3.28	3.04	0.34	2.44	3.48	3.04	0.33	2.45	3.47	3.03	0.32	2.45	3.45
11	3.27	0.20	2.88	3.51	3.32	0.31	2.70	3.64	3.32	0.31	2.70	3.63	3.32	0.31	2.70	3.63
12	3.24	0.19	2.87	3.52	3.35	0.32	2.72	3.67	3.31	0.31	2.69	3.65	3.31	0.31	2.69	3.64
13	2.99	0.25	2.52	3.30	3.03	0.34	2.44	3.51	3.03	0.34	2.44	3.50	3.02	0.33	2.45	3.46
14	2.93	0.24	2.47	3.22	2.98	0.34	2.40	3.44	2.98	0.34	2.40	3.43	2.97	0.32	2.41	3.41

The Z_{eff} variation for He ion is up to 21%, 25%, and 20% for hypoxic and normoxic gels, Fricke gel, and PRESAGE gels, respectively. For other ions, variation is up to 34% for hypoxic and normoxic gels, Fricke gel, and 32% for PRESAGE gels. Generally, as shown in Fig.1 to Fig.8, Z_{eff} and N_e behavior with ion energy for all dosimeters studied in this work are similar high values at low energy range (10 – 100 keV) decreasing gradually with energy increasing till reaching its minimum values (0.2 MeV for He, around 0.8 MeV for B & C, and 1.2 MeV O ion), within mid-range (100 keV – 10 MeV).

Increasing again to reach maximum values at 2.75 keV, 6.5 MeV, 7 MeV, and 9 MeV for He, B, C, and O ion, respectively, and then it decreases to a minimum at 8, 22.5, 25, and 32.5 MeV. Another sharp increase to 10, 27.5, 30, and 40 MeV for He, B, C, and O ion occurs then decreases steadily till the end of the energy range. The exception is for PRESAGE and PRESAGE® that have maximum values at low energy and high values at mid energies. Higher

values for Z_{eff} are observed in PRESAGE and PRESAGE® for all types of ions whereas the lowest values are observed in water. The peaks of Z_{eff} values are shifted toward higher energies with the increase of incident ion Z number as shown for some selected gels in Fig. 9 to Fig 12 below.

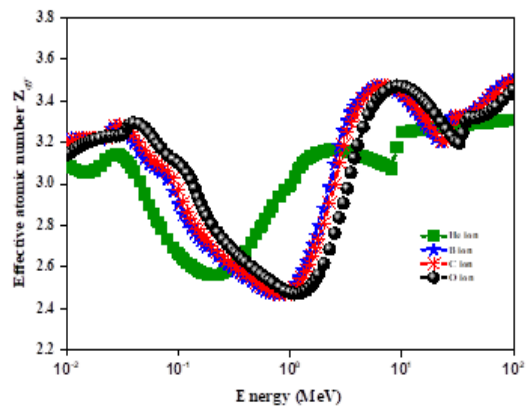


Fig. 9. Z_{eff} of selected gel dosimeters for different types of ions in MAGIC gel.

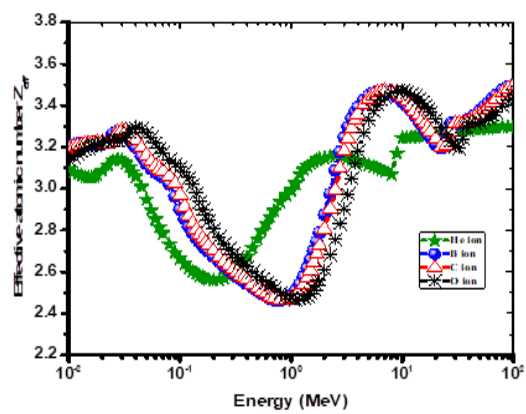


Fig. 10. Z_{eff} of selected gel dosimeters for different types of ions in ABAGIC gel.

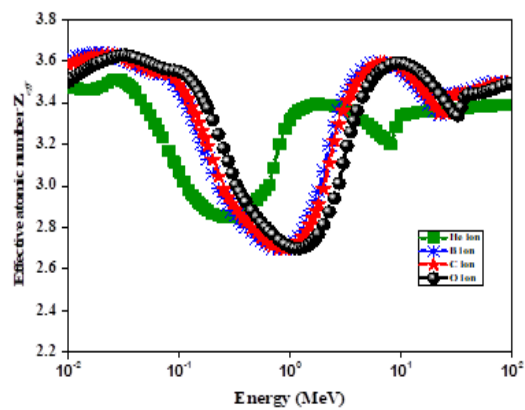


Fig. 11. Z_{eff} of selected gel dosimeters for different types of ions in PRESAGE.

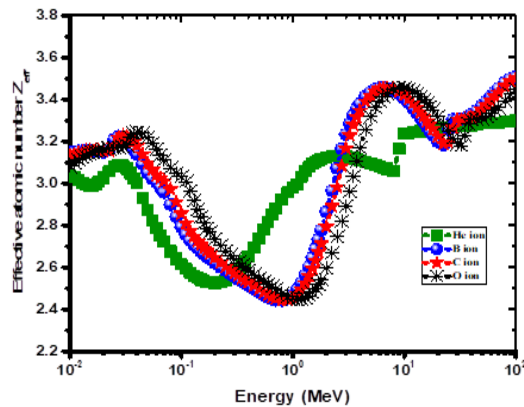


Fig. 12. Z_{eff} of selected gel dosimeters for different types of ions in Fricke gel.

A convenient method for evaluating the radiological characteristic equivalence of two materials is to compare Z_{eff} and N_e in a continuous energy region. Therefore, Z_{eff} s of the materials relative to water were also calculated to show the water equivalence of each material. It is found that Z_{eff} values of polymeric gels and Fricke gel and their behavior concerning ion energy are very close to those of water. Fig.13 to Fig.16 below shows the percentage difference of <7% for all types of incident ion. These gels could be considered as water equivalent material throughout the entire range of energy studied. PRESAGE gels show differences of up to 17.5%, 22%, 21%, and 25% for He, B, C, and O ion, respectively. It is worth saying that PRESAGE and PRESAGE@ show differences of 5% in the energy range 10 – 100 MeV of He ion. The highest differences for all gels studied occur between 40 and 300 keV energies for all ions.

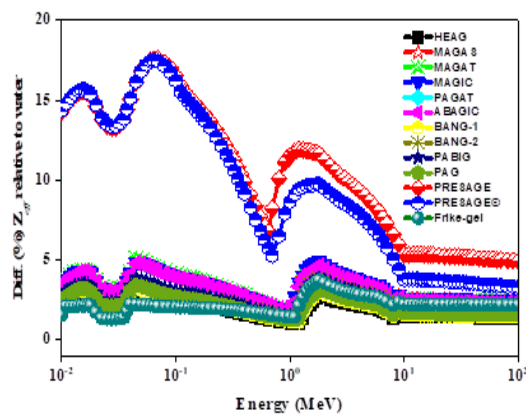


Fig. 13. Percentage difference in Z_{eff} of gel dosimeters relative to water for He ion interaction.

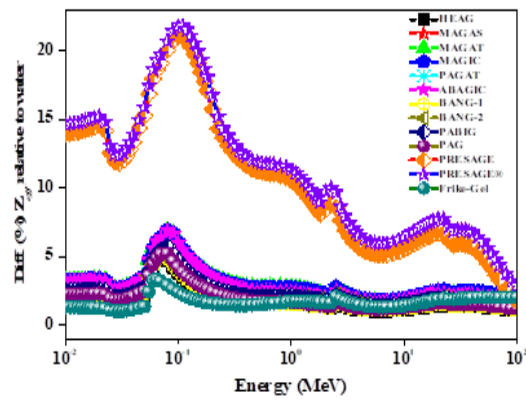


Fig. 14. Percentage difference in Z_{eff} of gel dosimeters relative to water for B ion interaction.

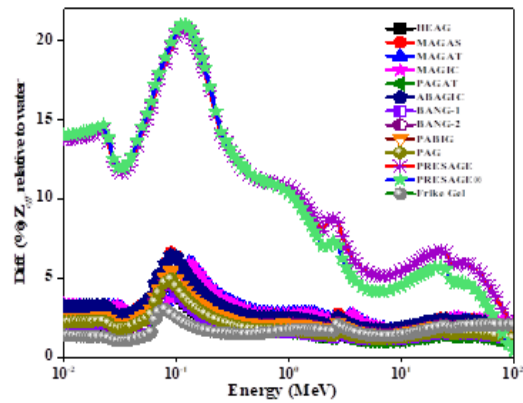


Fig. 15. Percentage difference in Z_{eff} of gel dosimeters relative to water for C ion interaction.

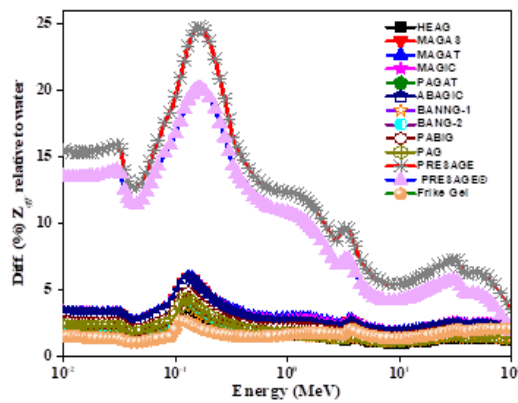


Fig. 16. Percentage difference in Z_{eff} of gel dosimeters relative to water for O ion interaction.

Fig. 5 to Fig.8 shows the variation of electron density of up to 10%, 14%, 15%, and 14% for He, B, C, and O ion, respectively, with ion energy. This variation shows the same behavior as Z_{eff} toward incident ion energy for all types of ions, which is expected since the values of N_e depends mainly on Z_{eff} . No experimental data were available concerning Z_{eff} and N_e for gels under study. There are only a few data of calculated Z_{eff} and N_e for PRESAGE, MAGAT, MAGIC, and Fricke gel interaction with He, B, and C ion in the limited energy range 0.01–10 MeV [9]. A good agreement is achieved in comparison.

4. Conclusion

In the present study, Z_{eff} and N_e of water, Fricke gel, and 10 polymeric gel dosimeters were calculated for He, B, C, and O ion interaction in the energy range 10 keV–100 MeV. We have shown that variation in Z_{eff} values is observed in the entire energy region from 10 keV to 100MeV. The lowest values of Z_{eff} were obtained in water, whereas the highest values were obtained in PRESAGE and PRESAGE[®]. These high values are due to the presence of a high Z element (Br, Z = 35) with a relatively high weight fraction within its constituents. The maximum values of Z_{eff} depend on ion type and shift toward higher energies with increasing the atomic number of the incident ion.

All polymeric gels and Fricke gel investigated found to be water-equivalent materials within the entire energy range studied. Further studies for different PRESAGE formulations regarding their water and tissue equivalence and other radiological properties are necessary when using them for dose measurements. Electron density is closely related to the effective atomic number and has the same quantitative energy dependence as Z_{eff} . Data reported here gives essential information about the interaction of different types of charged particles with different materials and could be useful in the energy range specified.

References

- [1] R. C. Murty, Nature **207**(4995), 398 (1965).
- [2] C. Baldock, IOP Publishing **777**(1), 012029 (2017).
- [3] M. L. Taylor, R. D. Franich, J. V. Trapp, P. N. Johnston, Australasian Physics & Engineering Sciences in Medicine **31**(2), 131 (2008).
- [4] M. L. Taylor, R. D. Franich, J. V. Trapp, P. N. Johnston, Radiation research **171**(1), 123 (2009).
- [5] M. Kurudirek, Nuclear Instruments and Methods in Physics Research Section B: Beam Interactions with Materials and Atoms **336**, 130 (2014).
- [6] M. Kurudirek, T. Onaran, Radiation Physics and Chemistry **112**, 125 (2015).
- [7] M. Kurudirek, Applied radiation and Isotopes **94**, 1 (2014).
- [8] M. Kurudirek, Radiation Physics and Chemistry **102**, 139 (2014).
- [9] M. Kurudirek, Detectors and Associated Equipment **795**, 239 (2015).
- [10] M. Kurudirek, O. Aksakal, T. Akkuş, Radiation and environmental biophysics **54**(4), 481 (2015).
- [11] M. Kurudirek, International Journal of Radiation Biology **92**(9), 508 (2016).
- [12] M. Büyükyıldız, The European Physical Journal Plus **132**(9), 391 (2017).
- [13] S. Brown, A. Venning, Y. De Deene, P. Vial, L. Oliver, J. Adamovics, C. Baldock, Applied Radiation and Isotopes **66**(12), 1970 (2008).
- [14] T. Gorjiara, Z. Kuncic, S. Doran, J. Adamovics, C. Baldock, Medical physics **39**(11), 7071 (2012).
- [15] J. F. Ziegler, M. D. Ziegler, J. P. Biersack, Nuclear Instruments and Methods in Physics Research Section B: Beam Interactions with Materials and Atoms **268**(11-12), 1818 (2010).

- [16] J. F. Ziegler, M. D. Ziegler, J. P. Biersack, SRIM (<http://www.srim.org/>), 12 (2014).
- [17] M. H. Eisa, A. H. A. Alfedeel, Digest Journal of Nanomaterials and Biostructures, **15**(1), 59(2020)
- [18] D. F. Jackson, D. J. Hawkes, Physics Reports **70** (3), 169 (1981).

Effective Atomic Numbers and Electron Densities of Some Human Tissues, Tissue Substitute Substances and Water for Proton, C and O Heavy Charged Particles Interaction in the Energy Range 10 keV – 1GeV

Maria S. Abdelrahim¹
A. H. Alfak¹
H. S. Bush³
S. Eltahir Ali⁴
KH. M. Haroun²
A. M. Ibraheem⁴

¹Sudan University of Science and Technology, Khartoum, Sudan

²Alzaim Alazhari University, Khartoum, Sudan

³Islamic University of Madinah, Madinah, Saudi Arabia

⁴Taif University, Taif, Saudi Arabia

Abstract. Various parameters of dosimetric interest such as effective atomic numbers and electron densities have been used to evaluate the water and tissue equivalence of some human tissues. Such as adipose tissue (ICRU-103), Lung Tissue, ICRP and muscle, skeletal (ICRP-ICRU 201), muscle, striated (ICRP-ICRU-202), Bone compact (ICRU-119), Bone, Cortical (ICRU-120), and six substitute substances, A-150 ICRU-099, LN10-75 LUNG, MS20 (ICRU-200), Muscle Equiv. Liq. with Sucrose (ICRU-203), Muscle Equiv. Liq. without Sucrose (ICRU-204), and B100 (ICRU-111). These parameters were computed for the total interactions with Proton, C ion and O ion in the wide energy range of 10KeV - 1GeV. The water and tissue equivalent properties have been investigated with respect to Z_{eff} and N_e values to evaluate their ability to be used with heavy charged particles applications. Some conclusions were drawn depending on variation of Z_{eff} throughout the energy range and tissue and water equivalency. Data reported here should be useful in determining best water and the best tissue equivalent substances for proton, C and O ion interaction within the energy range specified.

Key words: effective atomic number, electron density, heavy charged ions, water equivalence- human tissues, tissue substitutes, and SRIM code.

Introduction

With the increasing use of charged particles in various fields such as industry, medicine and agriculture, the study of their interaction with different composite materials has become an important issue for radiation physicists. For practical applications in medicine, therapy and diagnosis it is important to study charged particle interaction with dosimeters, human tissues, and substitutes which are used to simulate the human tissues and organs in diagnostic and therapeutic radiology. Charged particle therapy (CPT) is currently based on the use of protons or carbon ions for the treatment of deep-seated and/or radio-resistant tumors, which offer significant advantages in comparison to conventional megavolt photon therapy, because of the radiobiological advantages (depth to dose distribution, reduction of radiation dose in patients' body, smaller sensitivity for oxygen-depleted tissues). Charged particles now in use in CPT are ^1H , ^4He , ^{12}C , and ^{16}O , which are considered the most relevant candidates for advancing particle therapy, and is presently available in the most advanced particle therapy clinical centers (Tommasino et al., 2015: 429-438). There are various parameters used to characterize the materials in terms of radiation response such as mass stopping power for electrons, protons and

heavy ions, from which other parameters of dosimetric interest like effective atomic number and electron density could be derived; these help in the basic understanding of radiation interactions with multi-element materials. It was pointed out by Hine (1952: 725) that the effective atomic number cannot be expressed by a single number due to the different partial interaction processes at different energy regions and the various atomic numbers present in the compound have to be weighted differently. Effective atomic number (Z_{eff}), for multi-element materials, is calculated from the atomic numbers of the constituent elements, weighted according to the different partial interaction process by which the ion interacts, so it is an energy-dependent parameter (Murty, 1965: 398-399). Closely related to effective atomic number, is the electron density, N_e , which refers to the number of electrons per unit mass of a multi-element material, and it represent the probability of finding an electron at a particular point in space.

It becomes a common practice to study the radiological properties of materials such as dosimeters, human tissues and phantom material, with respect to their effective atomic number and electron density, and use them as a tool for evaluation of radiation equivalence of two materials, that is water equivalence and tissue equivalence of tissue and tissue substitute (Parthasaradhi et al., 1989: 653-654).

In literature several studies of Z_{eff} and electron density N_e of human tissues, and substitutes are been carried out for electron, proton and He ion in a wide range of energies (Kurudirek, 2016: 508-520; Kurudirek, 2014: 1-7), for other ions these studies was done within limited energy range. There is a need of studying these parameters for the interaction of heavy charged particles such as Proton, He, C and O ion and other ions that has important rule in radiotherapy. This is the motivation behind this work.

In this paper, radiological properties of some human tissues were investigated with respect to their effective atomic number and electron density for Proton, C, O ion total interaction, in the energy range 10KeV – 1GeV. Variations of atomic number and electron density with energy have been investigated. In addition, water and tissue equivalence of the material have been investigated.

Material and Methods

The elemental composition of Adipose Tissue (ICRP ICRU-103), Muscle, Skeletal (ICRP ICRU-201), Muscle, Striated (ICRP ICRU-202), Bone, Compact (ICRU-119), Bone, Cortical (ICRP ICRU-120), A-150 Tissue-Equiv. Plastic (ICRU-099), MS_20 Tissue Substitute (ICRU-200), Muscle Equivalent Liquid with Sucrose (ICRU - 203), Muscle Equivalent Liquid Without Sucrose (ICRU - 204), B-100, Bone-Equivalent Plastic (ICRU-111) and Water was obtained from compound dictionary available within SRIM program (Ziegler, 2020), Lung Tissue, ICRP (White, 1989) and LN10-75 LUNG was obtained from (Singh and Gagandeep, 2002: 442-449).

In order to calculate Z_{eff} using interpolation method, SRIM code (Ziegler, 2020) has been used to obtain the elemental mass stopping powers within ion energy range 0.01-1GeV, spanning the minimum and the maximum elements present in the considered materials. The mass stopping power for each material was then calculated using Bragg's additive rule, and the Stopping cross sections (σ_{tissue}) were then obtained by dividing mass stopping power of the tissue by the total number of atoms present in one gram of the material. Finally, Z_{eff} values were calculated by the linear logarithmic interpolation of Z values between the adjacent elemental stopping cross section data. This calculation done following procedure adopted by Kurudirek (Kurudirek, 2014a: 1-7; Kurudirek, 2014b: 130-134; Kurudirek, 2014c: 139-146; Kurudirek and Onaran 2015: 125-138). The electron density N_e of the tissues has been calculated using the formula:

$$N_e = Z_{eff} N_A / \langle A \rangle \text{ (electron/g)}$$

Where N_A is the Avogadro's number and $\langle A \rangle$ is the relative atomic mass of the tissue. The uncertainties in the present work base on the uncertainties arise in derivation of stopping powers derived from SRIM software.

Tissue and water equivalence of substances under study is expressed as relative difference percent, as follows:

$$RD\% = \frac{Z_{eff}(\text{Material}) - Z_{eff}(\text{Water})}{Z_{eff}(\text{Material})}$$

Results and Discussion

The variation of effective atomic number (Z_{eff}) and electron density (N_e) with energy for proton, C and O ion total interaction in the energy range 0.01KeV – 100MeV, are shown graphically in Fig. 1 and Fig. 2, respectively.

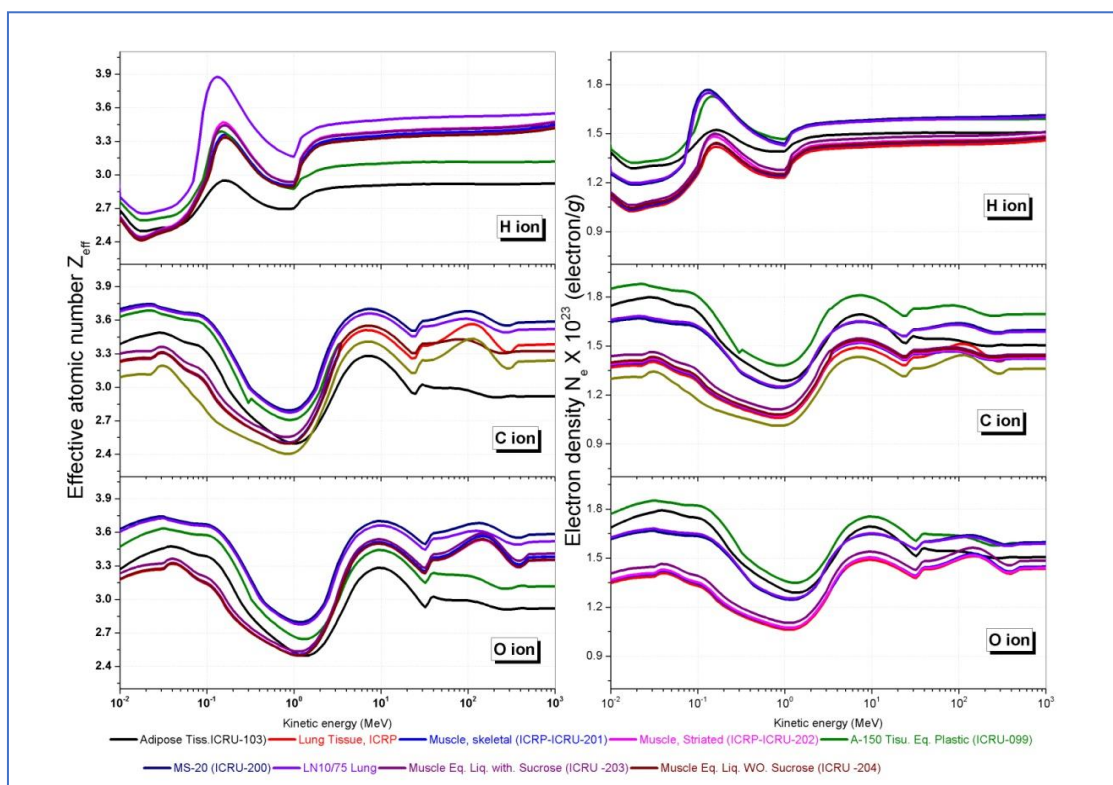


Fig. 1. Variation of Z_{eff} and N_e soft tissues and muscles with H, C and O ion energy

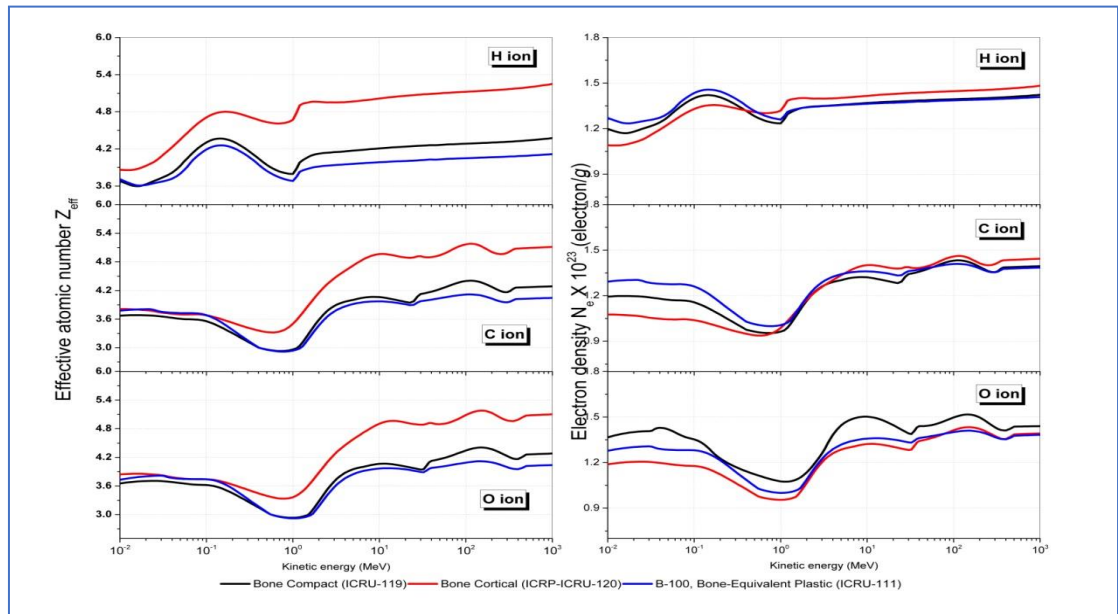


Fig. 2. Variation of Z_{eff} and N_e Bones compact, bone cortical and B-100, Bone-Equivalent Plastic (ICRU-111), with H, C and O ion energy

For Proton interaction, Z_{eff} has minimum values at lower energies and makes peak between 0.13 and 0.17 MeV, it start to increase again after 1 MeV and then keep constant. For C and O ion interaction, high values where observed at low ion energies, and in relatively high energies at (7.0 - 8.0 MeV) for C ion and 10 MeV for O ion. The minimum values are observed at intermediate energies of (0.8-1.0 MeV) and (1.1-1.4MeV) for C and O ion respectively.

For materials under study, highest value of Z_{eff} were observed for LN10/75 LUNG for all ions and MS-20 (ICRU 200) for proton interaction only. Meanwhile lowest Z_{eff} values were observed for Adipose Tissue (ICRP ICRU-103) for proton interaction and at energies greater than 1.0 MeV of C and O ion interaction. Lung Tissue ICTP, Muscle, Equiv. Liq. Without Sucrose (ICRU-204) and Muscle, Skeletal (ICRP ICRU-201) possesses lowest values for C and O ion below 1.0 MeV. In general, peaks were shifted towards higher energies with increasing atomic number of ion. As shown in Fig. 1. and Fig. 2, it is clear that variation of electron density N_e have same trends as variation of Z_{eff} , as expected.

Table1. Below shows basic statistical information on Z_{eff} and N_e dependence on incident ion energy. The highest variation in Z_{eff} for ion interaction is 35% (Tissue Substitute MS-ICRU-200), 33% (Lung ICRP) and 33% (Lung ICRP and Skeletal (ICRP ICRU-201)) for Proton, C and O ion respectively

Table 1. Statistical information on Z_{eff} and N_e of human tissues and substitutes for Proton, C and O ion interaction, (1) Adipose Tissue (ICRP ICRU-103), (2) Lung Tissue, ICRP (3) Muscle, Skeletal (ICRP ICRU-201) (4) Muscle, Striated (ICRP ICRU-202), (5) Bone, Compact (ICRU-119), (6) Bone, Cortical (ICRP ICRU-120) (7) A-150 Tissue-Equivalent Plastic (ICRU-099), (8) MS_20 Tissue Substitute (ICRU-200), (9) LN10-75 Lung, (10) Muscle Equivalent Liquid with Sucrose (ICRU - 203), (11) Muscle Equivalent Liquid Without Sucrose (ICRU - 204), (12) B-100, Bone-Equivalent Plastic (ICRU-111), (13) Water

S.N	Proton					C ion					O ion			
Z_{eff}	Mean	STD	Min	Max		Mean	STD	Min	Max		Mean	STD	Min	Max
1	2.82	0.14	2.50	2.95		3.03	0.28	2.50	3.28		3.04	0.28	2.50	3.28
2	3.13	0.33	2.41	3.44		3.17	0.33	2.50	3.57		3.17	0.33	2.50	3.57
3	3.14	0.33	2.42	3.45		3.16	0.32	2.50	3.55		3.17	0.33	2.51	3.57
4	3.18	0.34	2.45	3.48		3.16	0.32	2.50	3.55		3.16	0.32	2.50	3.53
5	4.13	0.23	3.60	4.38		3.79	0.44	2.93	4.41		3.78	0.43	2.94	4.41
6	4.81	0.39	3.86	5.25		4.32	0.67	3.32	5.18		4.31	0.66	3.33	5.18
7	3.02	0.20	2.59	3.39		3.21	0.29	2.64	3.44		3.22	0.29	2.64	3.44
8	3.42	0.35	2.66	3.97		3.48	0.29	2.79	3.70		3.48	0.29	2.80	3.70
9	3.36	0.33	2.65	3.88		3.44	0.29	2.77	3.66		3.44	0.29	2.78	3.66
10	3.18	0.34	2.44	3.47		3.19	0.30	2.55	3.55		3.20	0.32	2.53	3.59
11	3.12	0.32	2.42	3.42		3.16	0.32	2.49	3.55		3.16	0.32	2.50	3.54
12	3.96	0.17	3.61	4.26		3.72	0.36	2.92	4.12		3.72	0.36	2.92	4.12
13	2.99	0.31	2.34	3.31		3.13	0.46	2.40	5.17		3.04	0.32	2.41	3.43
S.N	Proton (H ion)					C ion					O ion			
N_e	Mean	STD	Min	Max		Mean	ST	Min	Max		Mean	STD	Min	Max
1	1.45	0.07	1.29	1.52		1.56	0.15	1.29	1.80		1.57	0.15	1.29	1.79
2	1.33	0.14	1.02	1.46		1.34	0.14	1.06	1.51		1.34	0.14	1.06	1.51
3	1.34	0.14	1.03	1.47		1.35	0.14	1.07	1.52		1.36	0.14	1.07	1.53
4	1.36	0.14	1.04	1.49		1.36	0.14	1.07	1.52		1.36	0.14	1.07	1.52
5	1.34	0.07	1.17	1.42		1.23	0.14	0.95	1.43		1.23	0.14	0.95	1.43
6	1.36	0.11	1.09	1.48		1.22	0.19	0.94	1.46		1.22	0.18	0.94	1.46
7	1.54	0.10	1.32	1.73		1.64	0.15	1.35	1.86		1.64	0.15	1.35	1.85
8	1.52	0.16	1.19	1.77		1.55	0.14	1.24	1.67		1.55	0.13	1.25	1.67
9	1.52	0.15	1.20	1.75		1.55	0.14	1.25	1.68		1.55	0.13	1.25	1.68
10	1.38	0.15	1.06	1.51		1.39	0.14	1.11	1.55		1.39	0.14	1.10	1.56
11	1.35	0.14	1.05	1.48		1.36	0.14	1.08	1.54		0.37	0.14	1.08	1.53
12	1.36	0.06	1.23	1.46		1.28	0.12	1.00	1.41		1.2	0.12	1.00	1.41
13	1.26	0.13	0.99	1.39		1.32	0.20	1.01	2.17		1.28	0.14	1.01	1.44

The Z_{eff} difference percent relative to water (DR%) has been also calculated to evaluate degree of water equivalence of the given substances for different ions interaction, and represented graphically in Fig. 3. It has been observed that A-150 Tissue-Equiv. Plastic (ICRU-099), Muscle Equivalent Liquid Without Sucrose (ICRU - 204), Skeletal (ICRP ICRU-201), Muscle, Muscle Equivalent Liquid with Sucrose (ICRU-203) and Muscle, Striated (ICRP ICRU-202), have the best water equivalence in the entire energy range with relative difference of $\leq -3\%$, $\leq 4\%$, $\leq 5\%$, $\leq 5\%$, $\leq 6\%$ for H ion. Also, Lung Tissue, ICRP, Muscle, Striated (ICRP ICRU-202), Muscle Equivalent Liquid with Sucrose (ICRU - 203), Muscle Equivalent Liquid without Sucrose (ICRU-204) show diff. of $\leq 5\%$ through entire energy range for C, and O ion.

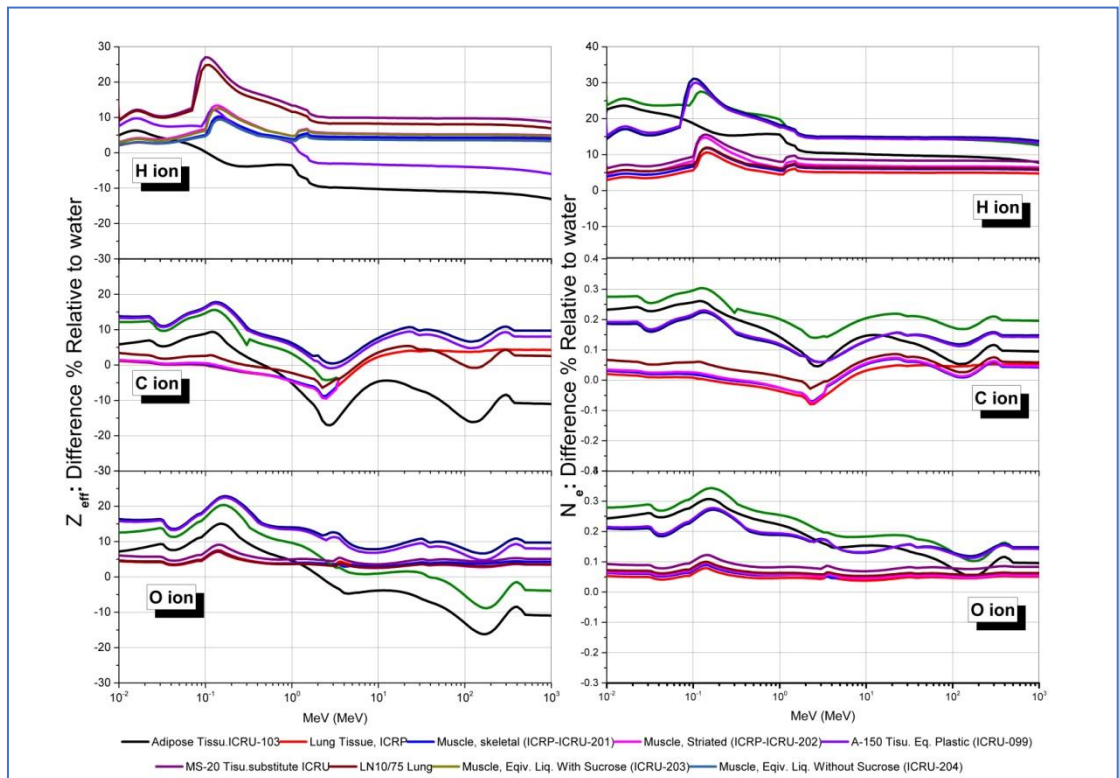


Fig. 3. Differences in Z_{eff} of tissues and muscles relative to water

The Z_{eff} difference percent relative to tissue (DR %) has been also calculated for some tissue of human organs relative to tissue substitute and shown graphically in Fig. 5. It is found that A-150 Tissue-Equiv. Plastic (ICRU-099), simulates Adipose through the entire energy range for all ions studied, with differences less than 6% while shows high differences (up to 15%), for H ion in the energy range of (0.01-1.0 MeV). Also, LN10/75 Lung shows good tissue equivalence with Lung Tissue ICRP with differences less than 5% at energies of (2-1000MeV), (3-1000MeV), (5-1000MeV) for H, C and O ion interaction, high difference up to (26% at 0.1 MeV), (22% at 0.14MeV) and (21% at 0.18MeV) is observed for proton, C and O ion respectively, mean while full matching is observed around 100 MeV for C and O ion. Muscle without matching well with muscle skeletal and muscle striated with relative differences of $<1.0\%$ and $<3\%$ for H ion, $<0.6\%$ and 0.1% for C ion, and 0.1% for O ion, with slightly high differences at 0.1-10MeV for both C and O ion. With respect to with sucrose, differences of 2% - 4% were observed at energy of (0.1-3.0MeV) for H and C ion, and difference is almost Zero for the rest of the energy regions. B100 shows well matching with compact 119, with low differences of

<5% for H ion, and between -4% at low energies below 1.0 MeV and 6% for the rest of range for C and O ion.

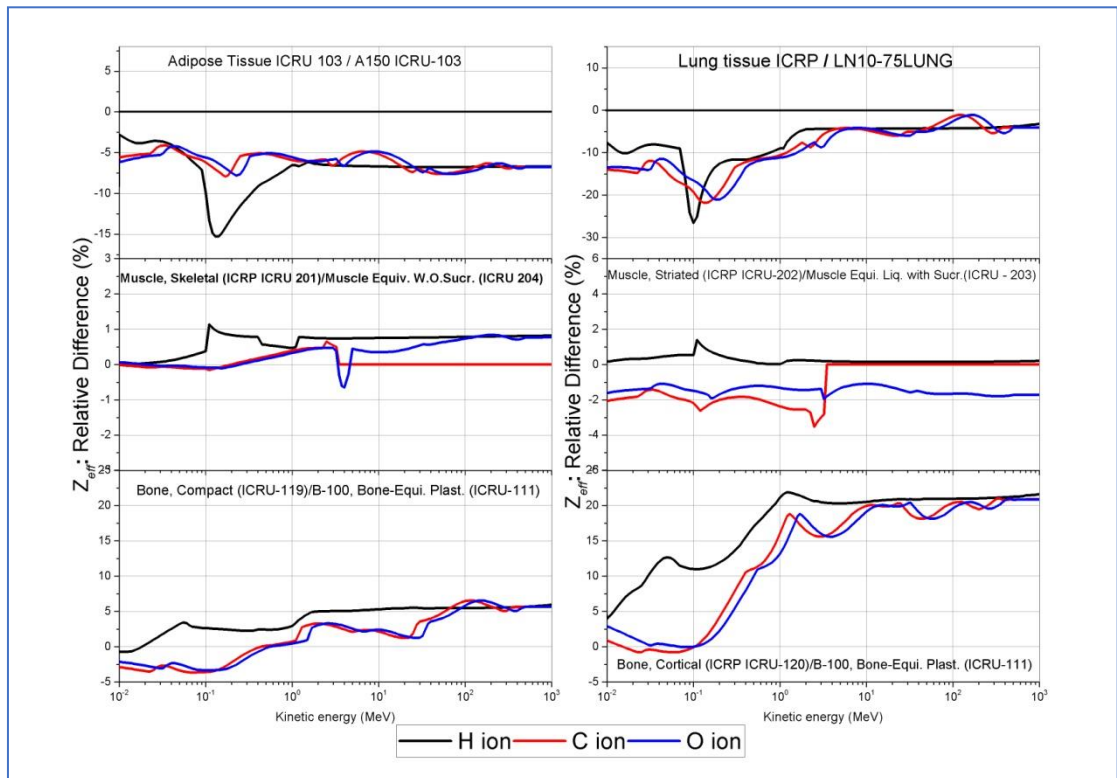


Fig. 4. Difference percent in Z_{eff} , all substances relative tissues

Conclusion

The effective atomic number and electron density of tissue and tissue substitute substances have been calculated in the energy range 10 keV-1 GeV for H, C and O ion total interaction.

We have shown that variation in Z_{eff} values is observed in the entire energy region from 10 keV to 1 GeV.

The lowest values of Z_{eff} were obtained in LN /75 LUNG for all ions, whereas the highest values were obtained in Bone cortical and bone compact. These high values are due to the presence of high Z element (Ca, $Z = 20$) with relatively high weight fraction within its constituents.

The maximum values of Z_{eff} depends on ion type and shift towards higher energies with increasing of the atomic number of the incident ion.

Electron density is closely related to the effective atomic number and has the same quantitative energy dependence as Z_{eff} .

The water and tissue equivalence properties of the given substances have been compared for different types of ions (H, C, and O ion).

A-150 Tissue-Eqiv. Plastic (ICRU-099), Muscle Equivalent Liquid Without Sucrose (ICRU - 204), Skeletal (ICRP ICRU-201), Muscle, Muscle Equivalent Liquid with Sucrose (ICRU-203) and Muscle, Striated (ICRP ICRU-202), have the best water equivalence in the entire energy range with relative difference of $\leq -3\%$, $\leq 4\%$, $\leq 5\%$, $\leq 5\%$, $\leq 6\%$ for H ion. Also, Lung Tissue, ICRP, Muscle, Striated (ICRP ICRU-202), Muscle Equivalent Liquid with Sucrose (ICRU - 203), Muscle Equivalent Liquid without Sucrose (ICRU-204) show diff. of $\leq 5\%$ through entire energy range for C, and O ion.

It is found that A-150 Tissue-Equiv. Plastic (ICRU-099), simulates Adipose Tissue ICRU 103 very well in the entire energy region for H, C and O ion interaction, except in the range of 10KeV-1.0 MeV for H ion interaction.

LN10/75 Lung shows good tissue equivalence with Lung Tissue ICRP with differences less than -5% for all ions, in the energy range 3MeV-1 GeV.

Muscle without was found to be equivalence to muscle skeletal and muscle striated with relative differences +/-1.0%

With respect to with sucrose, differences of 1% - -1% were observed at energy of (0.1-3.0MeV) for H and C ion, and difference is almost Zero for the rest of the energy regions.

Data reported here gives essential information about interaction of different types of charged particles with different materials and could be useful in the energy range specified.

References

Hine, G.J. (1952). The effective atomic numbers of materials for various gamma interactions. *Phys Rev.*, 85, 725.

Kurudirek, M. (2014a). Effective atomic numbers and electron densities of some human tissues and dosimetric materials for mean energies of various radiation sources relevant to radiotherapy and medical applications. *Radiation Physics and Chemistry*, 102, 139-146. <https://doi.org/10.1016/j.radphyschem.2014.04.033>

Kurudirek, M. (2014b). Effective atomic numbers of different types of materials for proton interaction in the energy region 1 keV–10 GeV. *Nuclear Instruments and Methods in Physics Research Section B: Beam Interactions with Materials and Atoms*, 336, 130-134. <https://doi.org/10.1016/j.nimb.2014.07.008>

Kurudirek, M. (2014c). Effective atomic numbers, water and tissue equivalence properties of human tissues, tissue equivalents and dosimetric materials for total electron interaction in the energy region 10 keV–1 GeV. *Applied radiation and Isotopes*, 94, 1-7. <https://doi.org/10.1016/j.apradiso.2014.07.002>

Kurudirek, M. (2016). Water and tissue equivalence properties of biological materials for photons, electrons, protons and alpha particles in the energy region 10 keV–1 GeV: a comparative study. *International journal of radiation biology*, 92(9), 508-520. <https://doi.org/10.1080/09553002.2016.1206225>

Kurudirek, M., Onaran, T. (2015). Calculation of effective atomic number and electron density of essential biomolecules for electron, proton, alpha particle and multi-energetic photon interactions. *Radiation Physics and Chemistry*, 112, 125-138. <https://doi.org/10.1016/j.radphyschem.2015.03.034>

Murty, R. (1965). Effective Atomic Numbers of Heterogeneous Materials. *Nature*, 207, 398-399. <https://doi.org/10.1038/207398a0>

Parthasaradhi, K., Rao, B.M., Prasad, S.G. (1989). Effective atomic numbers of biological materials in the energy region 1 to 50 MeV for photons, electrons, and He ions. *Medical physics*, 16(4), 653-654. <https://doi.org/10.1118/1.596325>

Singh, K., Gagandeep. (2002). Effective atomic number studies in different body tissues and amino acids. *Indian Journal of Pure & Applied Physics*, 40, 442-449. Available at:

<http://nopr.niscair.res.in/bitstream/123456789/26175/1/IJPAP%2040%286%29%20442-449.pdf>

Tommasino, F., Scifoni, E., Durante, M. (2015). New Ions for Therapy-International Journal of Particle Therapy, 2, 429-438. <https://doi.org/10.14338/IJPT-15-00027.1>

White, D.R., Booz, J., Griffith, R.V., Spokas, J.J., Wilson, I.J. (1989). Report 44. Journal of the International Commission on Radiation Units and Measurements, os23(1). <https://doi.org/10.1093/jicru/os23.1.Report44>

Ziegler, J.F. (2020). SRIM - The Stopping and Range of Ions in Matter. Available at: <http://www.srim.org>